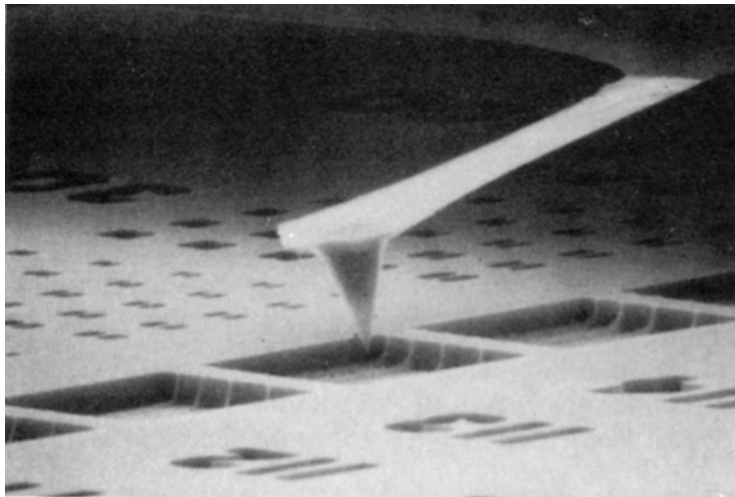


掃描探針顯微術(Scanning Probe Microscopy)



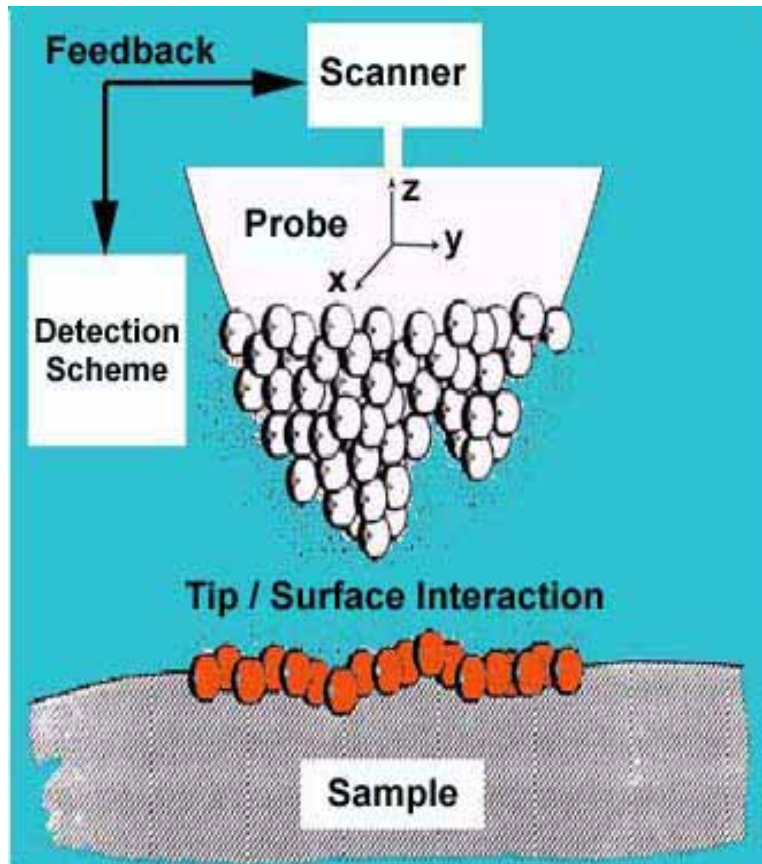
Ing-Shouh Hwang (ishwang@phys.sinica.edu.tw)

Institute of Physics, Academia Sinica, Taipei, Taiwan

References

1. G. Binnig, H. Rohrer, C. Gerber, and Weibel, Phys. Rev. Lett. **49**, 57(1982); and *ibid* **50**, 120(1983).
2. J. Chen, *Introduction to Scanning Tunneling Microscopy*, New York, Oxford Univ. Press (1993).
3. R. Wiesendanger, *Scanning Probe Microscopy and Spectroscopy*, Cambridge 1994.
4. Dawn Bonnell, "Scanning Probe Microscopy and Spectroscopy: Theory, Techniques, and Applications". Wiley-VCH 2001.

Scanning Probe Microscopy



A feedback control system is used to maintain a constant tip/surface interaction, which is very sensitive to the distance variation.

Scanning Tunneling Microscopy (STM)

--- G. Binnig, H. Rohrer et al, (1982)

Near-Field Scanning Optical Microscopy (NSOM)

--- D. W. Pohl (1982)

Atomic Force Microscopy (AFM)

--- G. Binnig, C. F. Quate, C. Gerber (1986)

Scanning Thermal Microscopy (SThM)

--- C. C. Williams, H. Wickramasinghe (1986))

Magnetic Force Microscopy (MFM)

--- Y. Martin, H. K. Wickramasinghe (1987)

Friction Force Microscopy (FFM or LFM)

--- C. M. Mate et al (1987)

Electrostatic Force Microscopy (EFM)

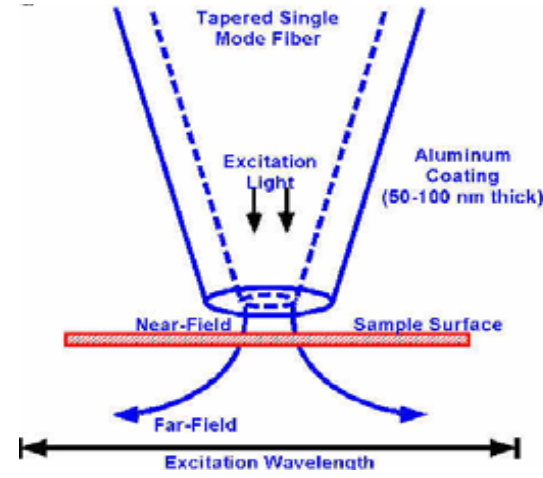
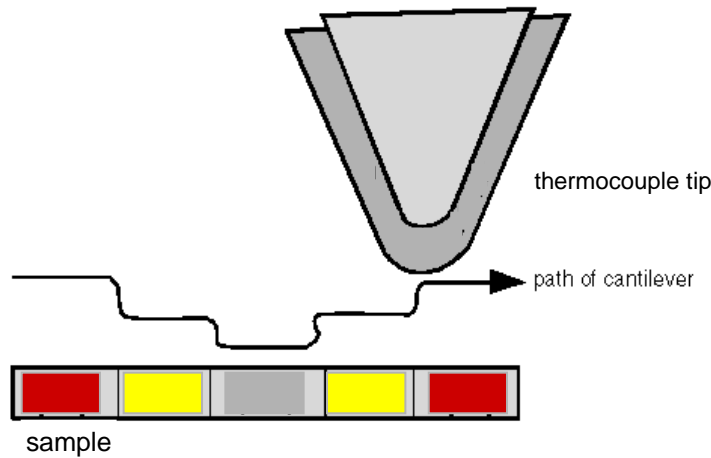
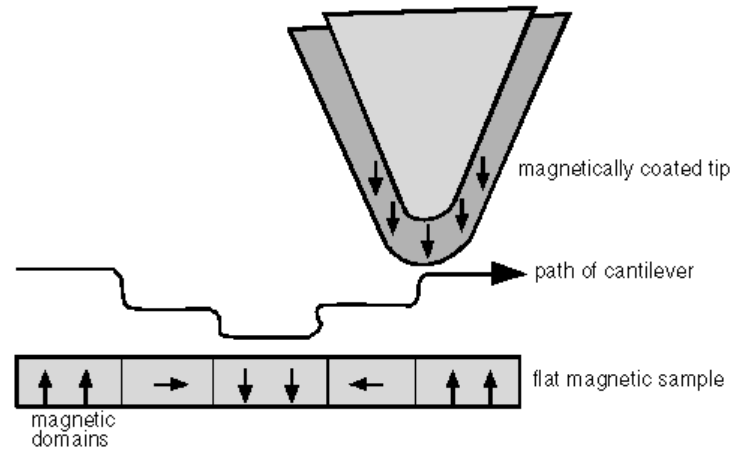
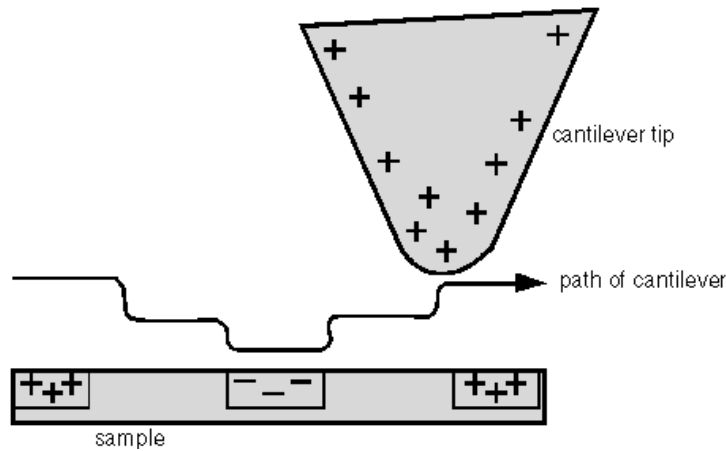
--- Y. Martin, D. W. Abraham et al (1988)

Scanning Capacitance Microscopy (SCM)

--- C. C. Williams, J. Slinkman et al (1989)

1. All SPMs are based on the ability to position various types of probes in very close proximity with extremely high precision to the sample under investigation.
2. These probes can detect electrical current, atomic and molecular forces, electrostatic forces, or other types of interactions with the sample.
3. By scanning the probe laterally over the sample surface and performing measurements at different locations, detailed maps of surface topography, electronic properties, magnetic or electrostatic forces, optical characteristics, thermal properties, or other properties can be obtained.
4. The spatial resolution is limited by the sharpness of the probe tip, the accuracy with which the probe can be positioned, the condition of the surface under study, and the nature of the force being detected.

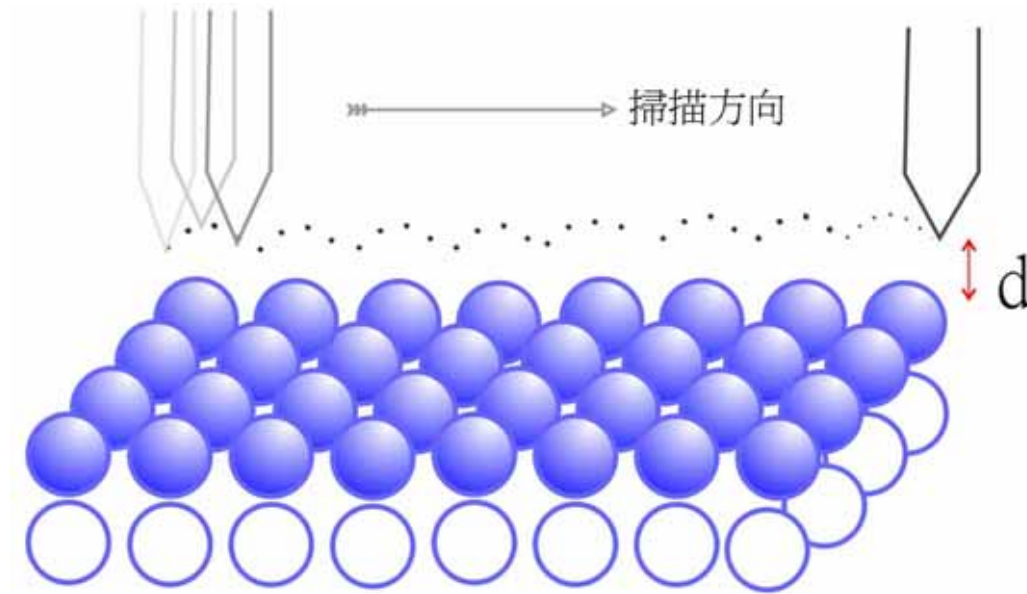
Different Probes



Microscope	Interaction	Information
STM	Tunneling current	3-D topography: size, shape and periodicity of features, surface roughness. Electronic structure, and possible elemental identity.
Contact or intermittent contact AFM	Interatomic and intermolecular forces	3-D topography: size and shape and periodicity of features, surface roughness.
Force-Modulated AFM	Interatomic and intermolecular forces	Hardness and surface elasticity at various locations.
LFM	Frictional forces	Differences of adhesiveness and friction at various locations.
MFM	Magnetic forces	Size and shape of magnetic features. Strength and polarity of magnetic fields at different locations.
SThM	Heat transfer	Thermal conductivity differences between surface features.
EFM	Electrostatic forces	Electrostatic field gradients on the sample surface due to dopant concentrations..
NSOM	Reflection, absorption and Fluorescence of light	Optical properties of surface features

Scanning Tunneling Microscopy

掃描穿隧顯微術

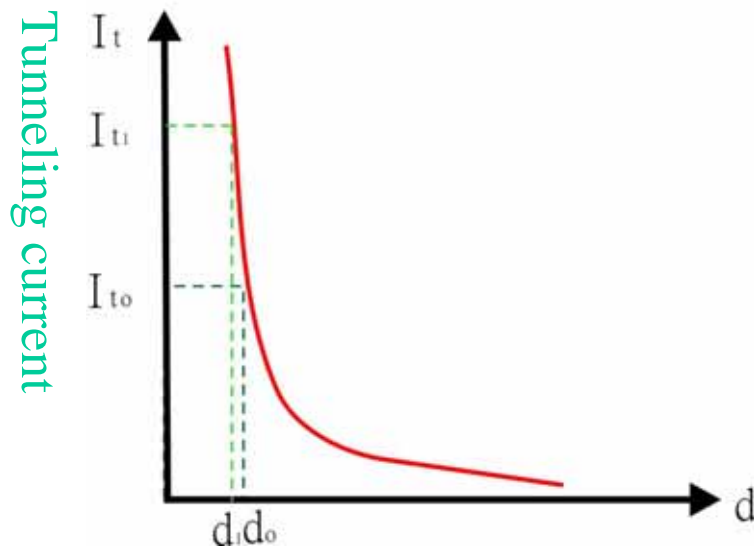
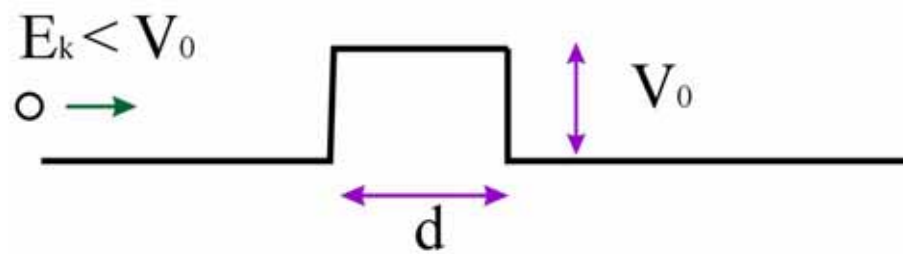


References

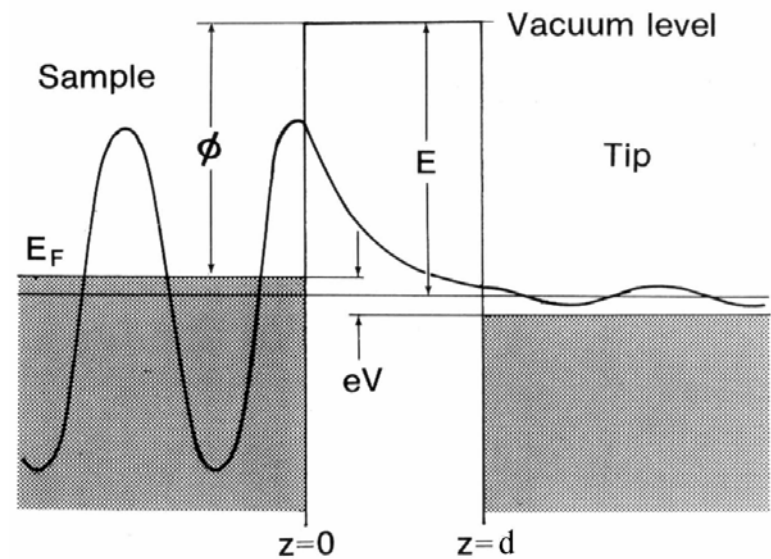
1. G. Binnig, H. Rohrer, C. Gerber, and Weibel, Phys. Rev. Lett. **49**, 57(1982); and *ibid* **50**, 120(1983).
2. J. Chen, *Introduction to Scanning Tunneling Microscopy*, New York, Oxford Univ. Press (1993).
3. 黃英碩, 科儀新知95, 18 (3), 4 (1996)。
4. 黃英碩, 科儀新知144, 26 (4), 7 (2005)。

Tunneling

Classical



Quantum
Mechanics



Tunneling current I_t

$$I_t \propto (V/d) \exp(-A\phi^{1/2}d)$$

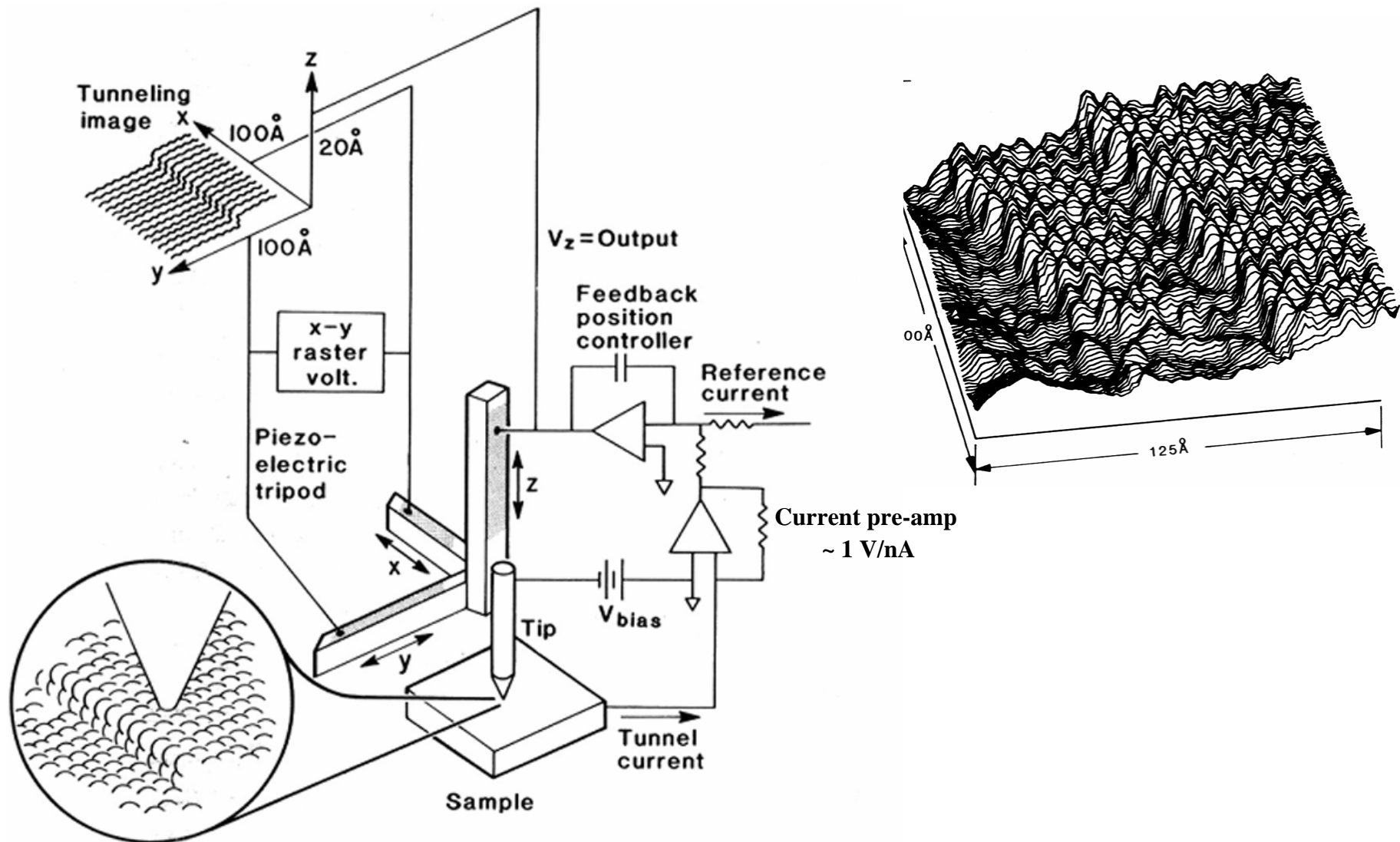
$$A = 1.025 \text{ (eV)}^{-1/2} \text{\AA}^{-1}$$

$$I_t = 10 \text{ pA} \sim 10 \text{nA}$$

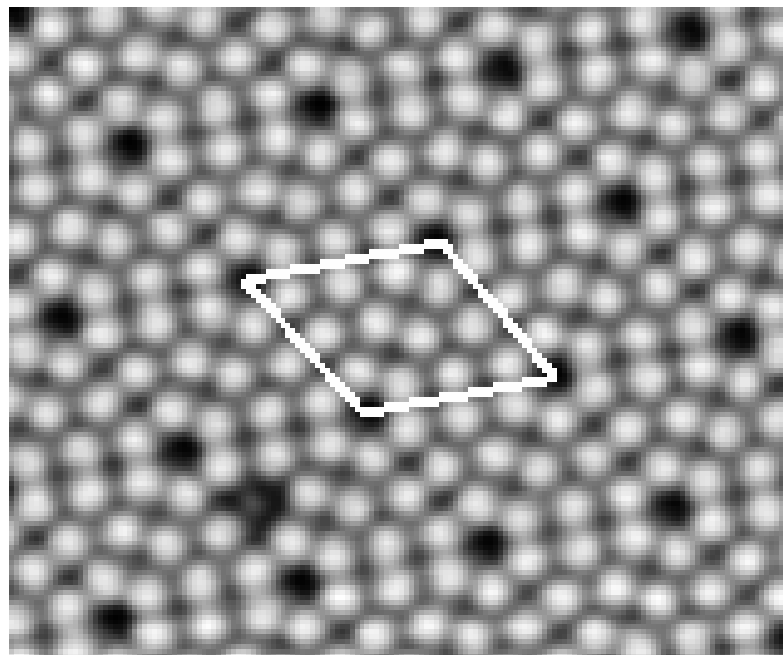
$$V = 1 \text{ mV} \sim 3 \text{ V}$$

d decreases by 1\AA , I_t increases by about one order of magnitude.

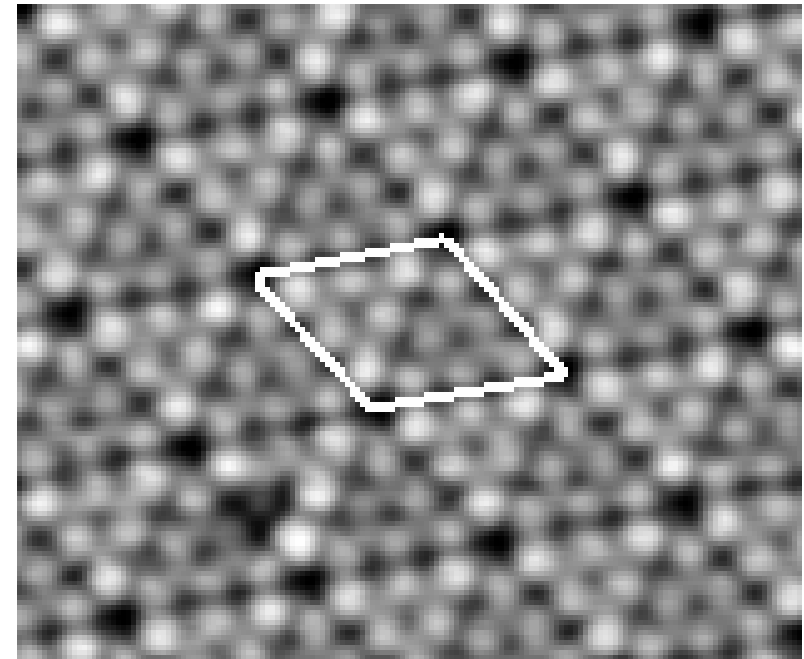
Schematics of STM



STM Images of Si(111)-(7×7)



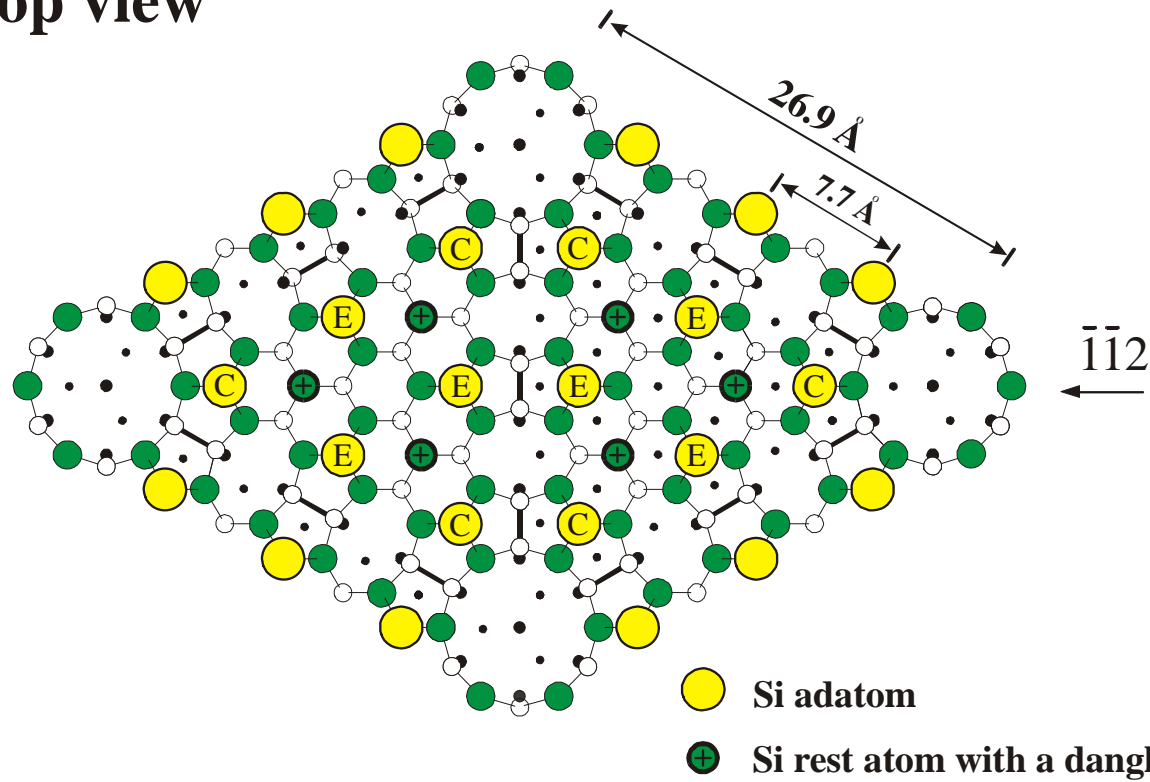
Empty-state image



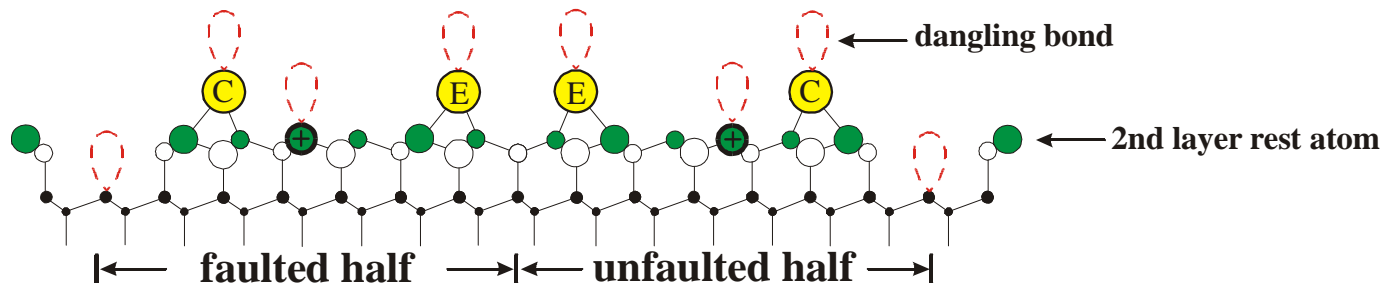
Filled-state image

Atomic Model of Si(111)-(7×7)

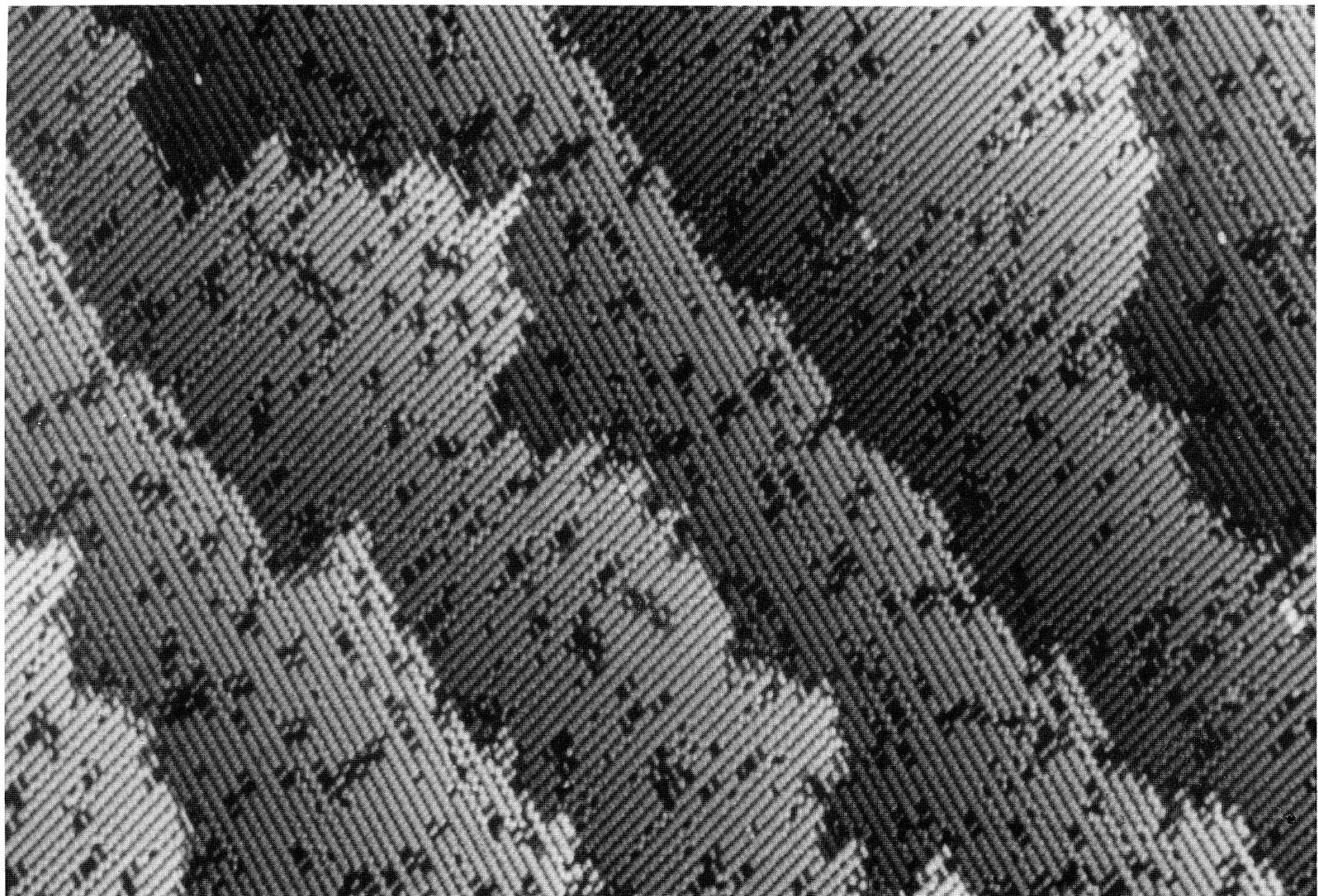
Top view



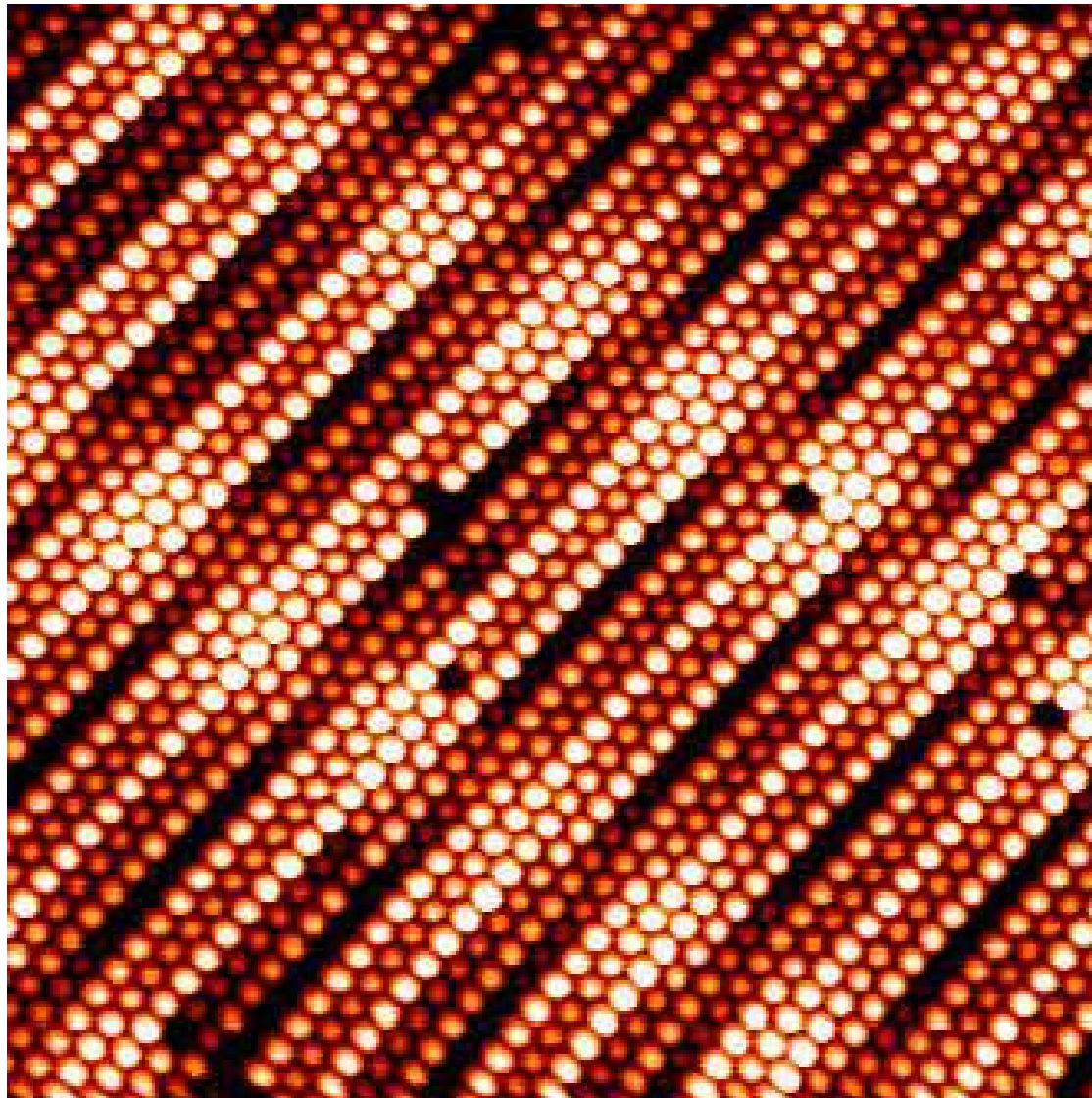
Side view



Atomic Structure of the Si(001) Surface

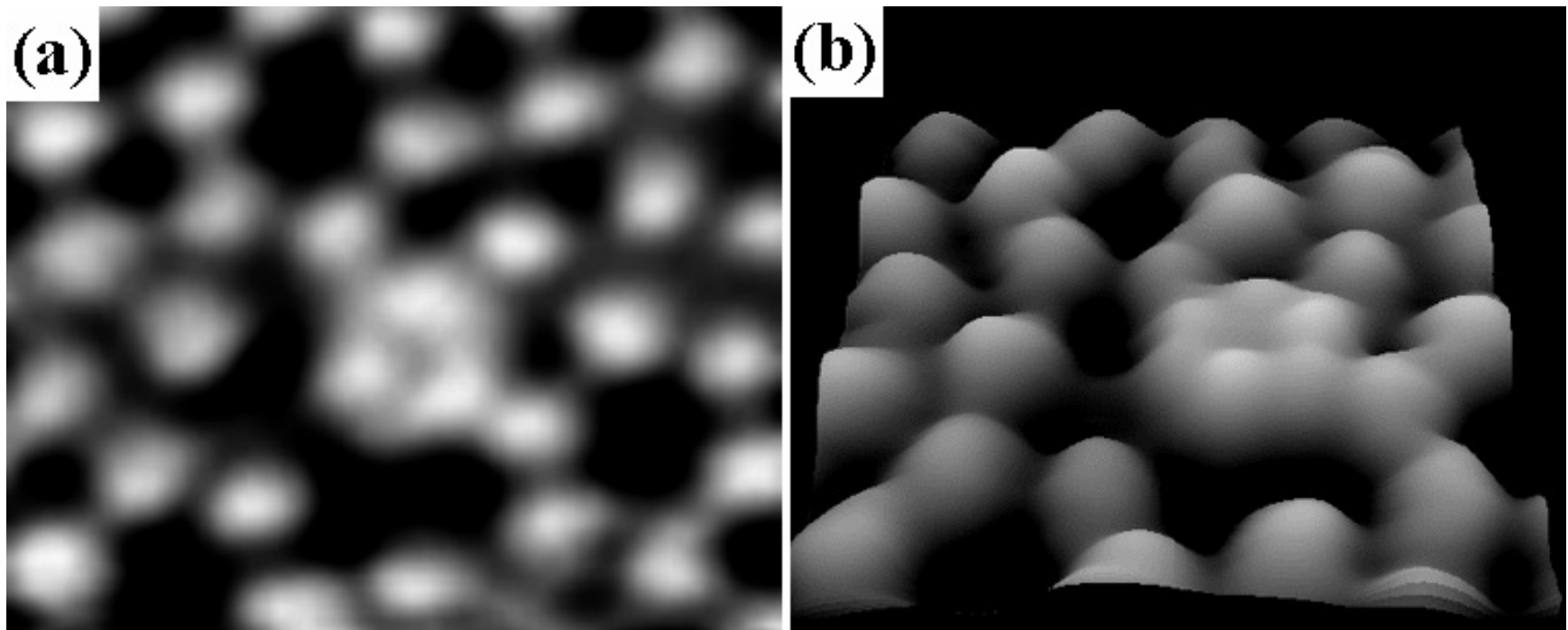


Atomic Structure of the Pt(001) Surface



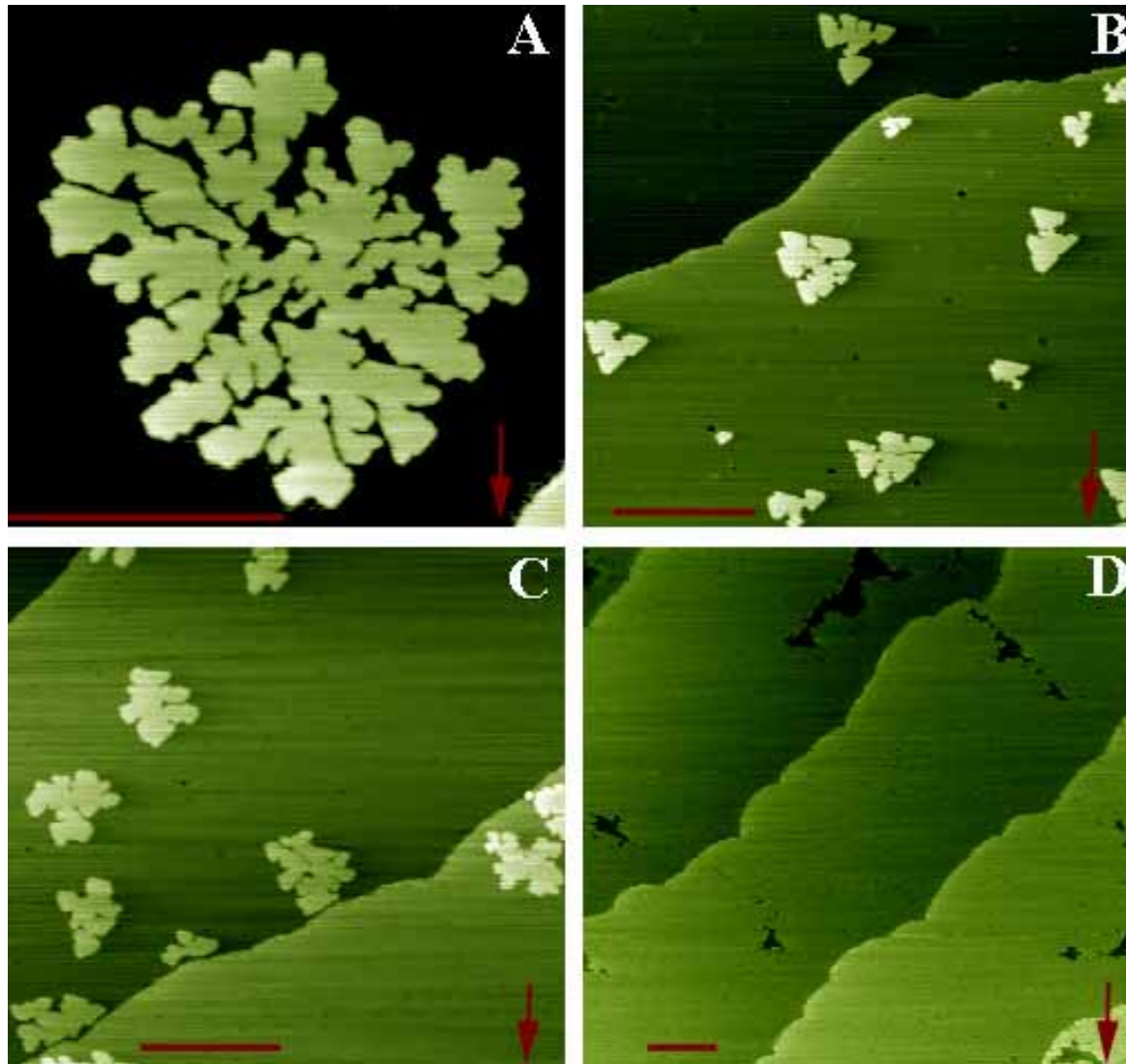
Surface Science 306, 10 (1994).

Si Magic Clusters



Physical Review Letters **83**, 120 (1999).

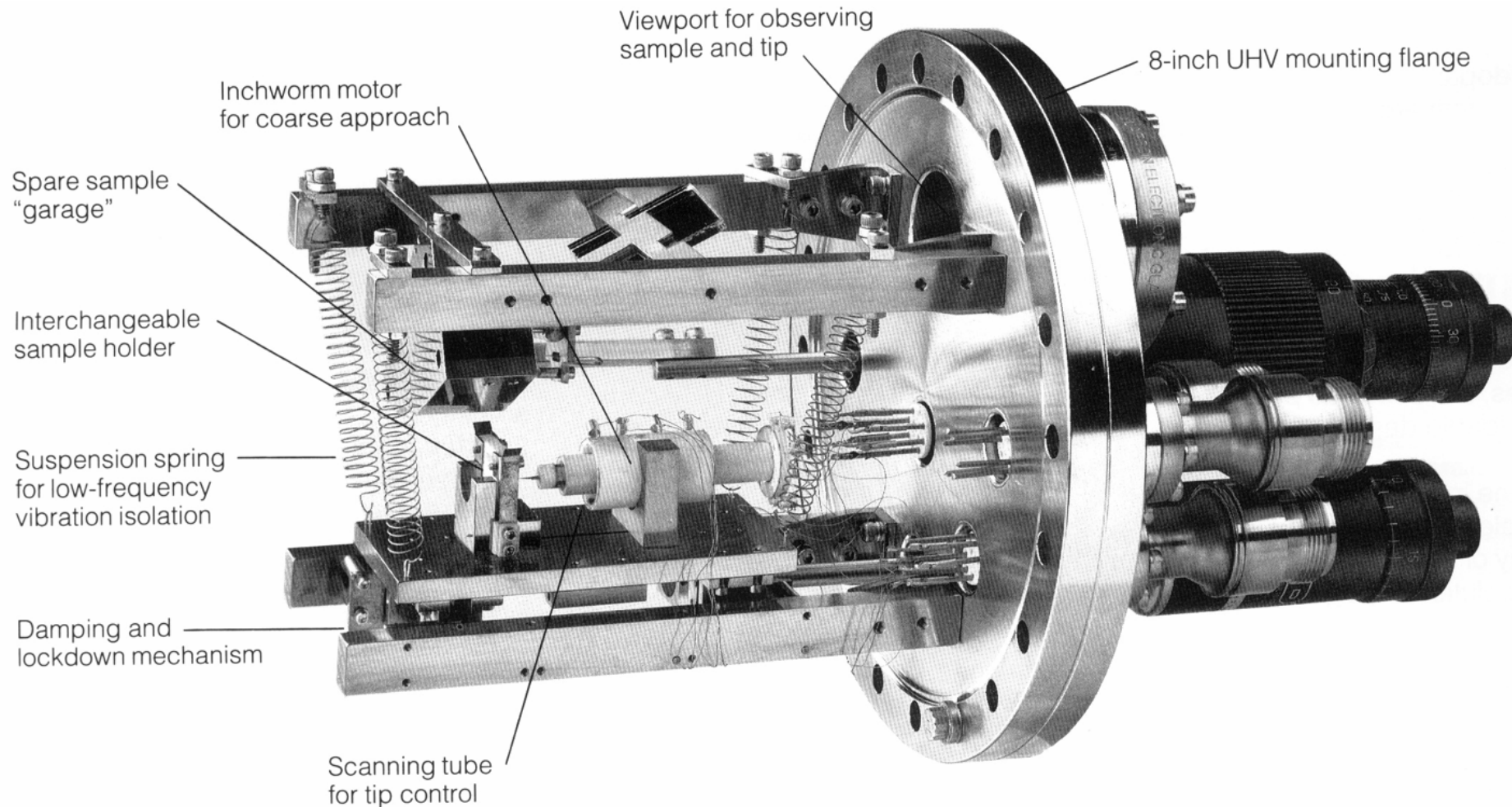
Nucleation and Growth of Ge at Pb/Si(111)



Physical Review Letters **83**, 1191 (1999).

Japanese Journal of Applied Physics **39**, Part 1, No. 7A, 4100 (2000).

Ultra-High Vacuum Scanning Tunneling Microscope



Inchworm-Type Linear Motor

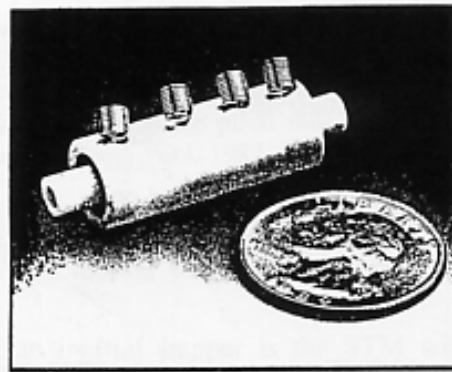
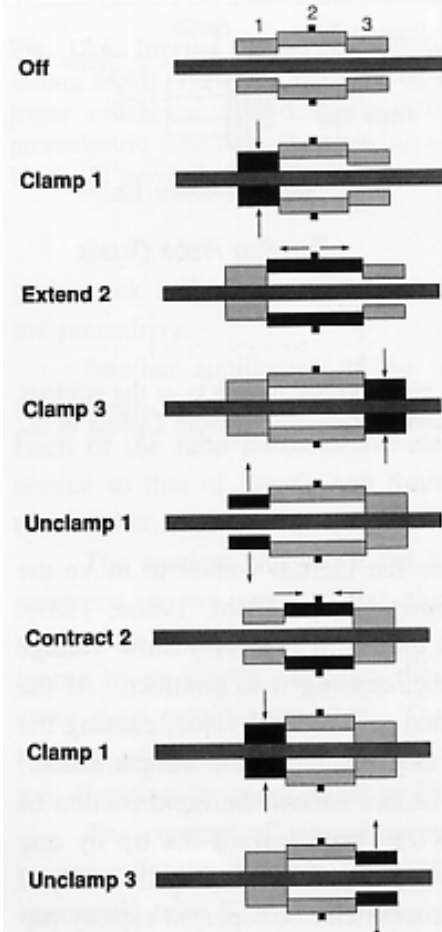
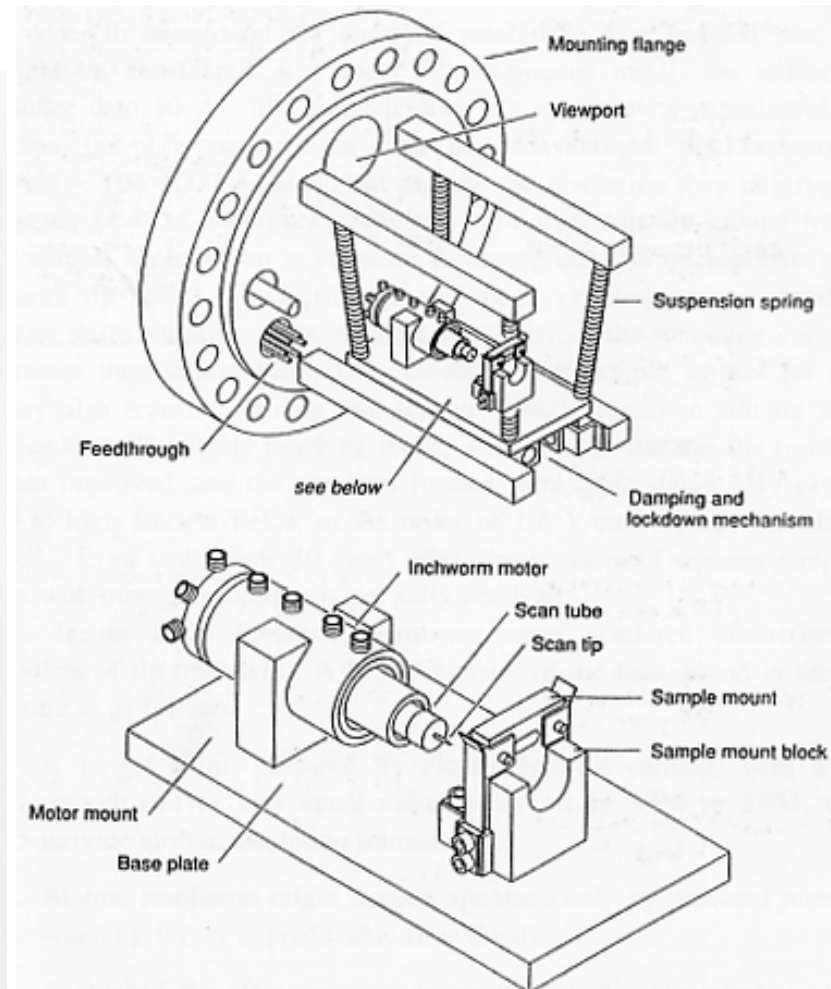
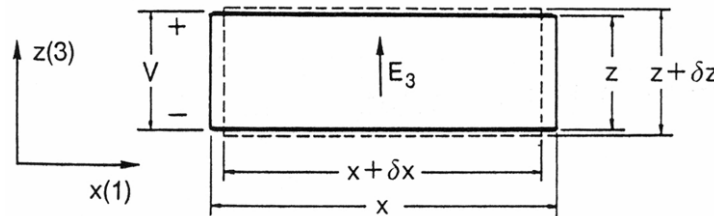


Fig. 12.8. The Inchworm®. It consists of an alumina shaft, slid inside a piezoelectric tube, which consists of three sections. Top, a photograph of the MicroInchworm® Motor, actual size. Right, walking mechanism: (1) Clamp the left-hand side by applying a voltage to section 1. (2) Extend section 2. (3) Clamp the right-hand end. (4) Unclamp section 1. (5) Contract the center section. (6) Clamp section 1. (7) Unclamp section 3. (Courtesy of Burleigh Instruments, Inc.)



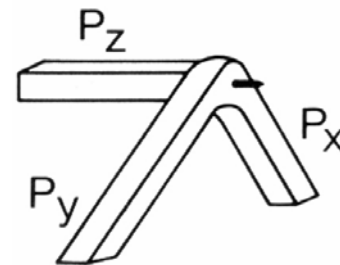
Piezoelectric Scanners



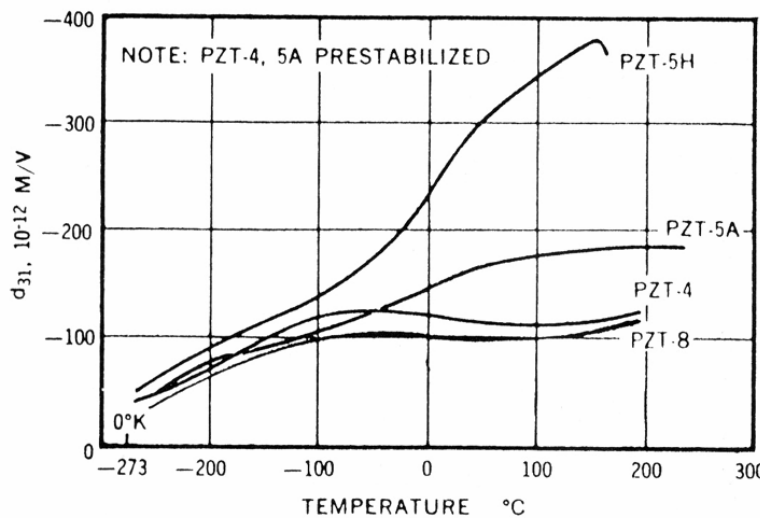
$$d_{31} = S_1/E_3, S_1 = \delta x/x, E_3 = V/z$$

$$d_{33} = S_3/E_3, S_3 = \delta z/z$$

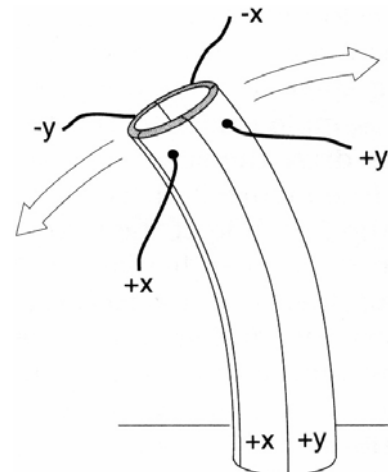
Tripod scanner



Variation of piezoelectric coefficient with temperature.



Tube scanner

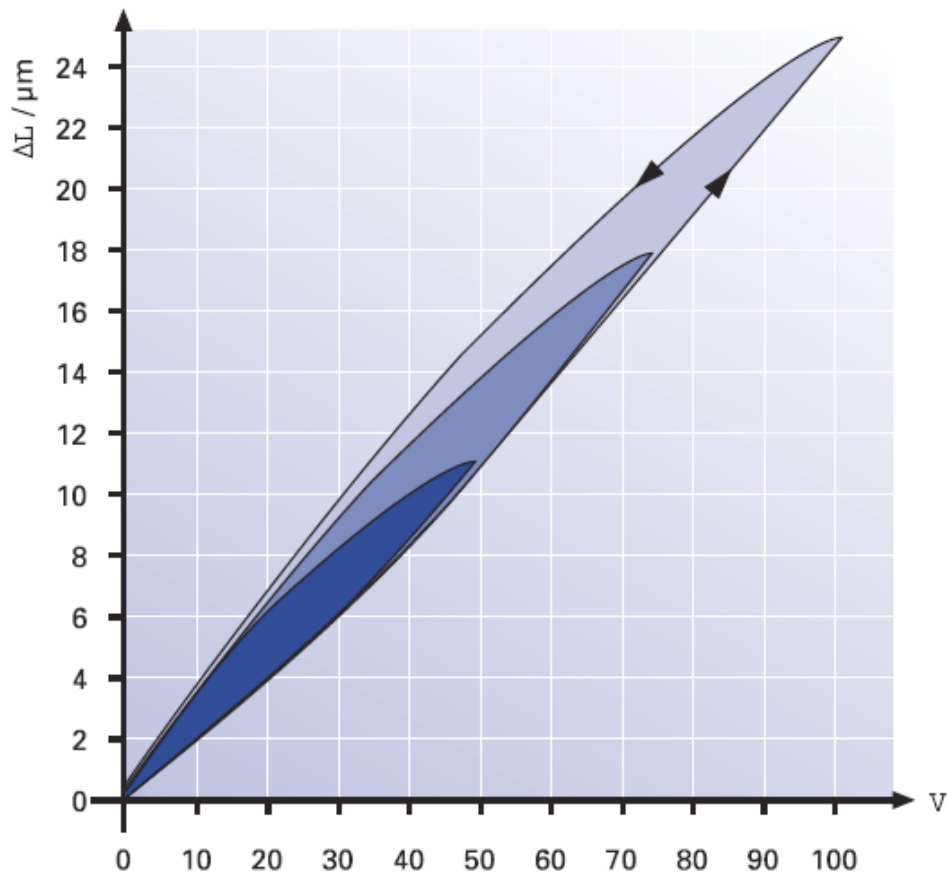


PZT Materials

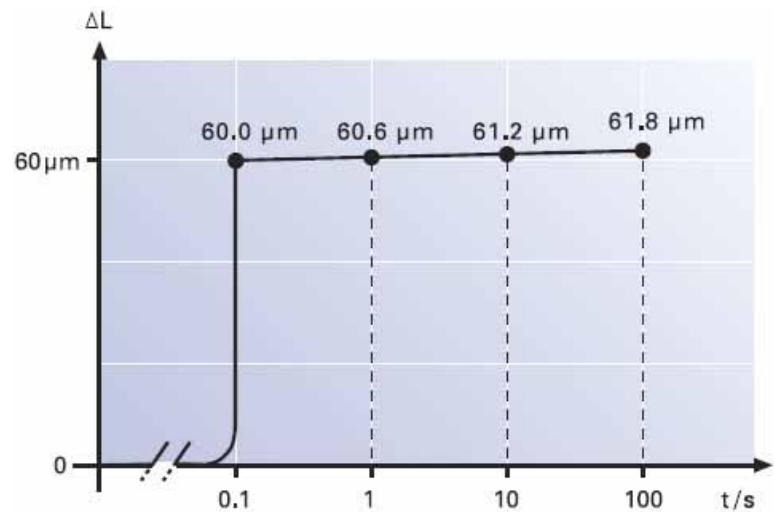
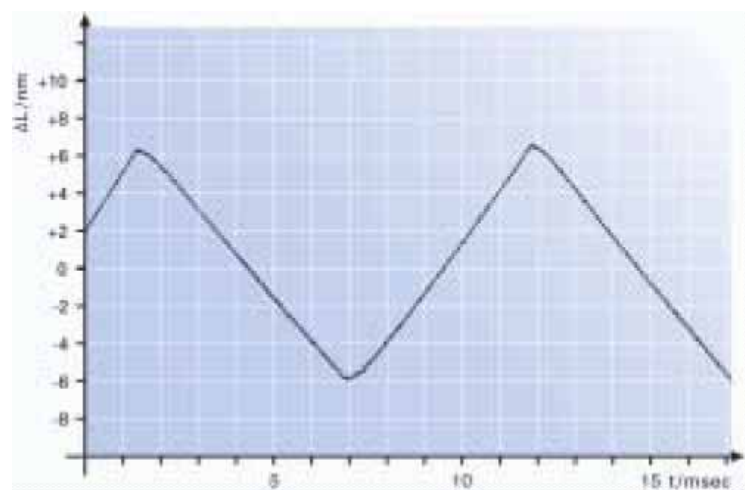
1. The piezoelectric effect was discovered by Pierre Curie and Jacques Curie in 1880.
2. The piezo materials used in STM are various kinds of lead zirconate titanate ceramics (PZT) --- a mixture of PbZrO_3 and PbTiO_3 . It consists of small ferroelectric crystals in random orientations.
3. An advantage for PZT ceramics over single crystal materials is that it can be shaped easily and poled at a desired direction.
4. PZT scanners are widely used in SPM because they have excellent resolution in displacement, high stiffness, and fast response. A major drawback of PZT materials is its lack of accuracy due to many nonlinear characteristics, such as hysteresis, creep, and recoil-generated ringing, which often cause distortion in SPM images. The positioning error of a PZT scanner can be as much as 10-15% of the full scanning range.
5. The piezoelectric constants vary with temperature in a complicated manner, and also with the particular batch of materials by the manufacturer and time (the aging effect).
6. Displacement calibration or compensation is needed for accurate measurement of length or size.

Hysteresis of a PZT Actuator

Hysteresis curves of an open-loop piezo actuator for various peak voltages



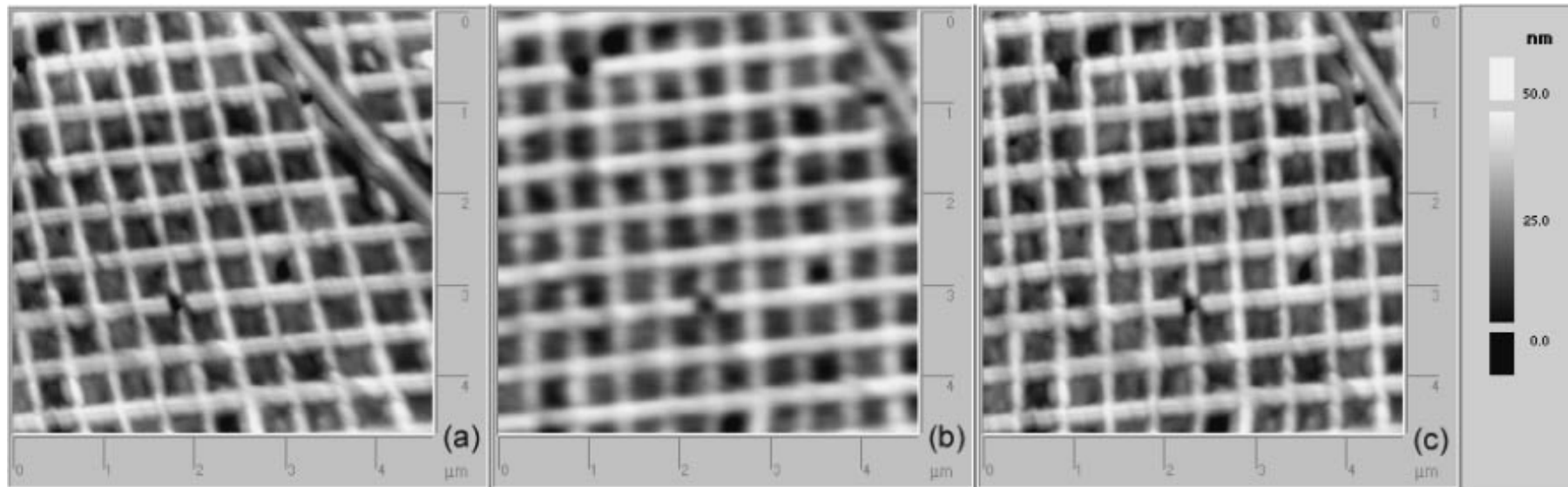
Response of a PZT translator to a 1 V, 200 Hz triangular drive signal



Creep of open-loop PZT motion

Topographic Images of AFM Square Grating

Without correction

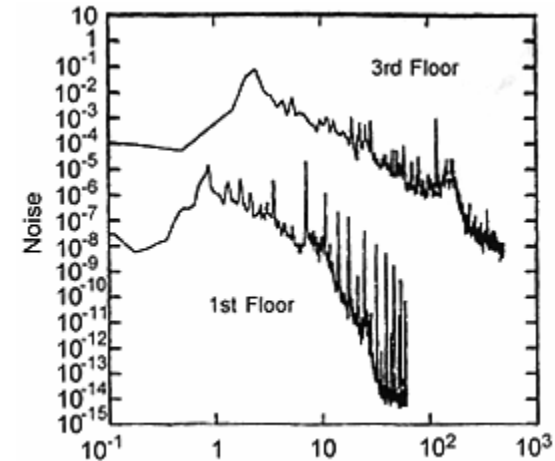
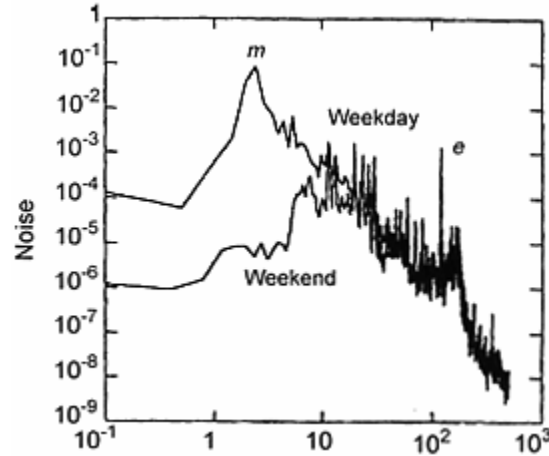
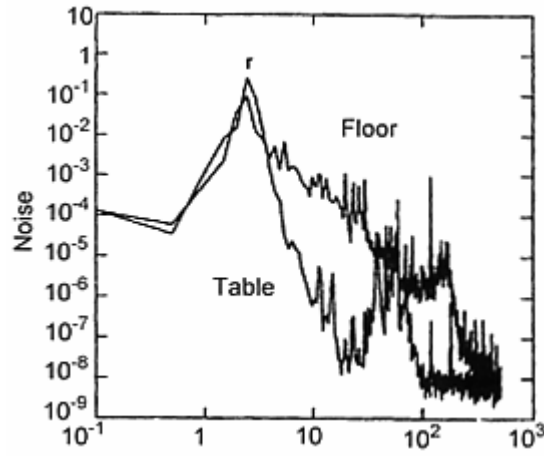


With correction in the x-direction

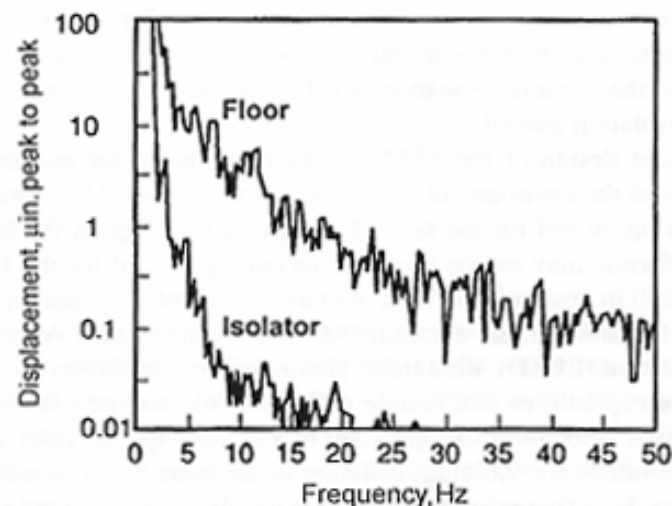
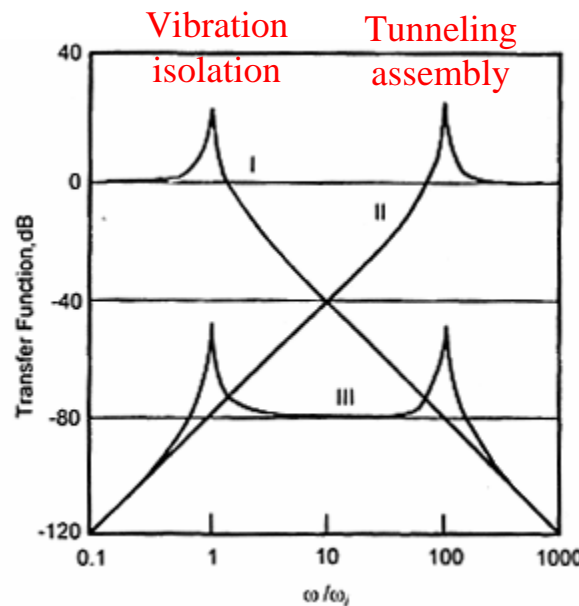
Jap. J. of Appl. Phys. **45**, 3B, 1917-1921.

Vibration Isolation

Power spectra of a tunneling signal



Calculated transfer function

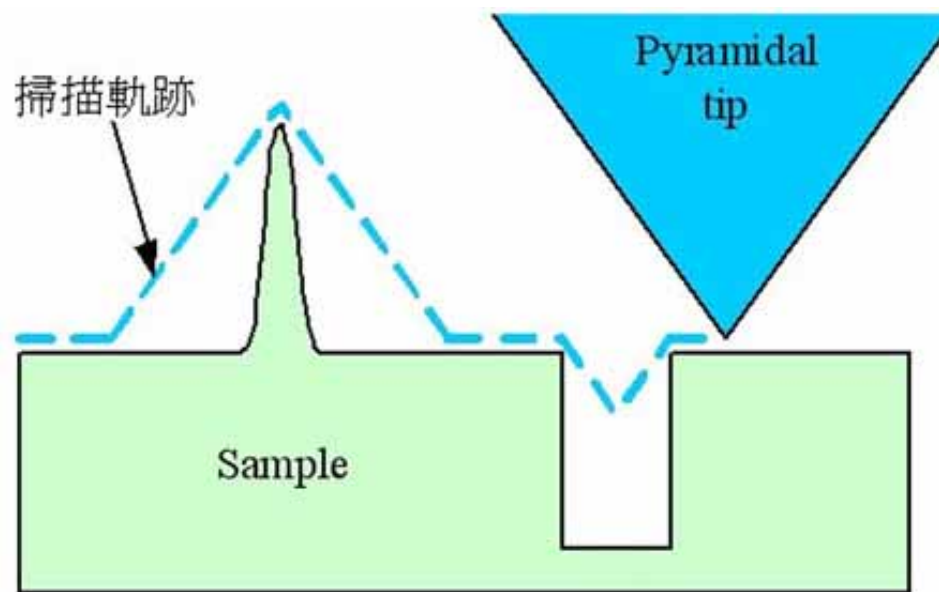
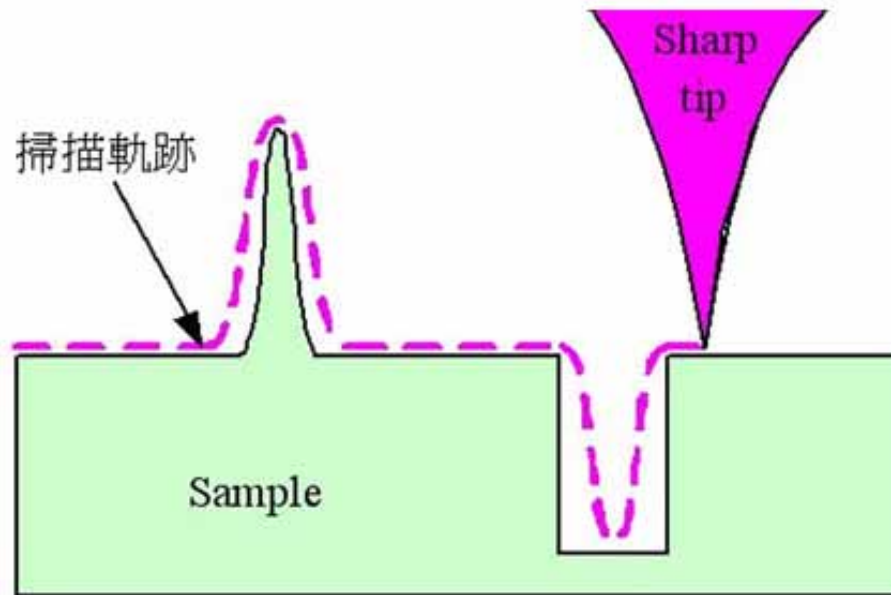


Vibration Isolation

Requirement in vibrational noise: $< 0.01\text{\AA}$ in z, and $< 0.1\text{\AA}$ in x and y.

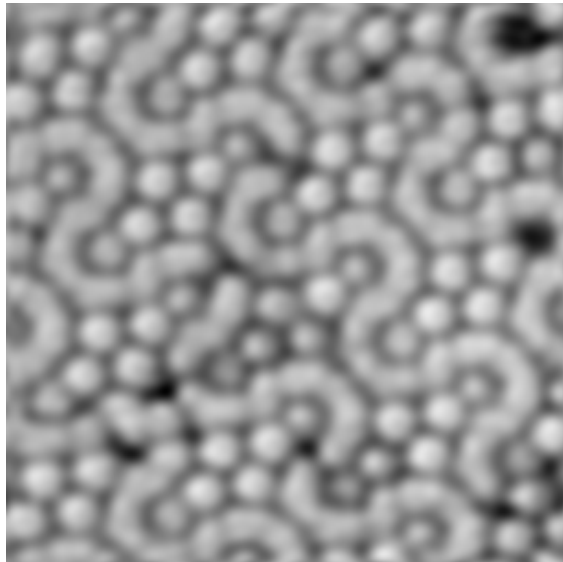
1. Building vibrations 5-100 Hz.
2. Acoustic noise 10-10k Hz
3. Table/chamber resonances 30-100 Hz
4. The design strategy is to reduce the resonance frequency of the vibration isolation system as low as possible, increase the resonance frequency of the tunneling assembly.
5. An effective way to damp the low-frequency vibrations is to suspend the microscope on long tension wires or levitate the table/chamber system on air legs. The performance can further be improved by increasing the mass of the system.
6. The microscope itself can be suspended with tension spring.
7. Vibrations in the medium-frequency can be damped by mounting the scanner assembly on a stack of materials of different elastic moduli or to suspend the scanner on tension springs with eddy current damping.

Tip Shape Effects

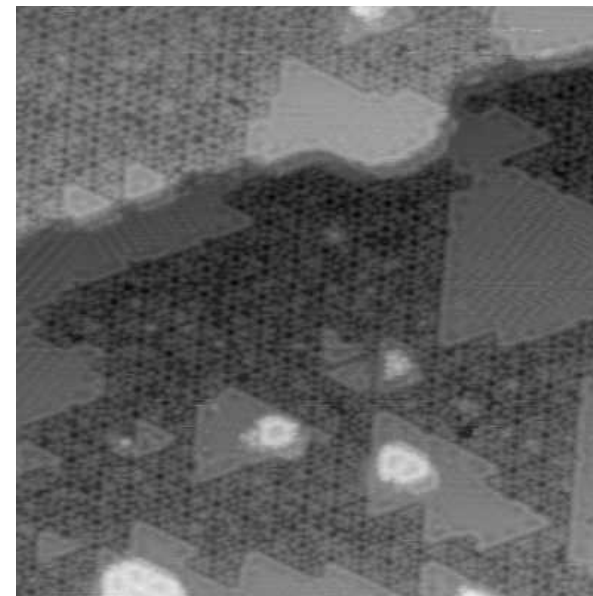
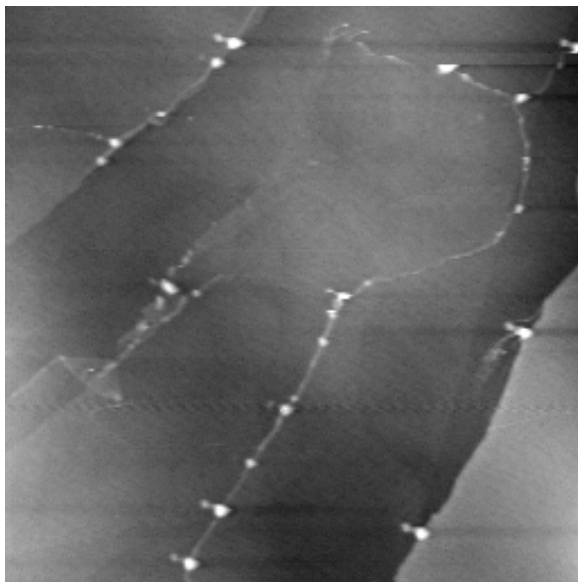
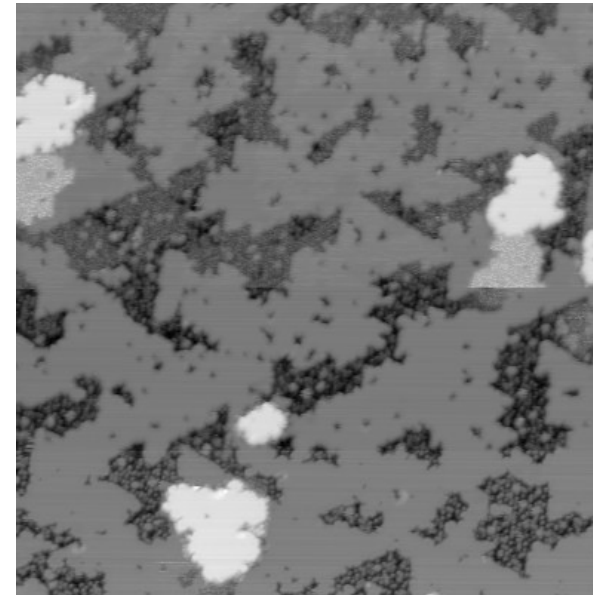


Artifacts of the Tip

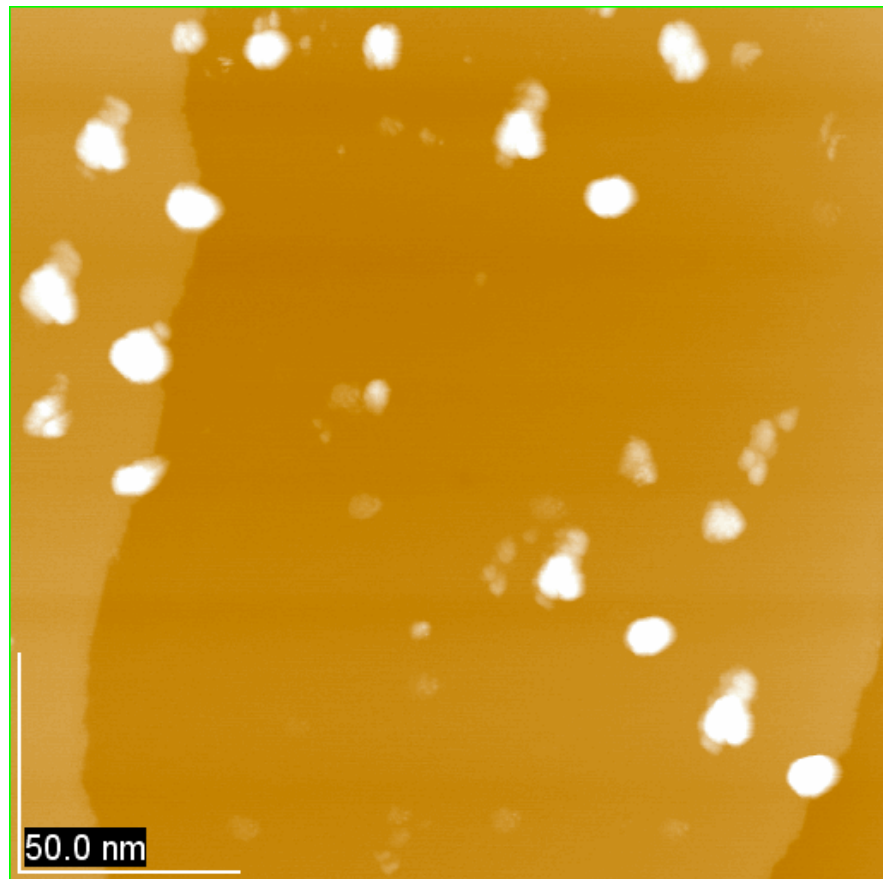
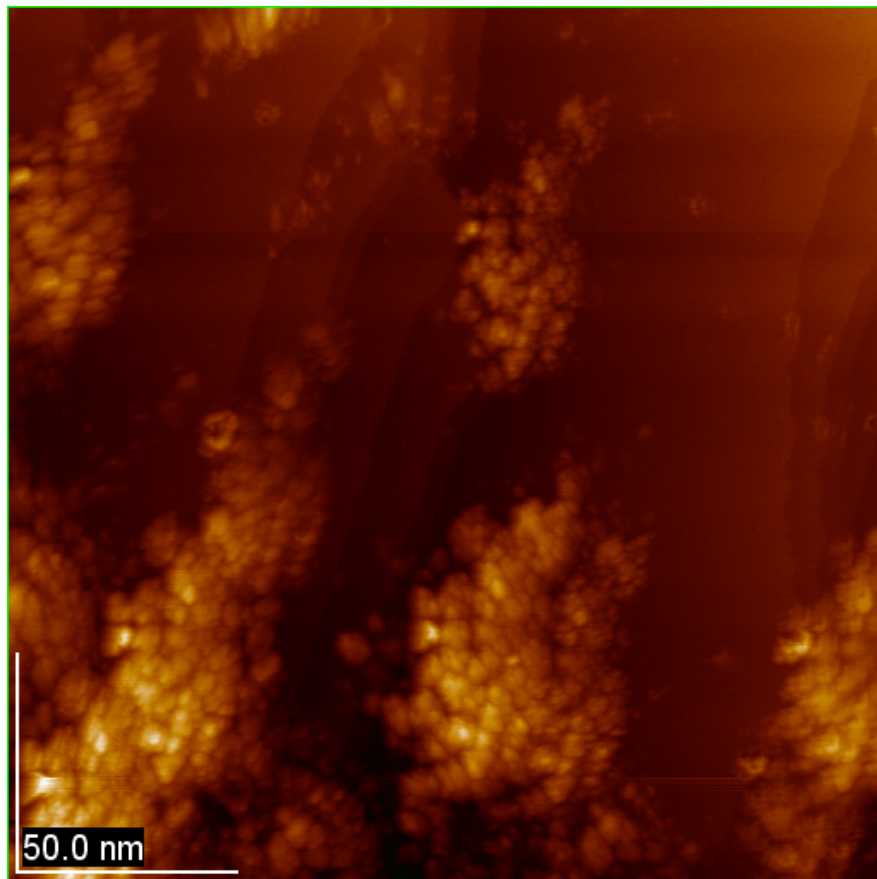
Si(111)-(7x7)



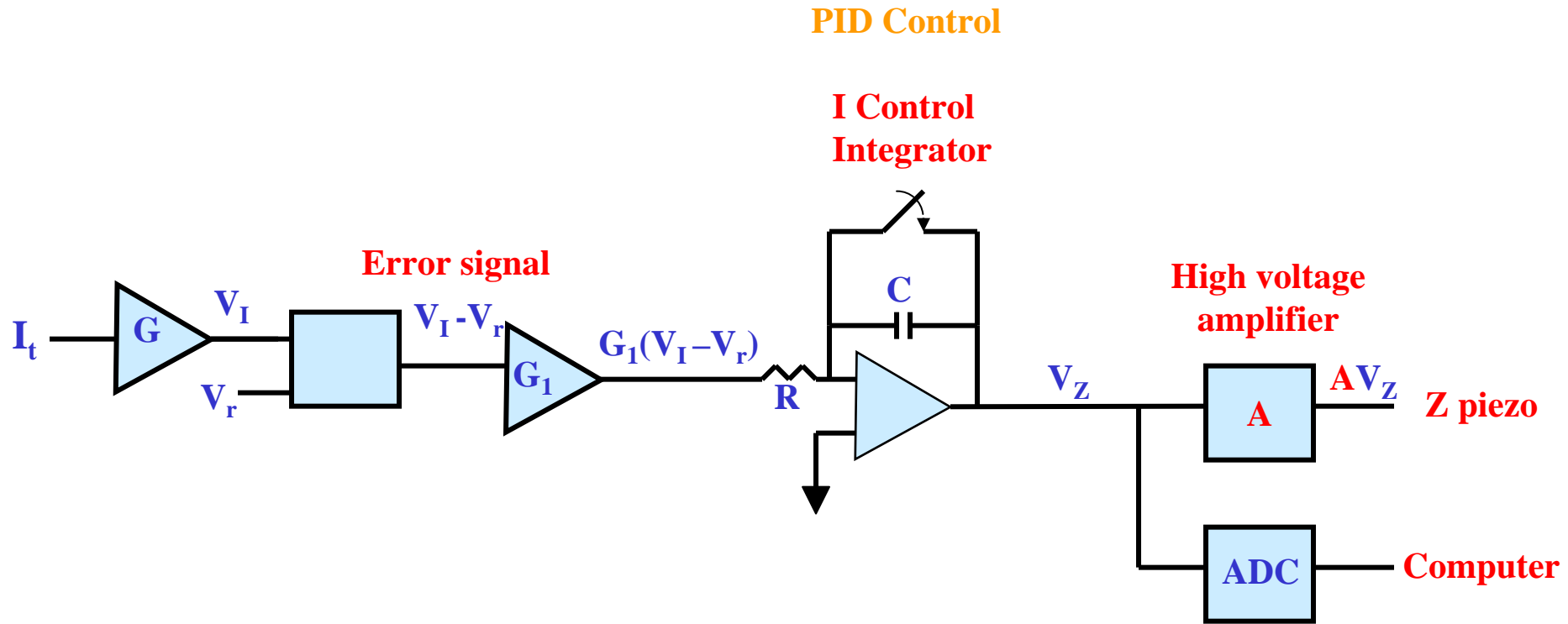
Pb/Si(111)



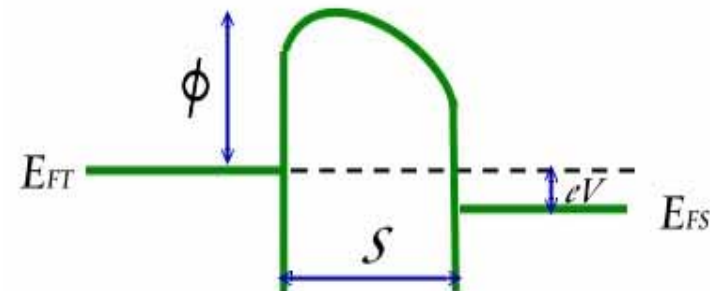
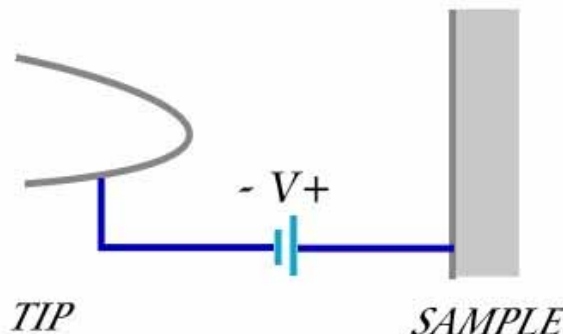
Artifacts of the Tip



STM Feedback Control



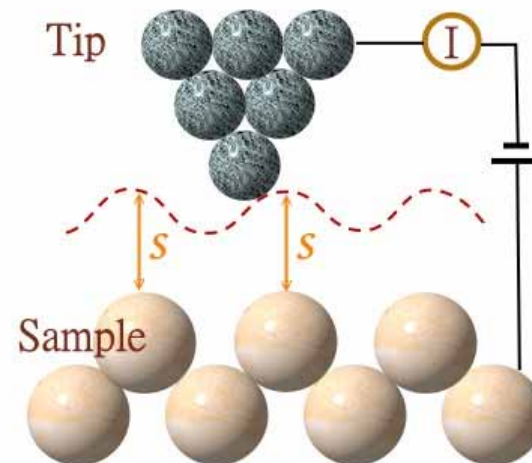
Theory of STM



From one-dimensional tunneling problem
tunneling current ($eV \ll \phi$)

$$I \propto \frac{V}{S} \exp\left(-A\phi^{\frac{1}{2}}S\right)$$

$$A = 1.025(eV)^{-\frac{1}{2}} A^0$$



Constant Current Mode

Tunneling Current

$$I_{T \rightarrow S} = \frac{2\pi e}{\hbar} \sum_{\mu\nu} f(E_\mu) [1 - f(E_\nu + eV)] |M_{\mu\nu}|^2 \delta(E_\mu - E_\nu - eV)$$

where $f(E)$ is Fermi function

E_μ is the energy of state μ , where μ and ν run over all the states of the tip and surface, respectively.

$M_{\mu\nu}$ is tunneling matrix element

$$M_{\mu\nu} \equiv \frac{\hbar^2}{2m} \int d\vec{s} (\psi_\mu^* \nabla \psi_\nu - \psi_\nu \nabla \psi_\mu^*)$$

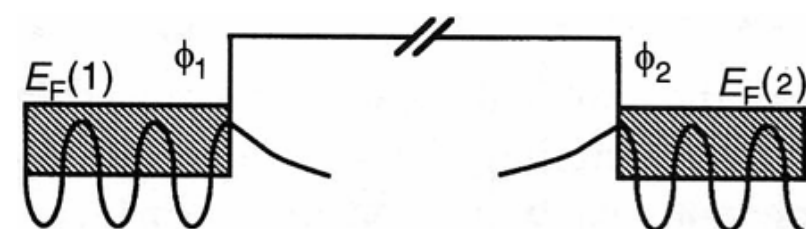
where ψ_μ is the wave function, and the integral is over any plane in the barrier region.

$$\begin{aligned} I &= I_{T \rightarrow S} - I_{S \rightarrow T} \\ &= A' \int_{-\infty}^{\infty} \rho_T(E) \rho_S(E + eV) |M(E)|^2 [f(E) - f(E + eV)] dE \end{aligned}$$

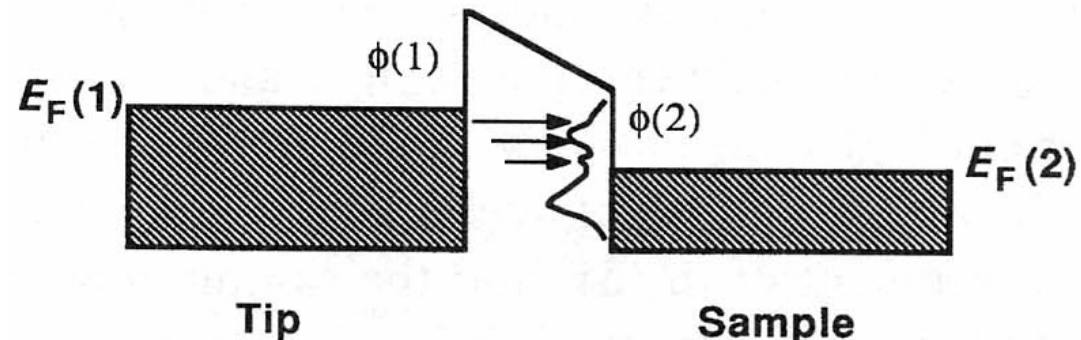
where ρ_S and ρ_T are the densities of states in the sample and the tip, respectively.

Electronic Structures at Surfaces

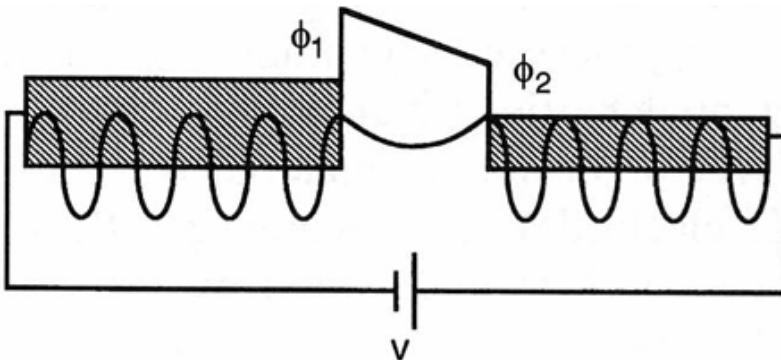
Not Tunneling



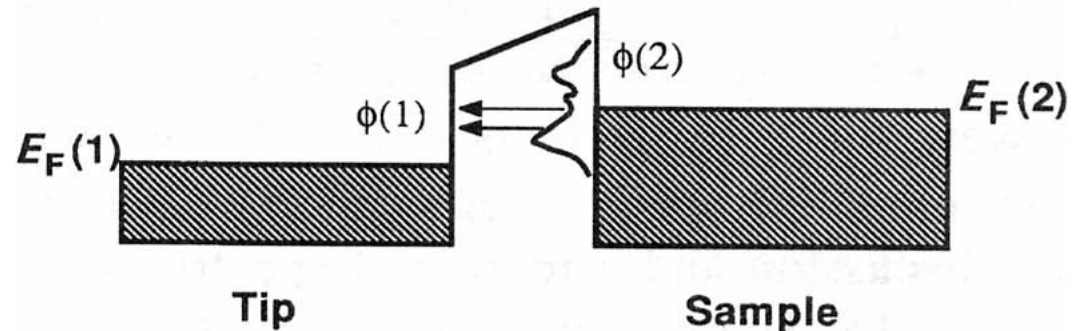
Empty-State Imaging



Tunneling



Filled-State Imaging



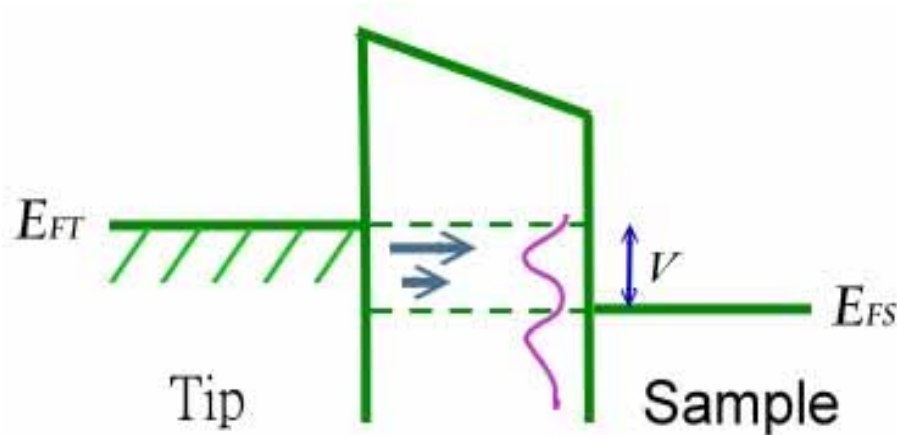
Tunneling Current

$$I \equiv A' \int_{-\infty}^{\infty} \rho_T(E) \rho_S(E + eV) |M(E)|^2 [f(E) - f(E + eV)] dE$$

Transmission probability of the electron

$$M(E) = \exp \left[-A \phi^{\frac{1}{2}} S \right]$$

Usually, we assume ρ_T is featureless (ie. $\rho_T \approx \text{const.}$), and the sample electronic states dominate the tunnel spectra.



However, the tips might have effect on the tunnel spectra, if

1. we have atomically sharp tips ,or
2. the tip has picked up a foreign atom.

Tunneling Barrier

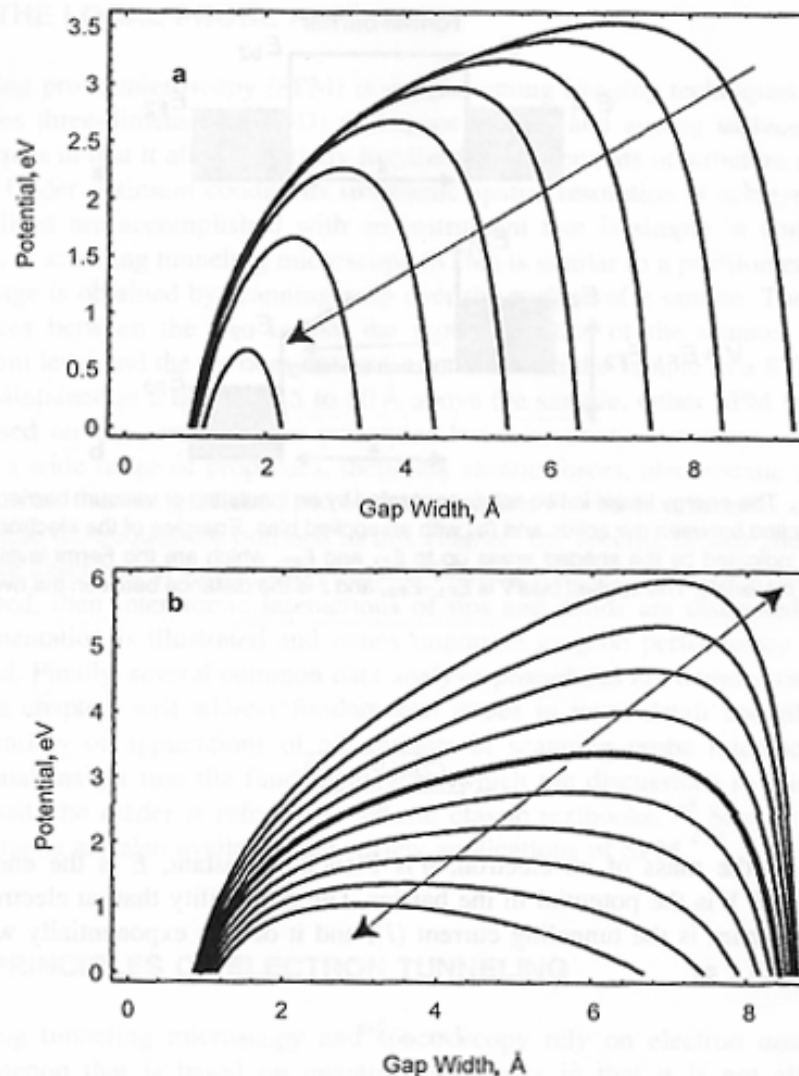


Figure 2.2. A more realistic depiction of the tunneling barrier, including the effect of image charge on the shape of the barrier. **a.** As the distance between the solids is decreased (arrow), the size and shape of the barrier change. **b.** The barrier also changes when a voltage is applied, the arrows show the response to opposite signs of bias.²⁵

Case I -----metals

In the low-voltage limit

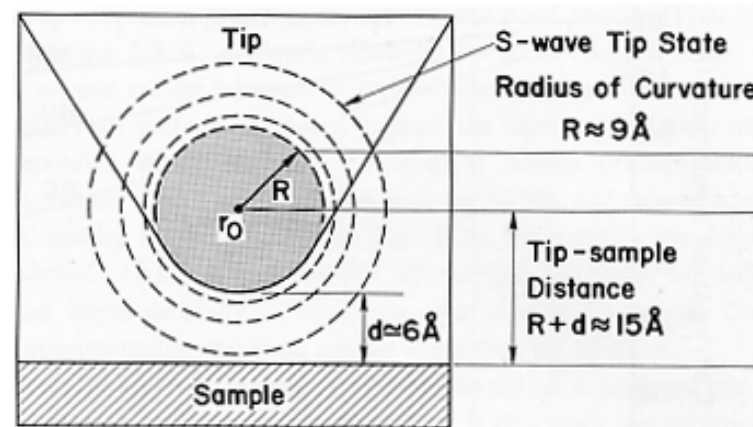
$$I \propto V \rho_s(\tilde{r}_t; E_F) \rho_t(E_F)$$

where $\rho_s(\tilde{r}_t; E_F)$ is the surface density of states of the sample at the center of the tip(\tilde{r}_t),

$$\rho_s(\tilde{r}; E) \equiv \sum_v |\psi_v(\tilde{r})|^2 \delta(E_v - E)$$

$\rho_t(E_F)$ is the density of states of the tip at the Fermi level and is often regarded as a constant.

The contour followed by the tip is a contour of constant Fermi-level density of states of the sample, measured at the center of curvature of the tip.



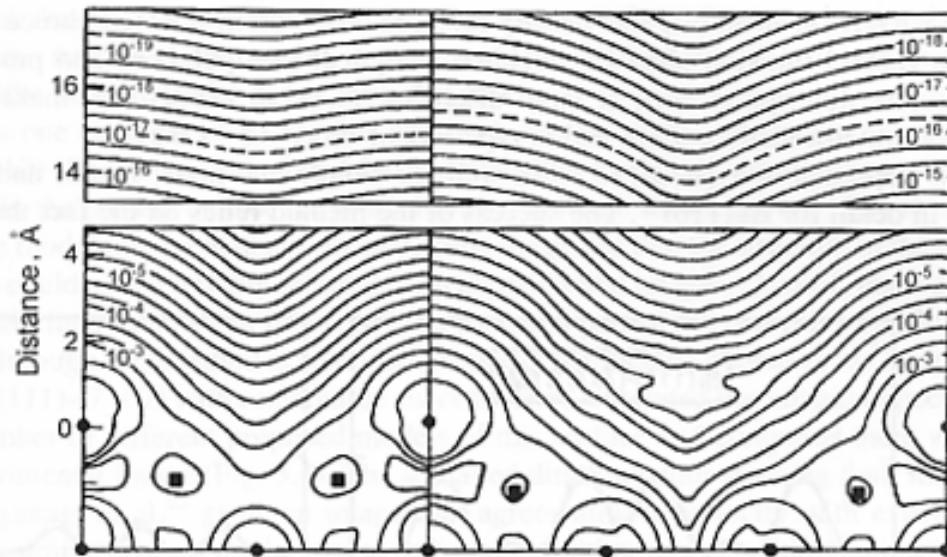
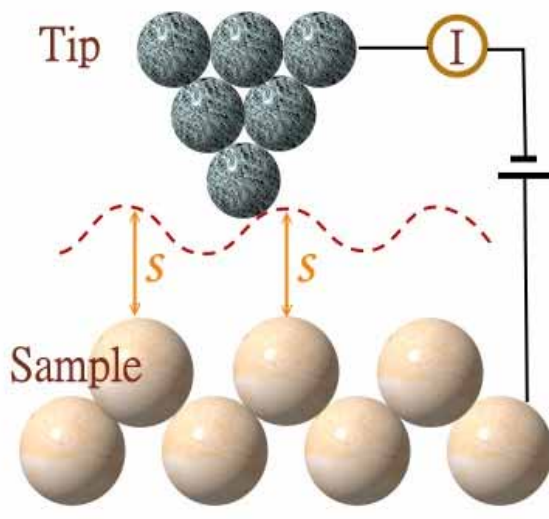
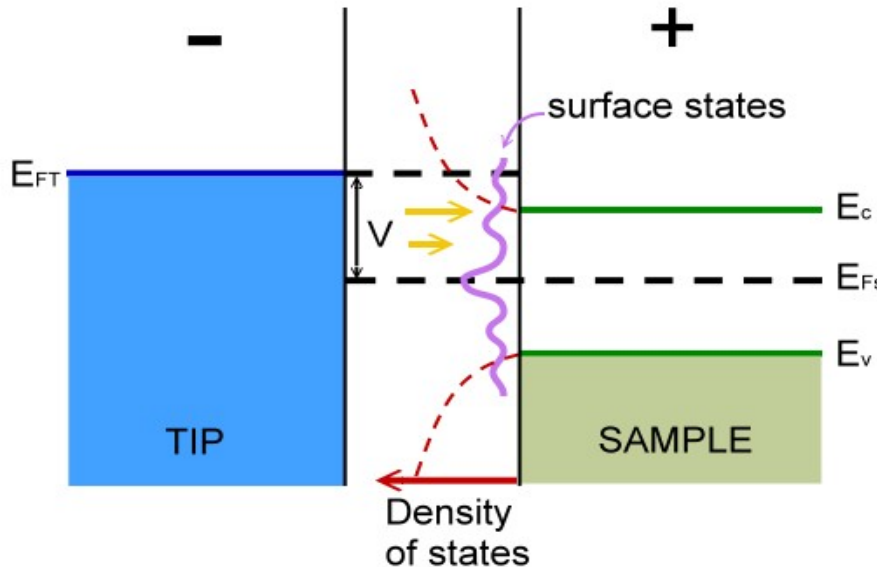


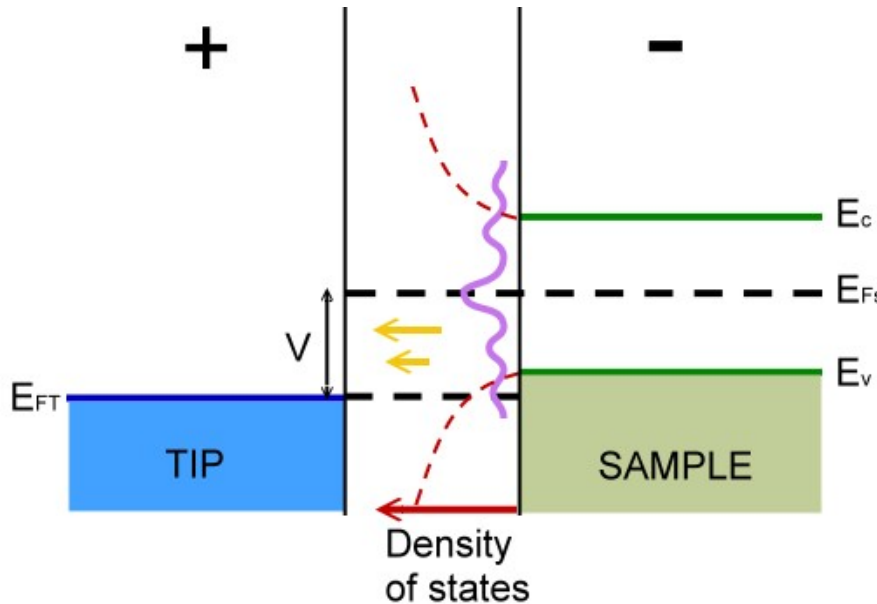
Figure 3.3. Calculated $\rho(r, E_F)$ for Au (110)-(2 \times 1) (left) and (3 \times 1) (right) surfaces. The figure shows the (110) plane through outermost atoms. Positions of nuclei are indicated by solid circles (in plane) and solid squares (out of plane). Contours of constant ρ are labeled in units of a.u.⁻³ eV⁻¹. Note the break in the vertical distance scale. Assuming a 0.9-nm tip radius in the s-wave tip model, the center of curvature of the tip is calculated to follow the dashed line. (Reprinted with

Example -----Semiconductor

1.Tip-negative



2.Tip -positive



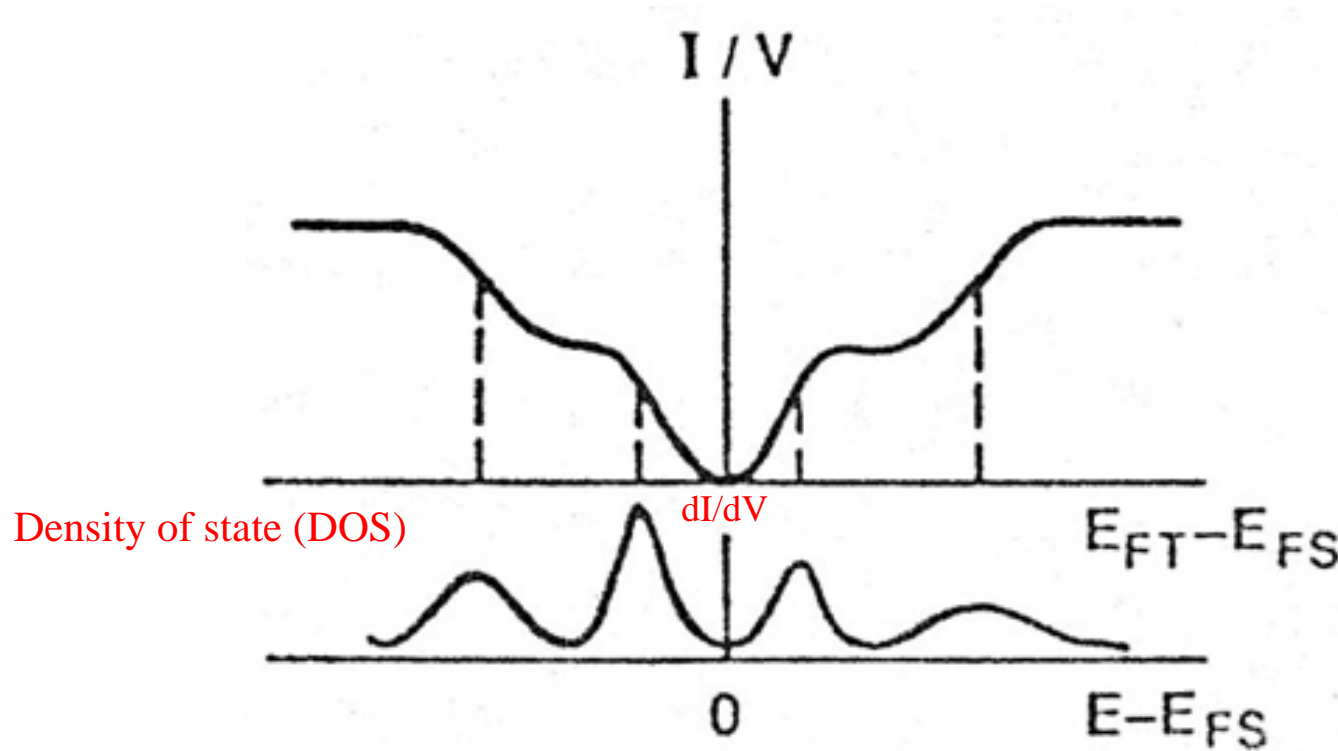
Science 234, 304 (1986).

Scanning Tunneling Spectroscopy

STM provides atomic-scale topographic information, and atomic-scale electronic information. However, the mixture of geometric and electronic structure information often complicates interpretation of observed feature.

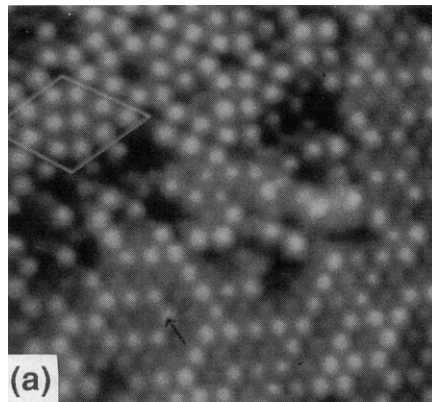
Several spectroscopic modes:

1. Voltage-dependent STM imaging.
2. Tunneling I-V curves, dI/dV .

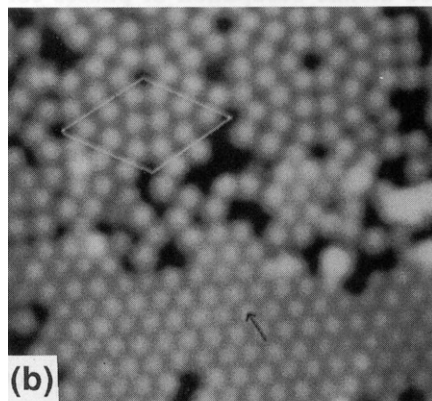


Pb/Si(111)

+1.8 V

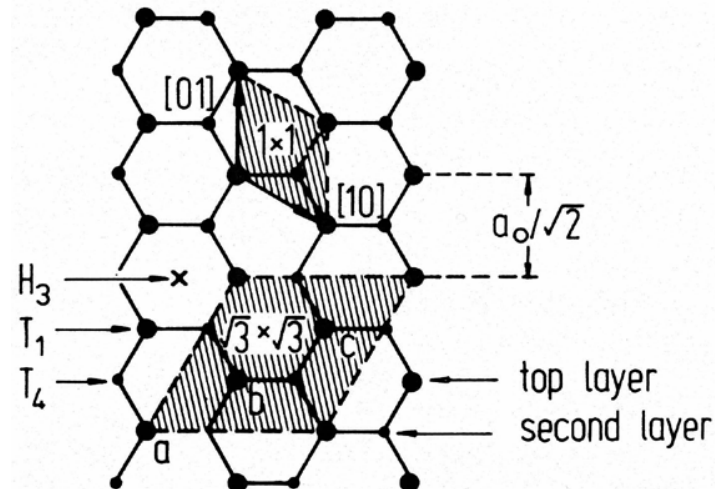
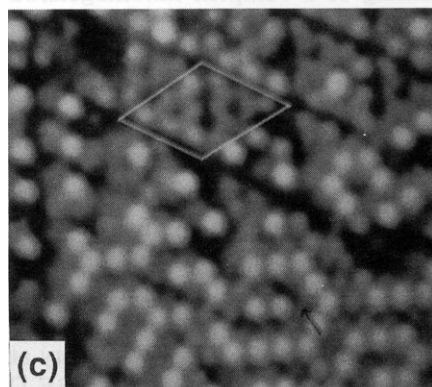


+2.4 V



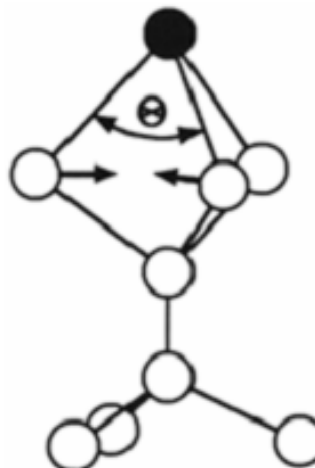
-1.8 V

Filled-state



T_4 site

$\sqrt{3} \times \sqrt{3}$

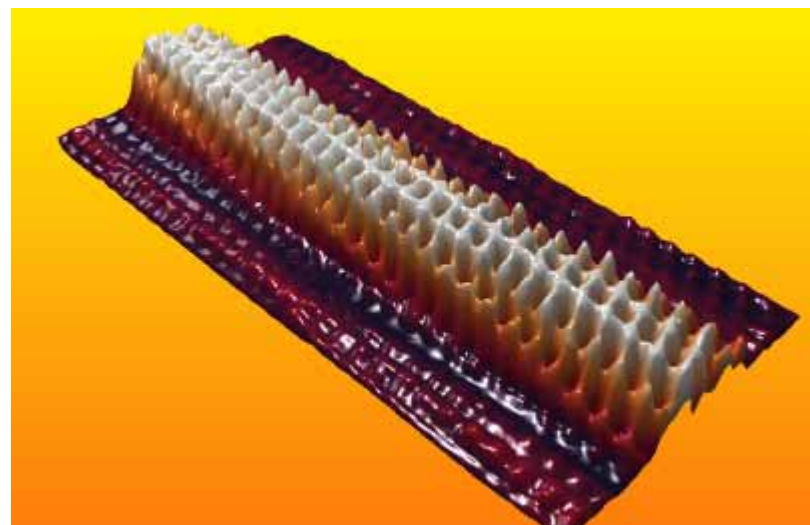
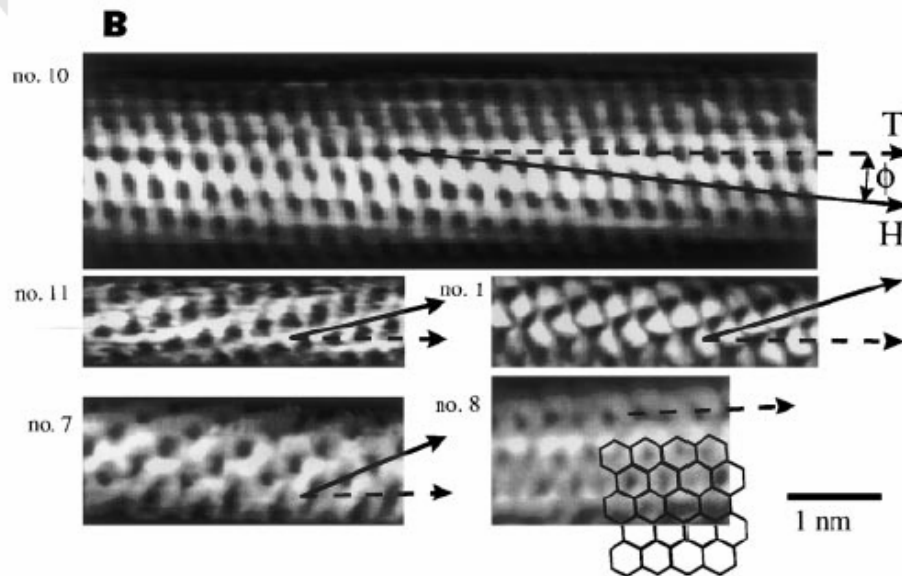
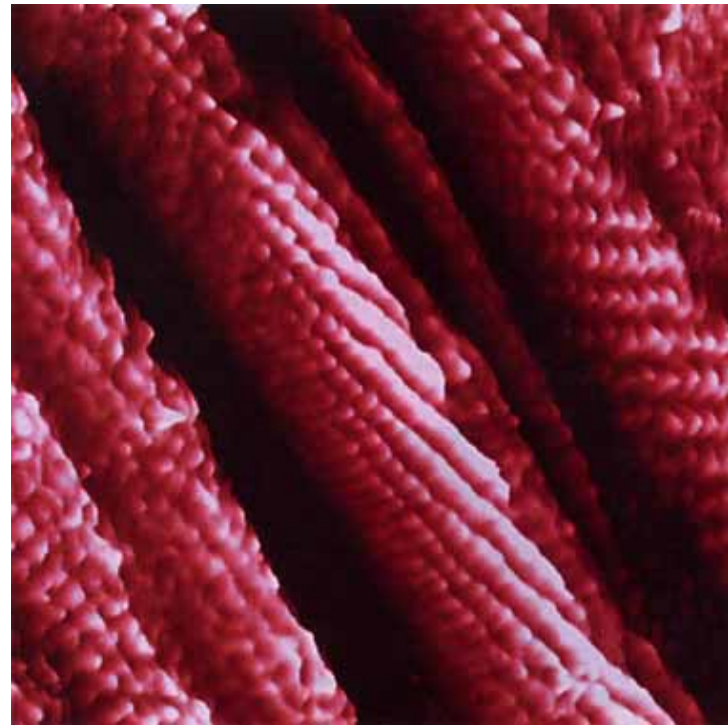
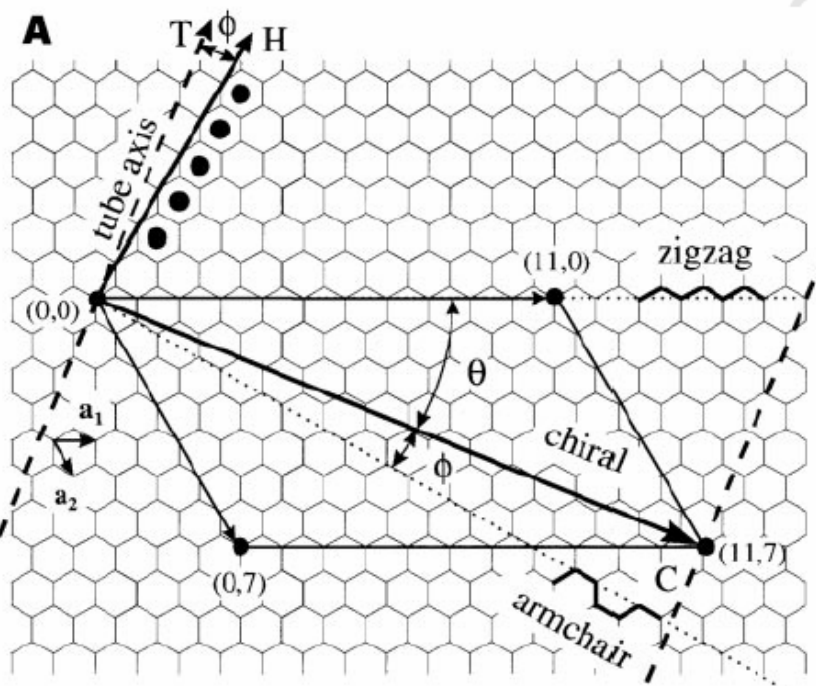


Scanning Tunneling Spectroscopy (STS)

$$\frac{dI}{dV} = \rho_s(r, eV) \rho_t(r, 0) T(eV, eV, r) + \int_0^{eV} \rho_s(r, E) \rho_t(r, E - eV) \frac{dT(E, eV, r)}{dV} dE$$

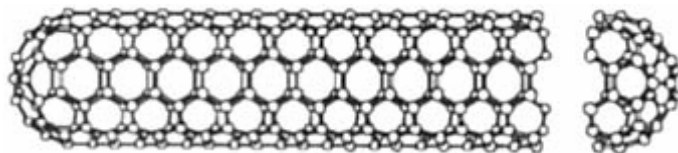
1. The tunneling transmission probability T is a smooth, monotonically increasing function of V . Thus dT/dV contributes a smooth background. Therefore, structure in dI/dV can usually be assigned to changes in the state density.
2. Extracting quantitative information about the sample density of states is difficult because the density of states of the tip and the tunneling transmission probability T are almost unknown.
3. Normalization of dI/dV by I/V was proposed to minimize the distance dependence of the tunneling probability (or the voltage dependence of the tunneling barrier).

Single-Wall Carbon Nanotubes

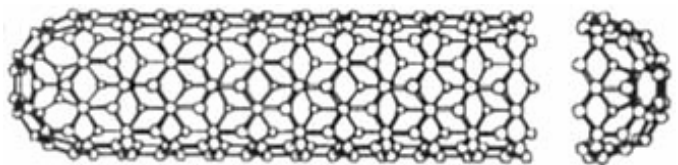


Electronic Structure of Single-Wall Nanotubes

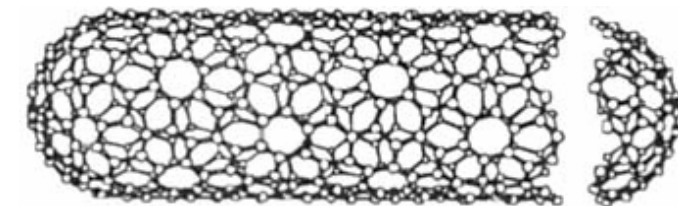
1. Armchair nanotubes $(n,n) \rightarrow$ metallic



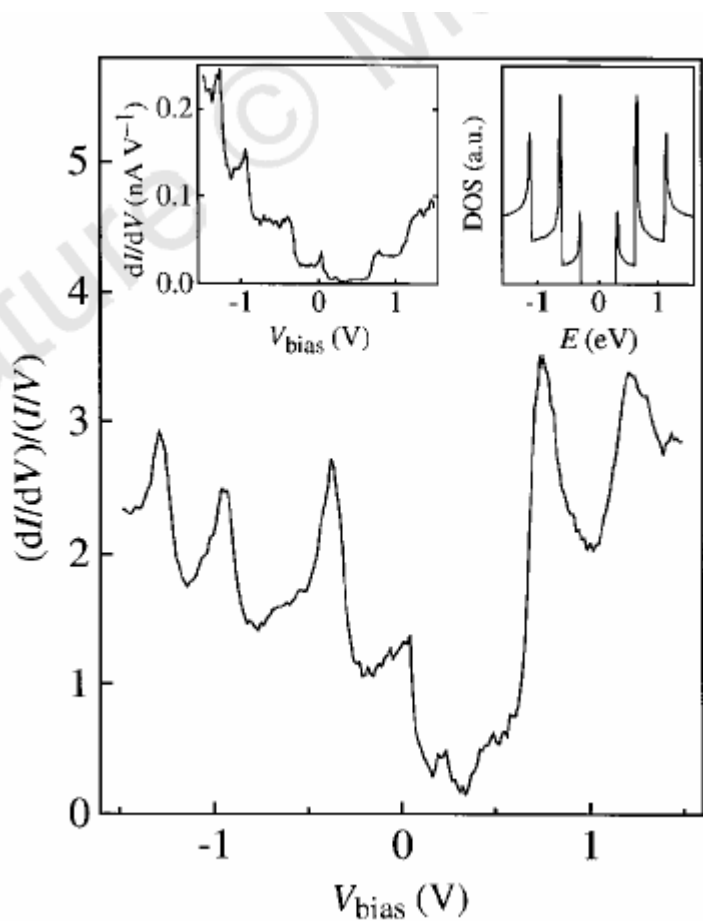
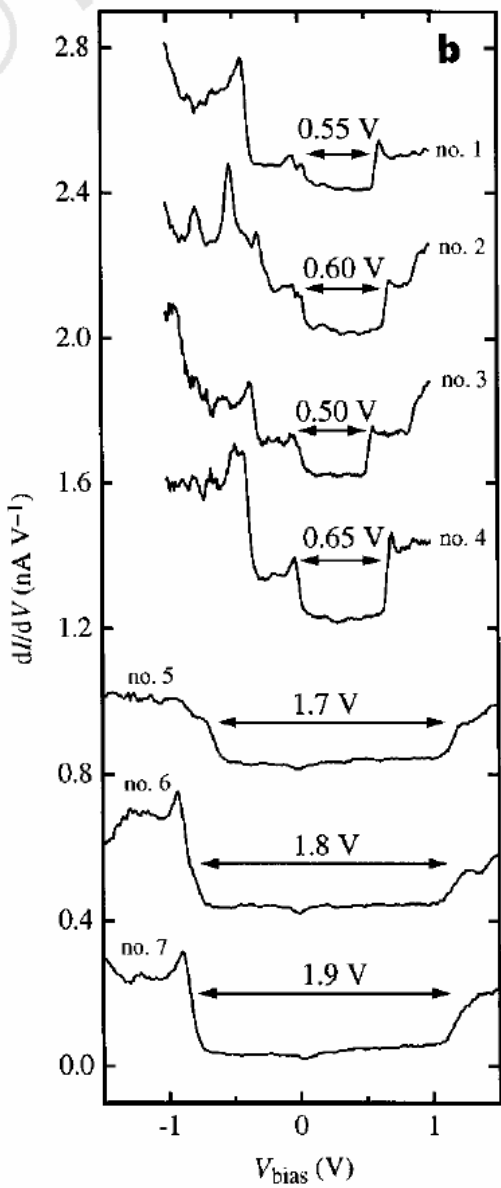
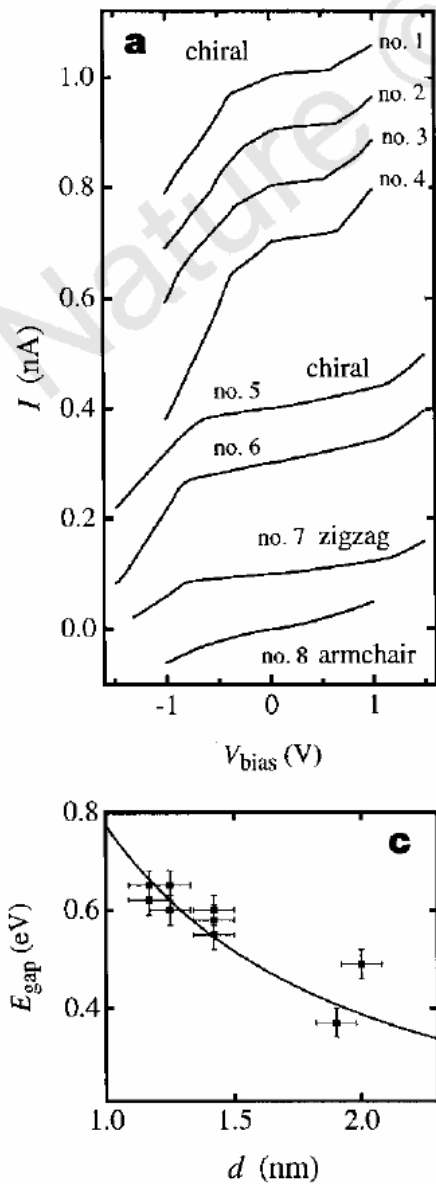
2. Zigzag nanotubes $(n,0) \rightarrow$ metallic, when $n=3q$
 \rightarrow semiconducting, otherwise



3. Chiral nanotubes $(n,m) \rightarrow$ metallic, when $m=n+3q$

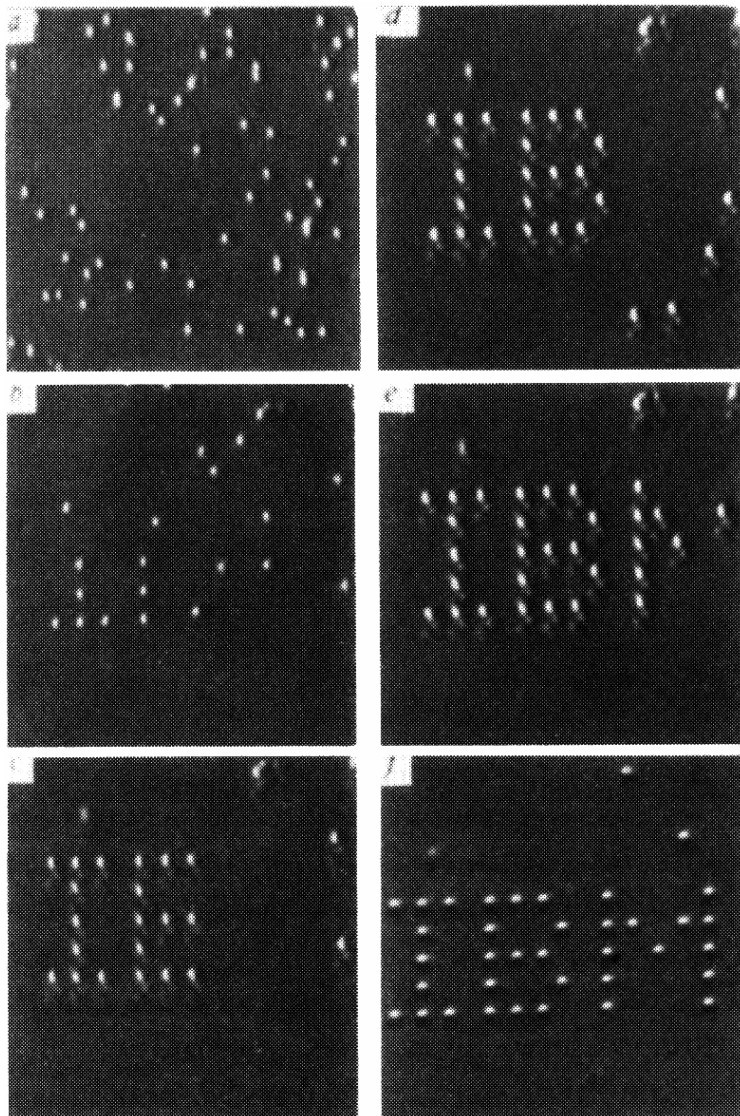


Electronic Structure of Single-wall Nanotubes

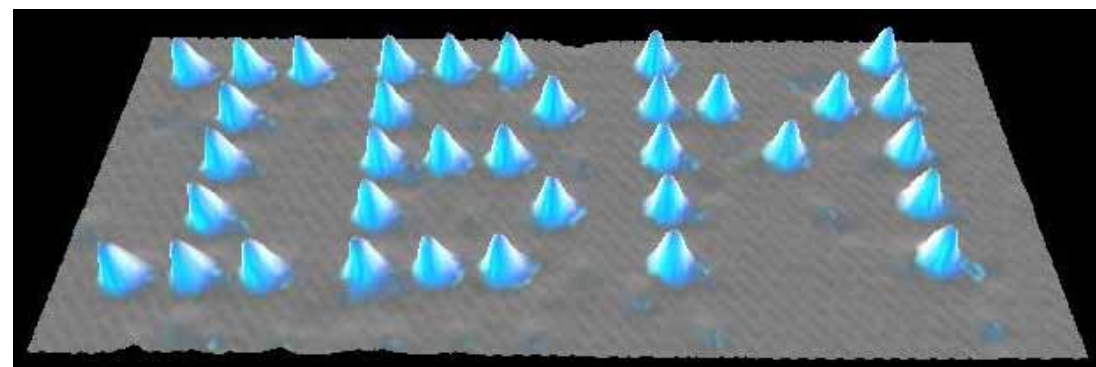


Nature 391, 59 (1998).

Atomic Manipulation with STM



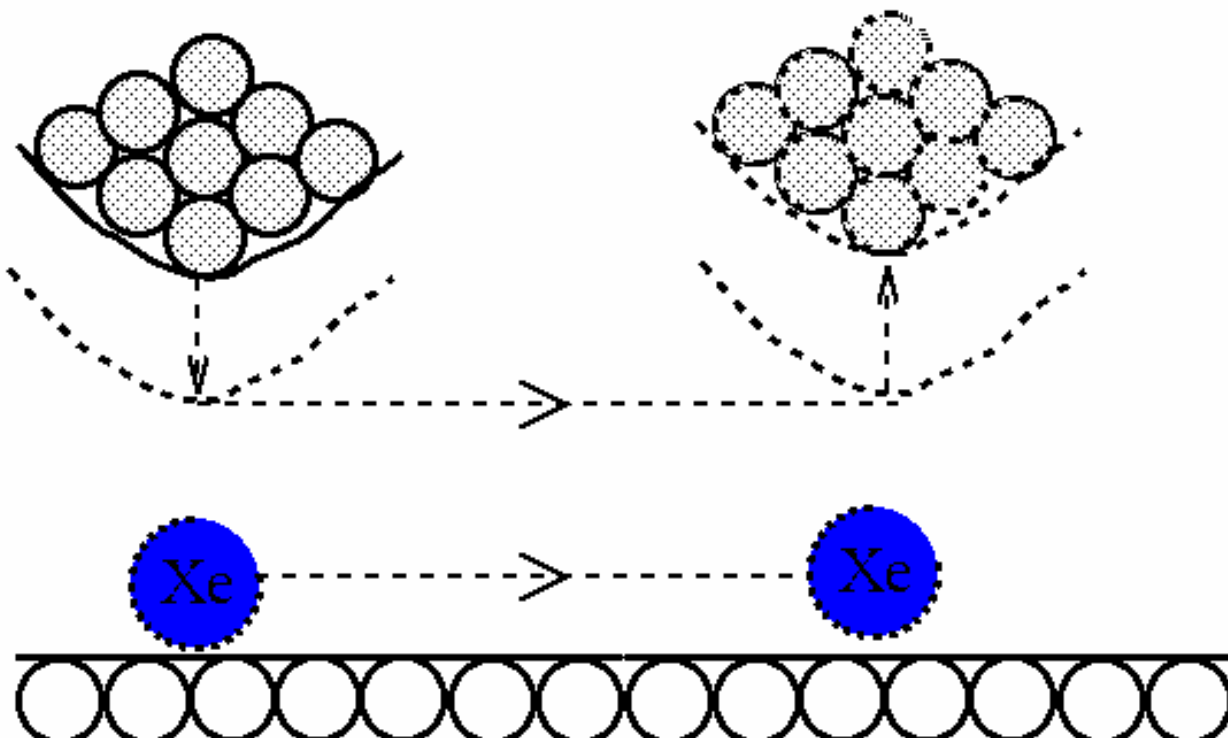
Nature 344, 524 (1990)



Xe on a Ni surface

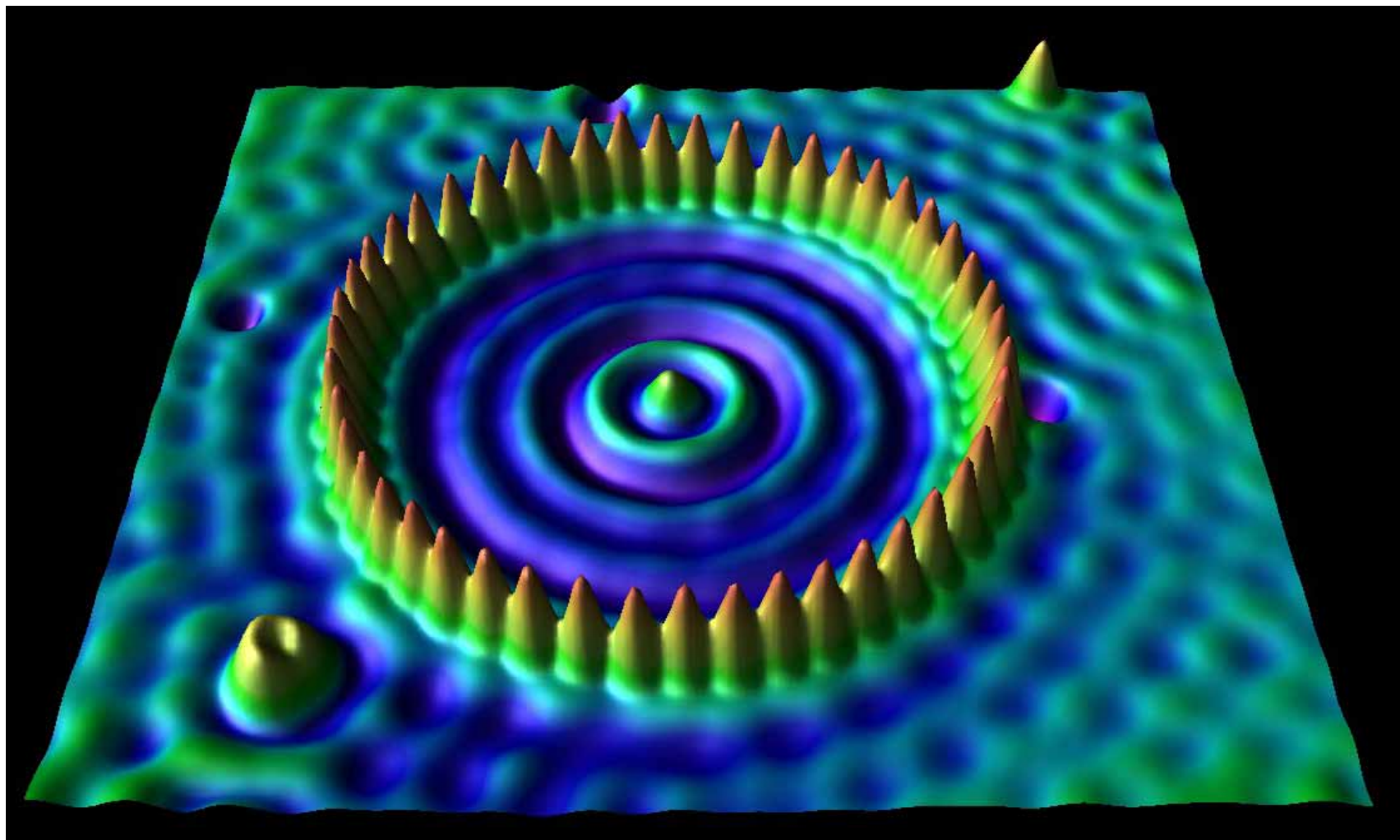
Positioning Atoms with an STM

D.M. Eigler & E.K. Schweizer Nature 344 524 (1990)



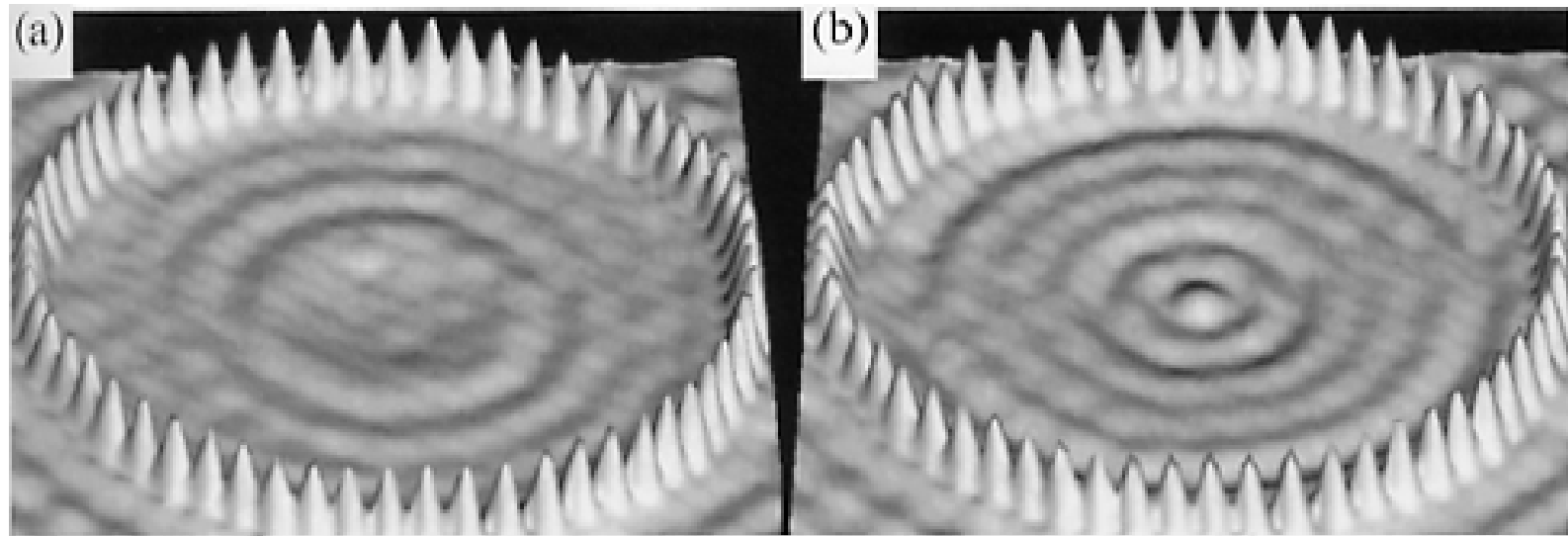
The STM tip is brought down near the atom, until the attraction is enough to hold it as the atom is dragged across the surface to a new position.

Quantum Correl



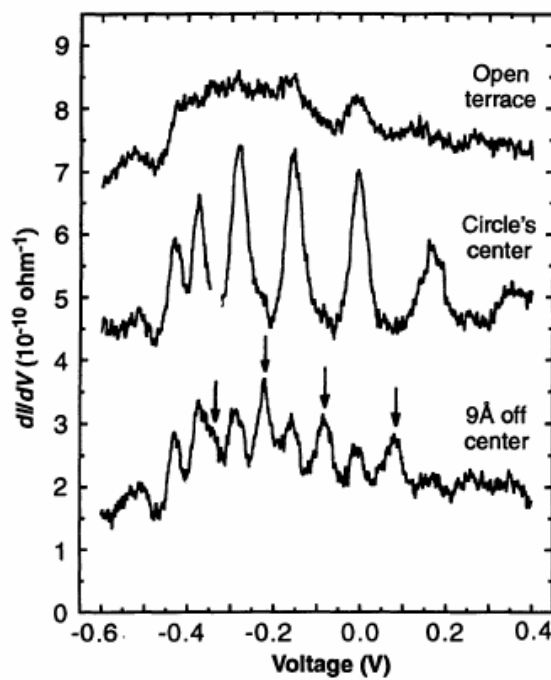
M.F. Crommie *et al.*, Science 262, 218 (1993).

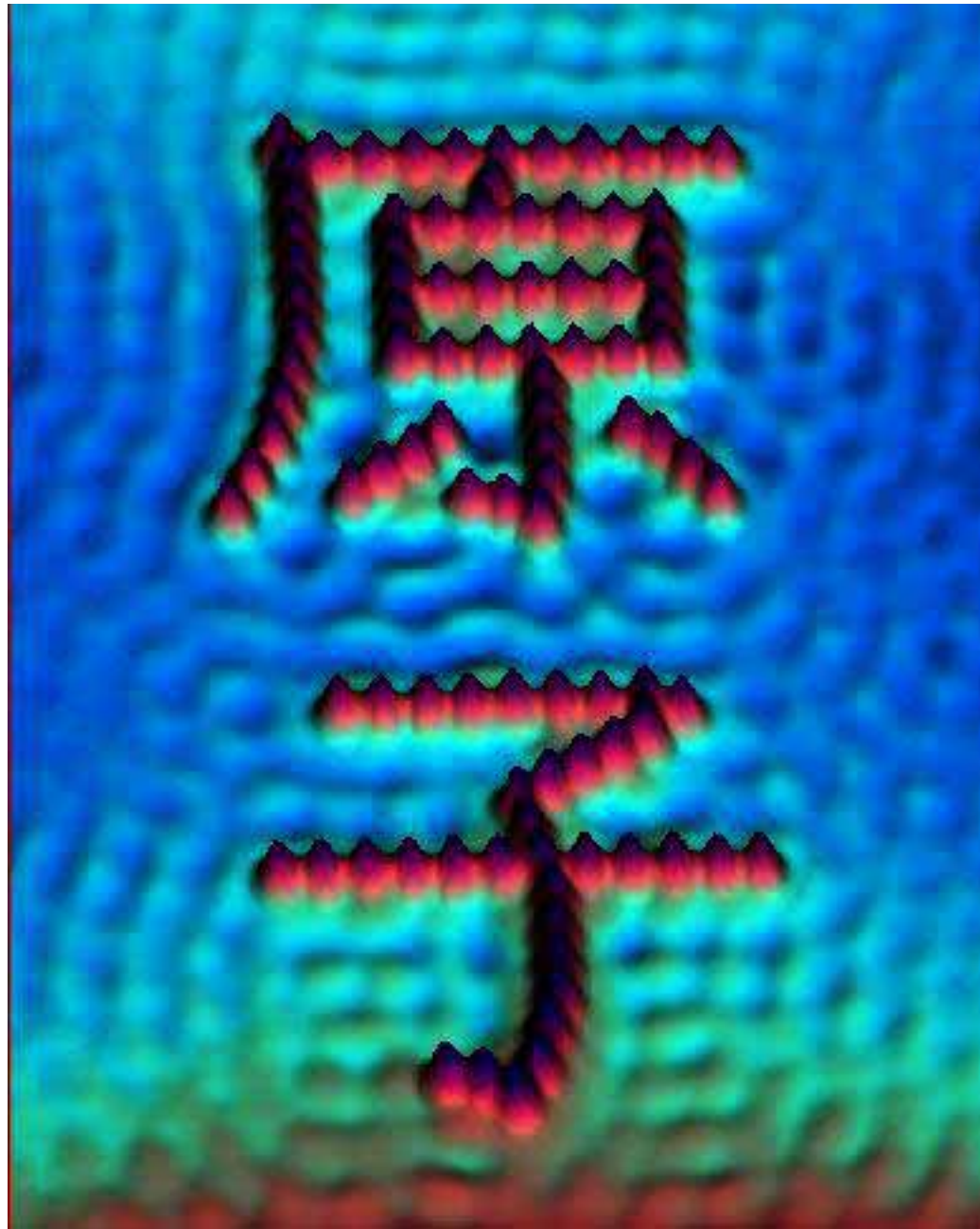
Energy-Dependent Friedel Oscillations



$V_t = + 10 \text{ mV}$

$V_t = - 10 \text{ mV}$





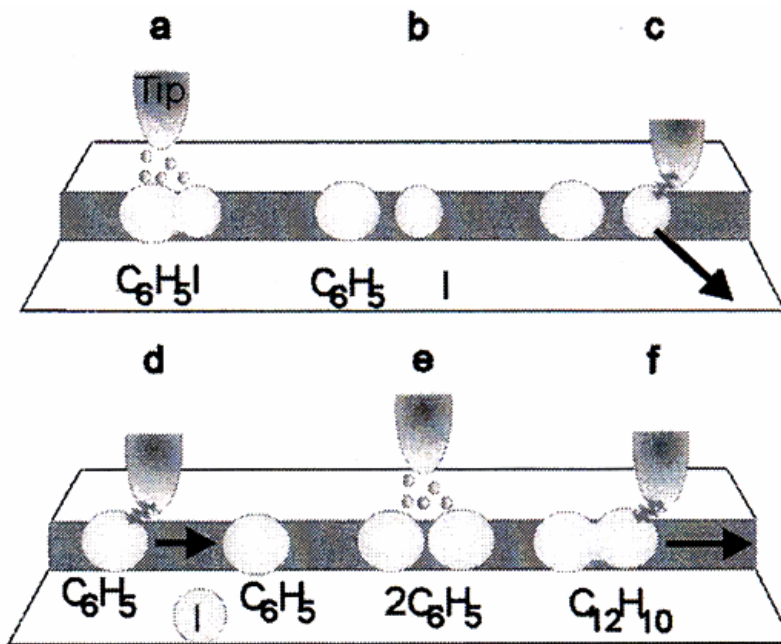
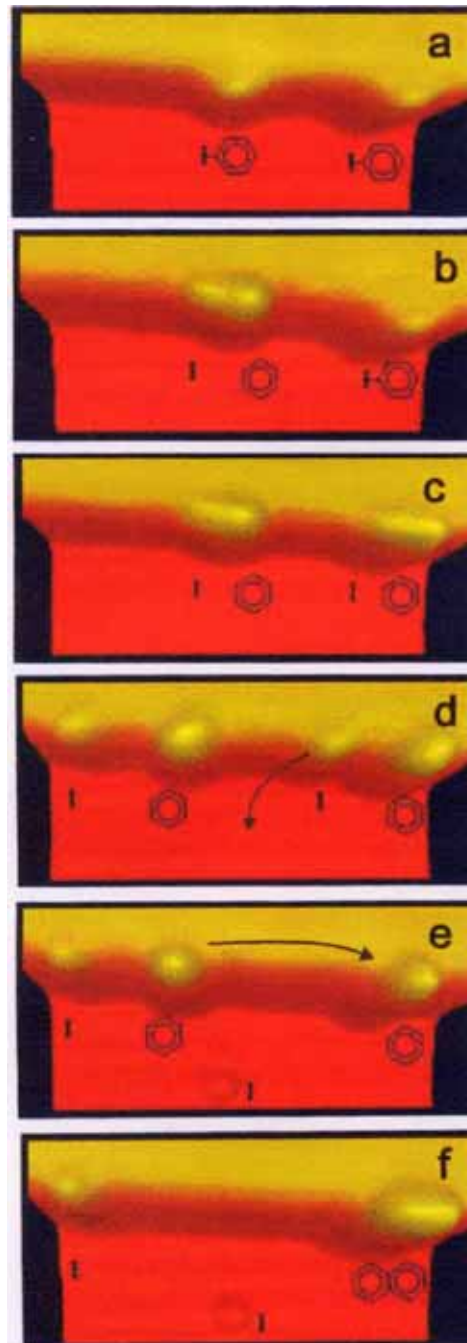
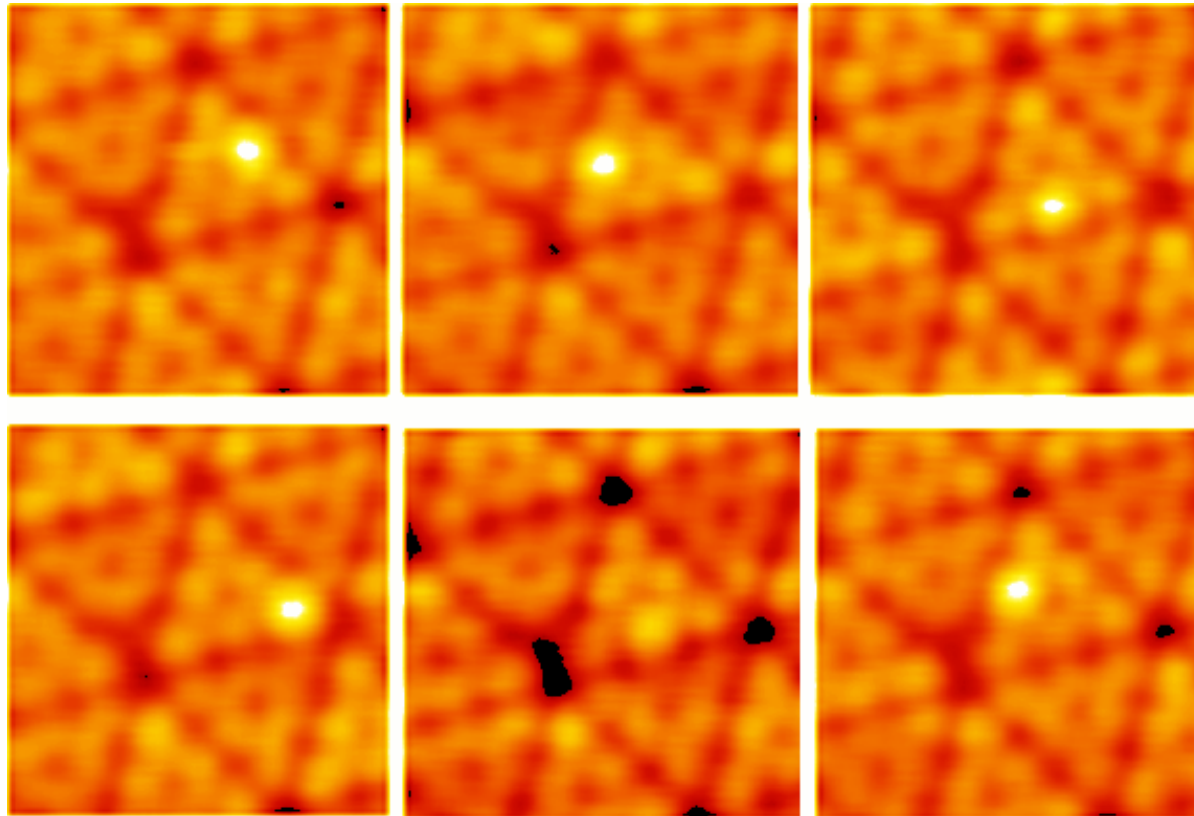


FIG. 1. Schematic illustration of the STM tip-induced synthesis steps of a biphenyl molecule. (a),(b) Electron-induced selective abstraction of iodine from iodobenzene. (c) Removal of the iodine atom to a terrace site by lateral manipulation. (d) Bringing together two phenyls by lateral manipulation. (e) Electron-induced chemical association of the phenyl couple to biphenyl. (f) Pulling the synthesized molecule by its front end with the STM tip to confirm the association.



Site Hopping of O₂ on Si(111)-7x7



O₂ molecule starts to hop between neighboring adatom sites at temperature about 300°C.

1. I.-S. Hwang, R.-L. Lo, and T.T. Tsong, Physical Review Letters **78**, 4797 (1997).
2. I.-S. Hwang, R.-L. Lo, and T.T. Tsong, Surface Science **399**, 173 (1998).

Arrhenius Plot for the Hopping from a Center Site to an Adjacent Center Site

Jumping rate
 $R = N/t = R_o \exp(-E_a/k_B T)$
Arrhenius relation

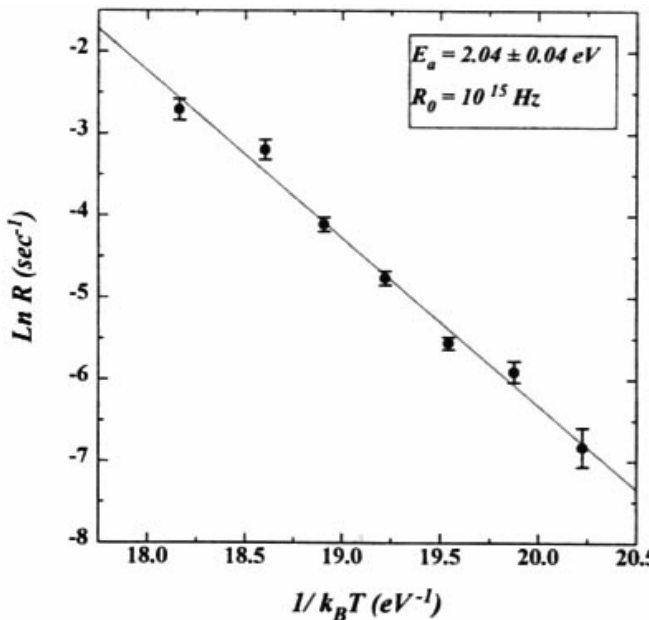
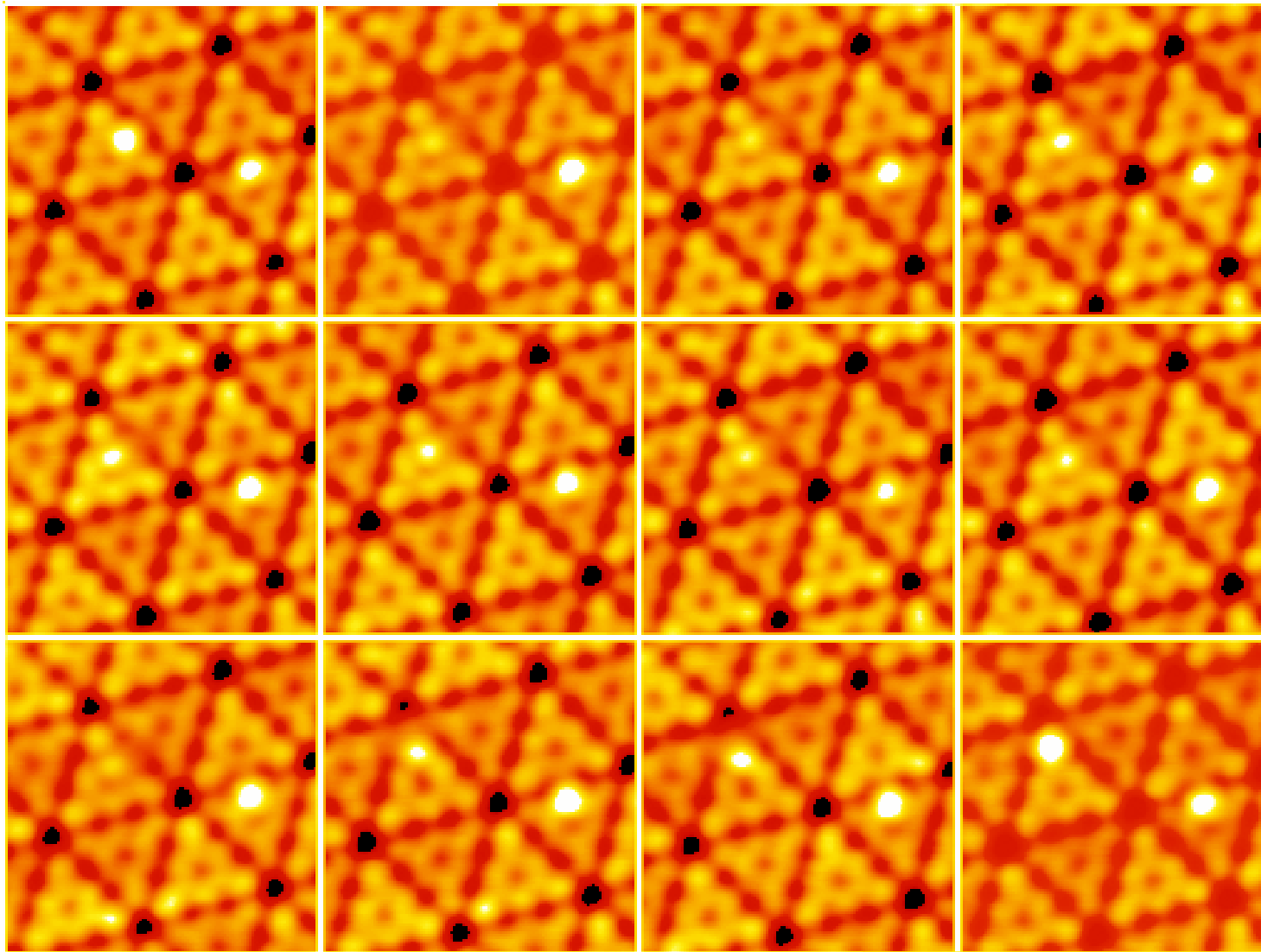


TABLE I. Parameters for site hopping of O_2 on Si(111)-(7 \times 7).

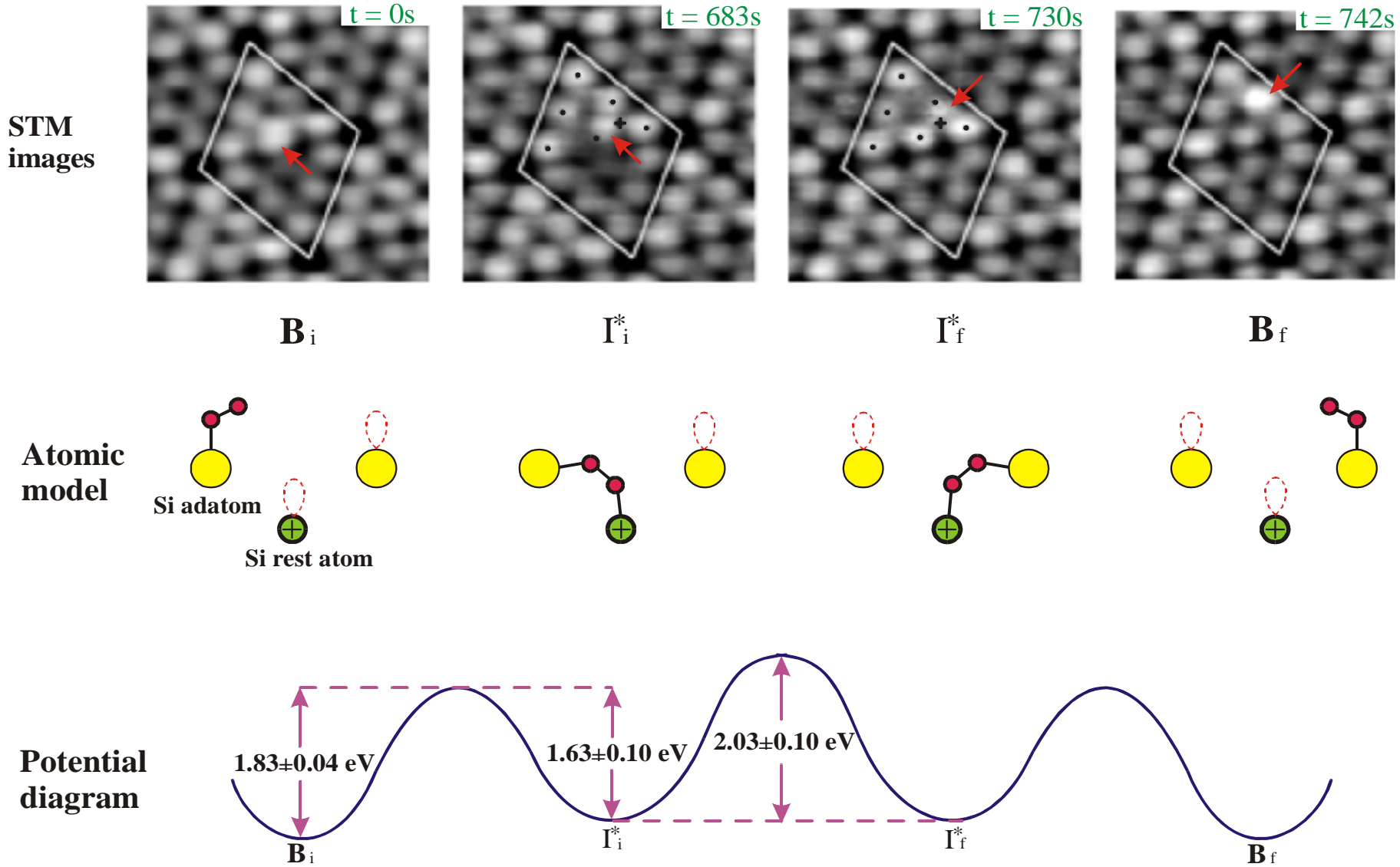
Hopping	Activation energy	Frequency factors
FE to FE	$2.04 \pm 0.04 \text{ eV}$	$10^{15.0} \text{ s}^{-1}$
FE to FO	$2.29 \pm 0.06 \text{ eV}$	$10^{16.2} \text{ s}^{-1}$
FO to FE	$2.13 \pm 0.11 \text{ eV}$	$10^{15.6} \text{ s}^{-1}$
UE to UE	$2.16 \pm 0.04 \text{ eV}$	$10^{15.9} \text{ s}^{-1}$
UE to UO	$2.01 \pm 0.10 \text{ eV}$	$10^{14.6} \text{ s}^{-1}$
UO to UE	$1.96 \pm 0.13 \text{ eV}$	$10^{14.1} \text{ s}^{-1}$

Continuous-Time Scanning

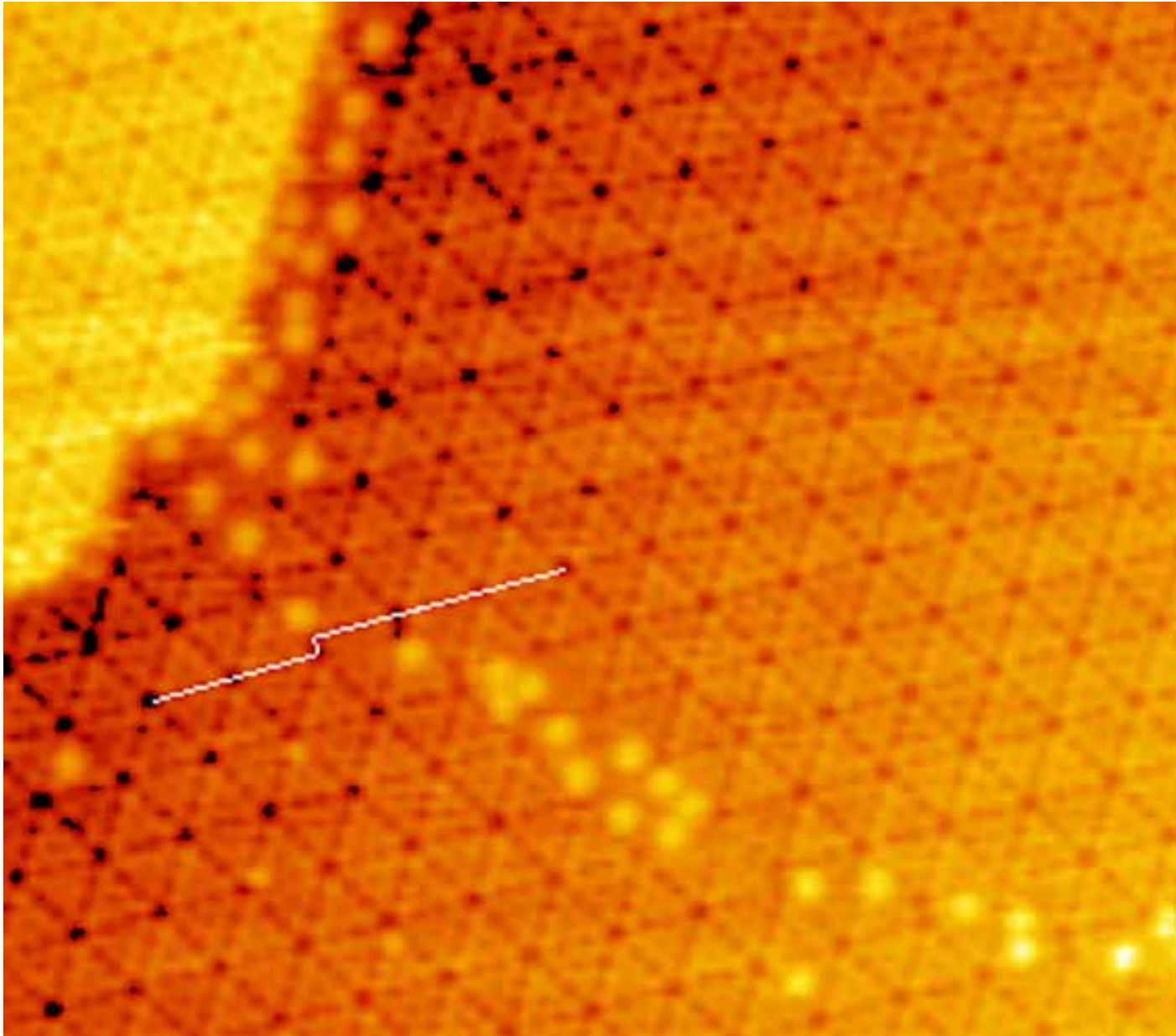


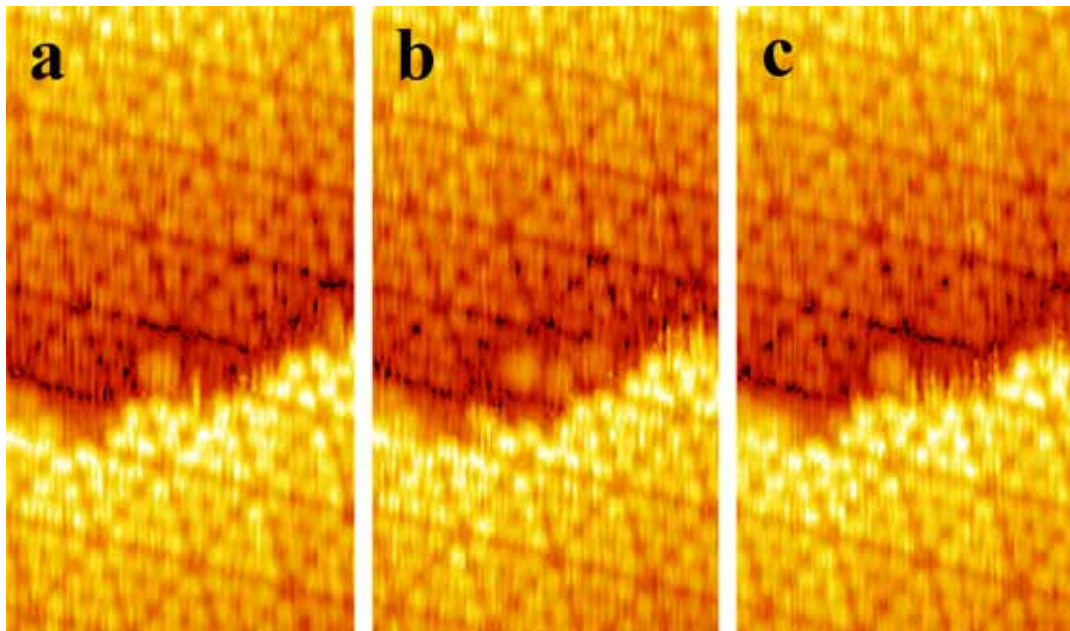
300 C, 1V(filled-state), 0.2 nA, 2.4 sec per image

Site Hopping of O₂ Molecule on Si(111)-(7x7)



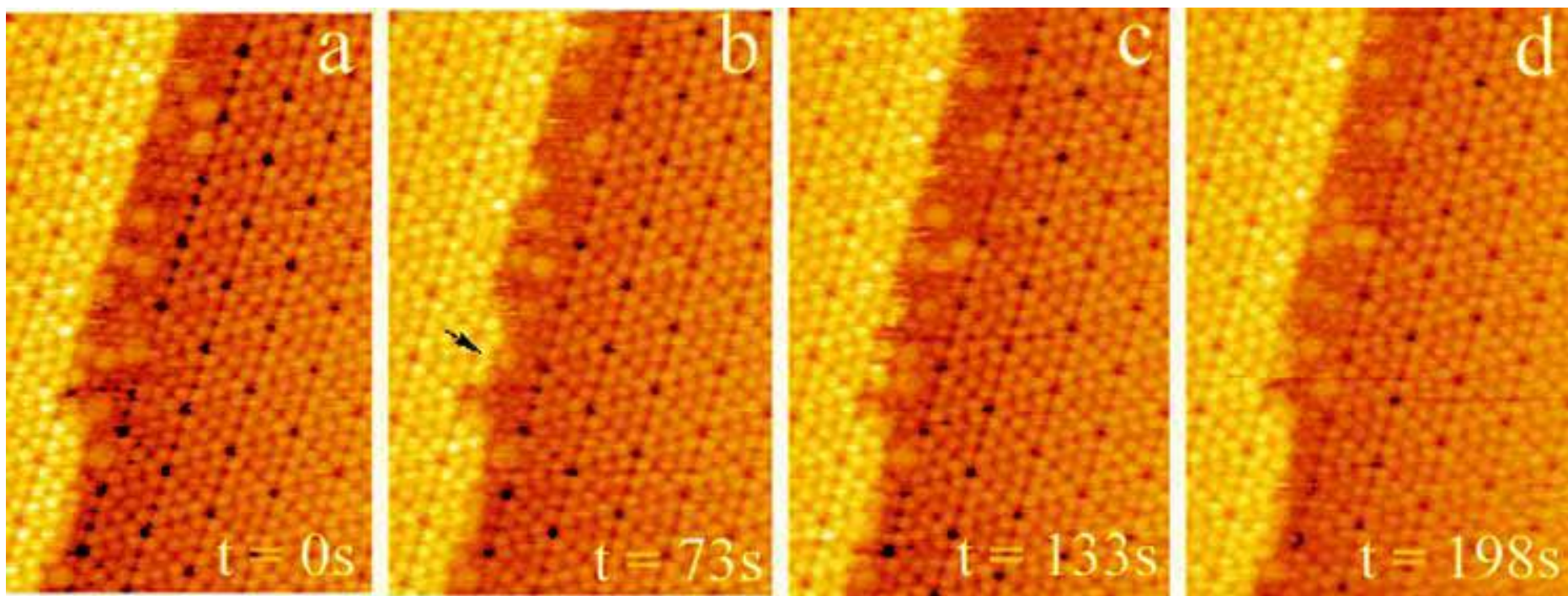
Silicon Magic Clusters on Si(111) Surfaces



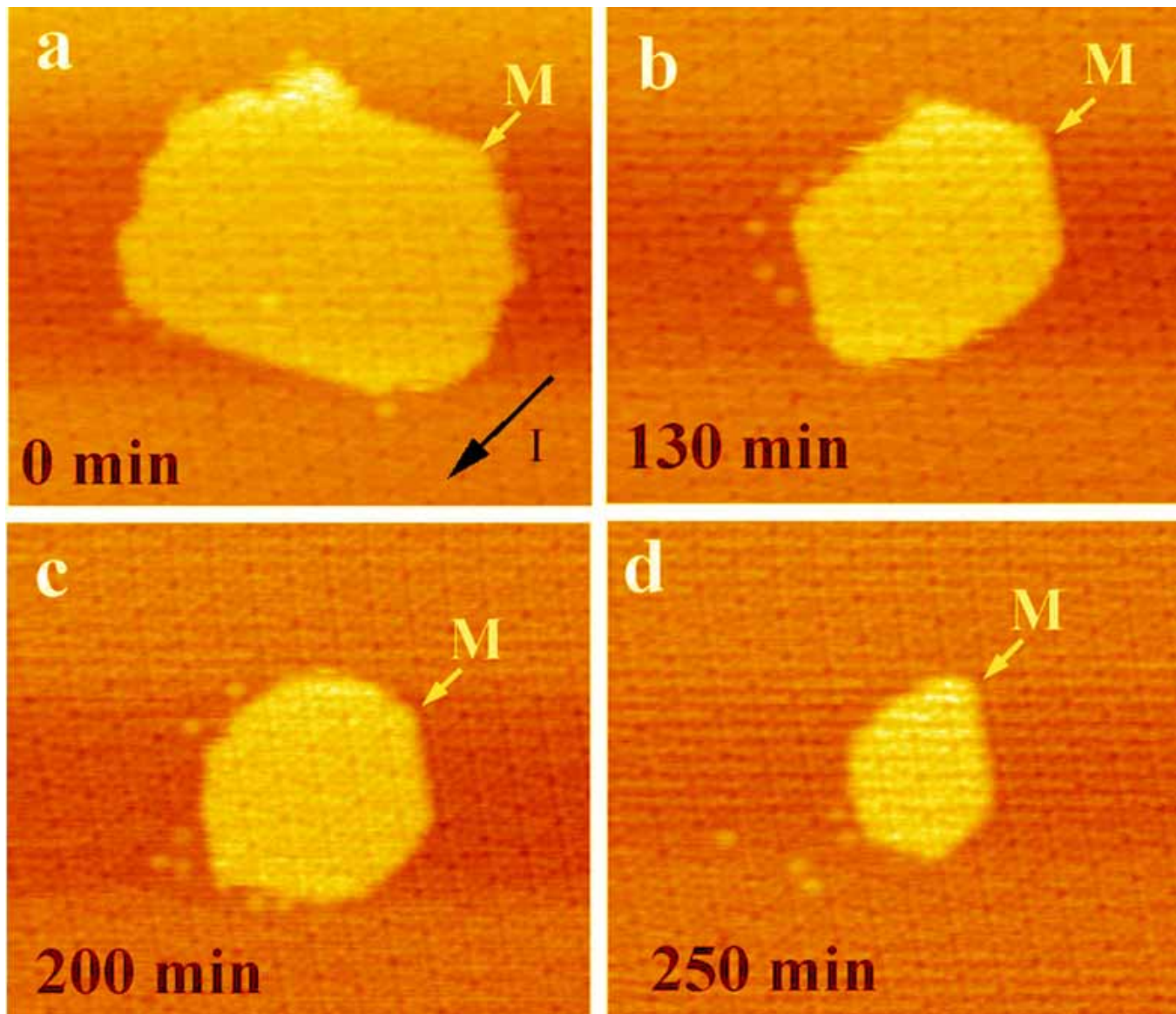


Time interval 4.6 s
Sample bias of -1.5V

450



The Decay Processes of 2D Islands

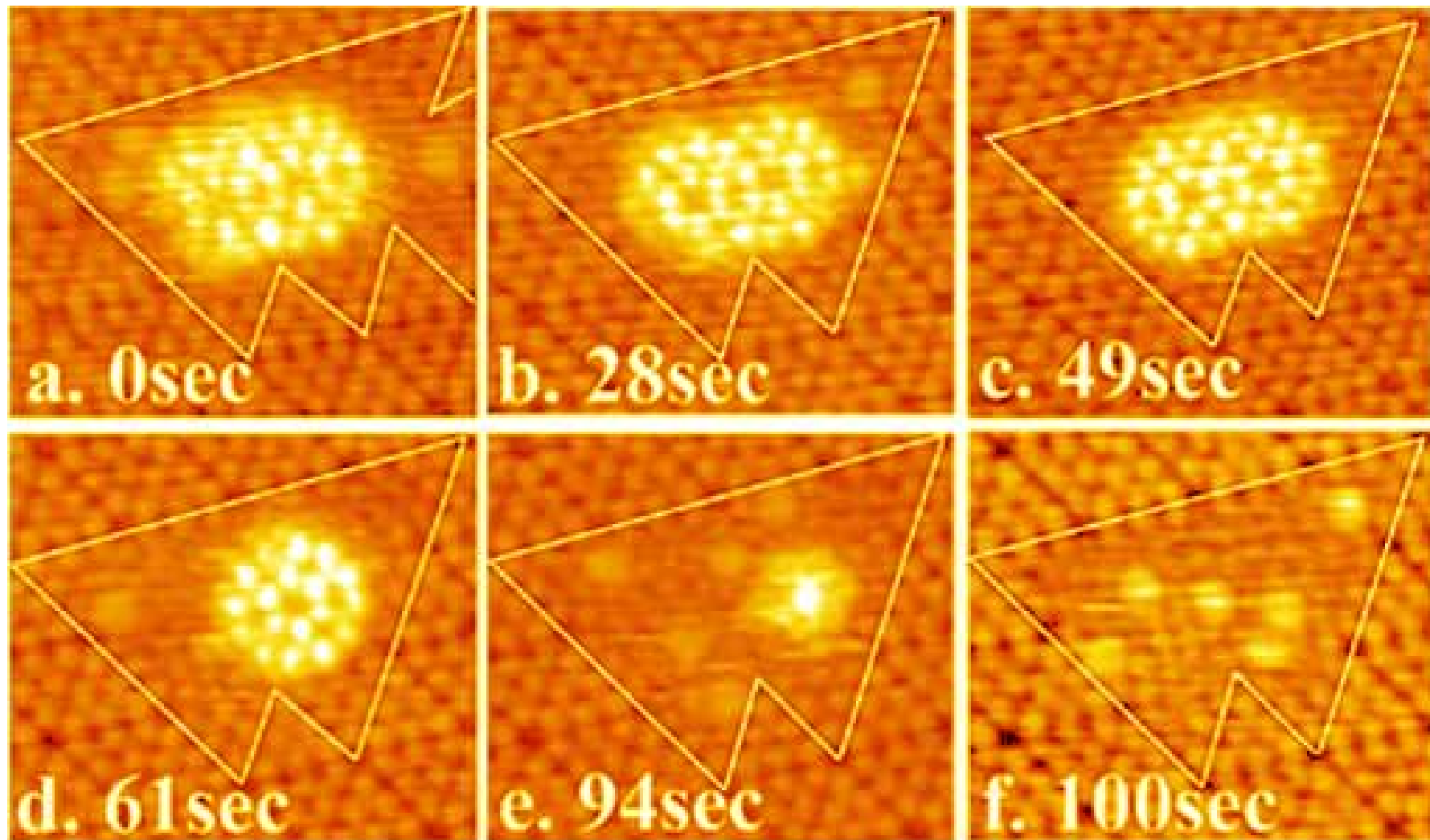


450Å × 380Å

Sample bias -2V

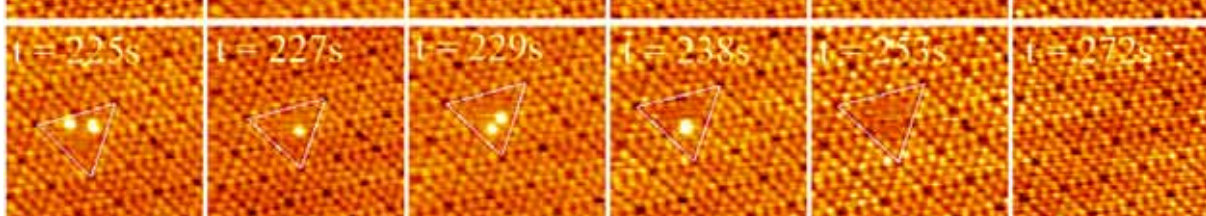
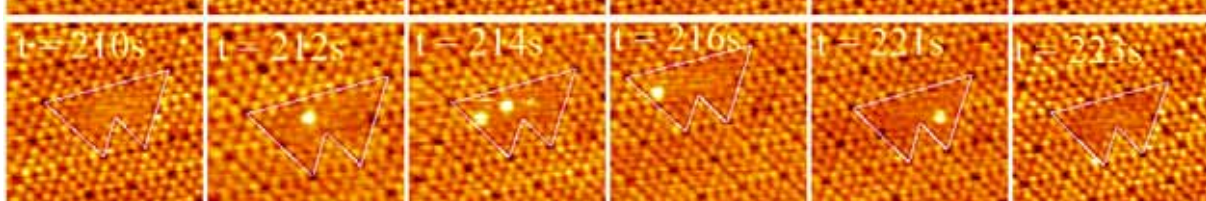
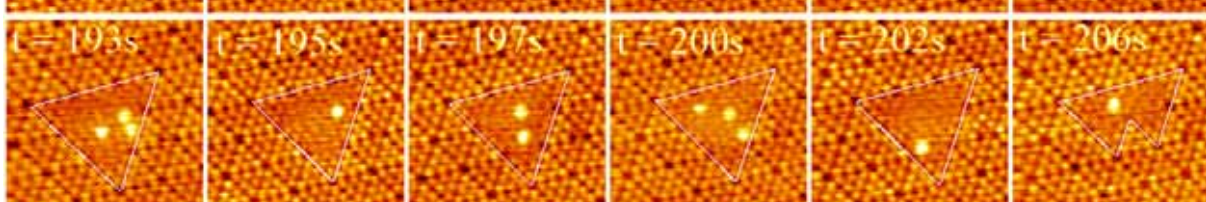
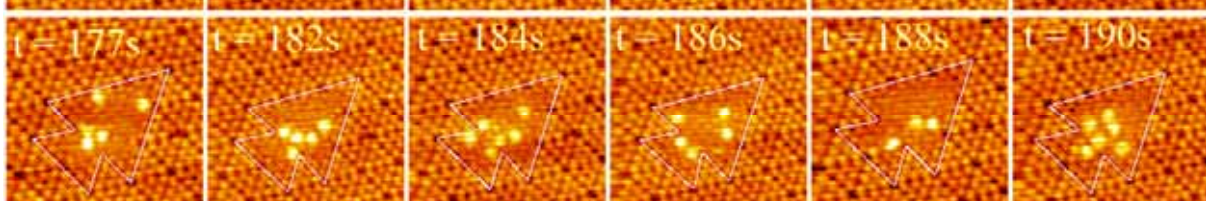
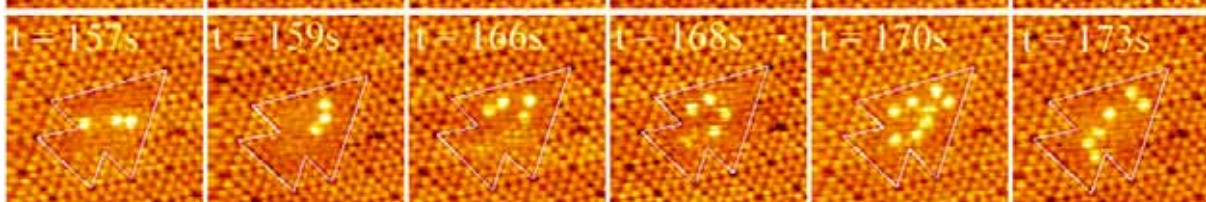
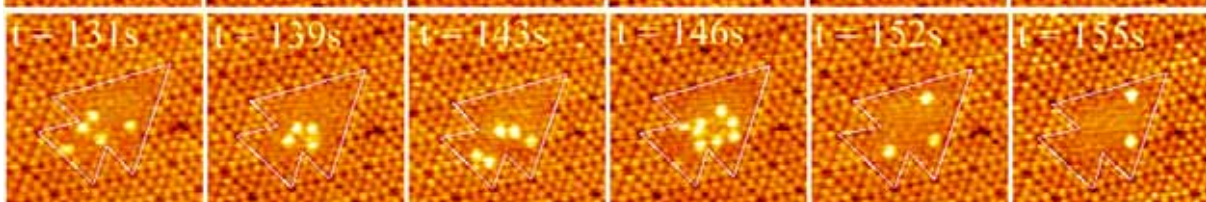
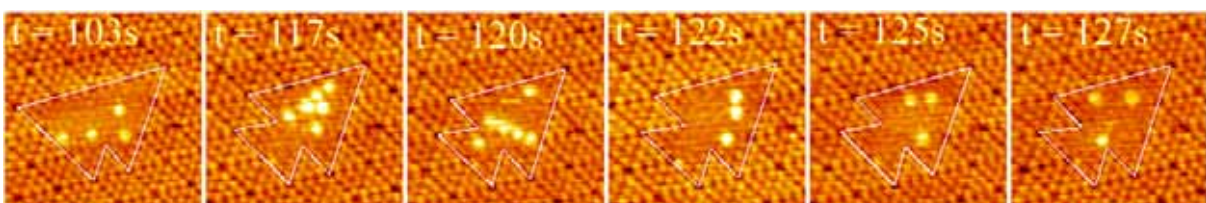
450

Decomposition of a Si Island into Magic Clusters

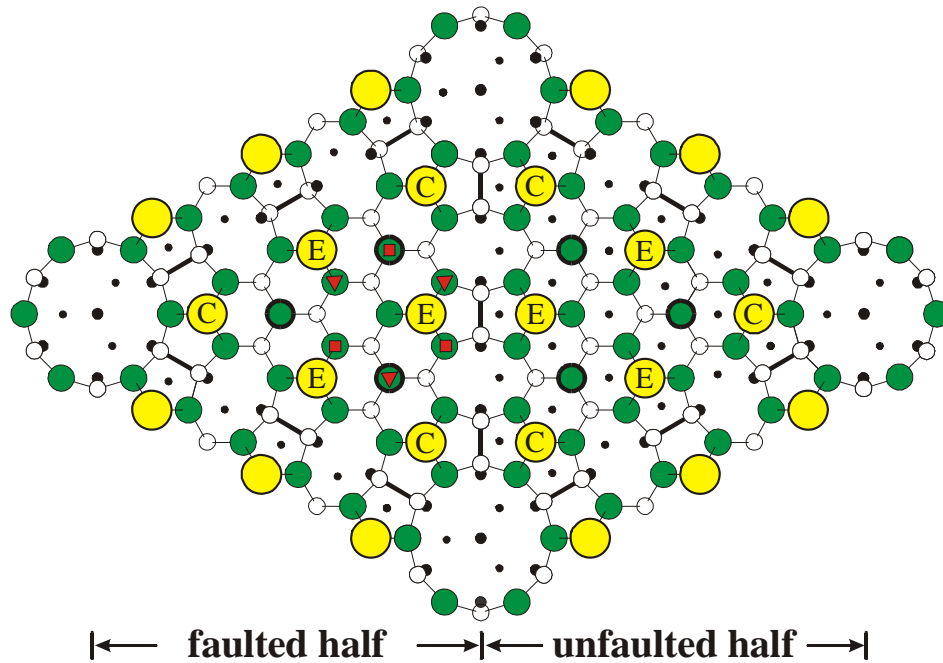


Sample bias -1.5V

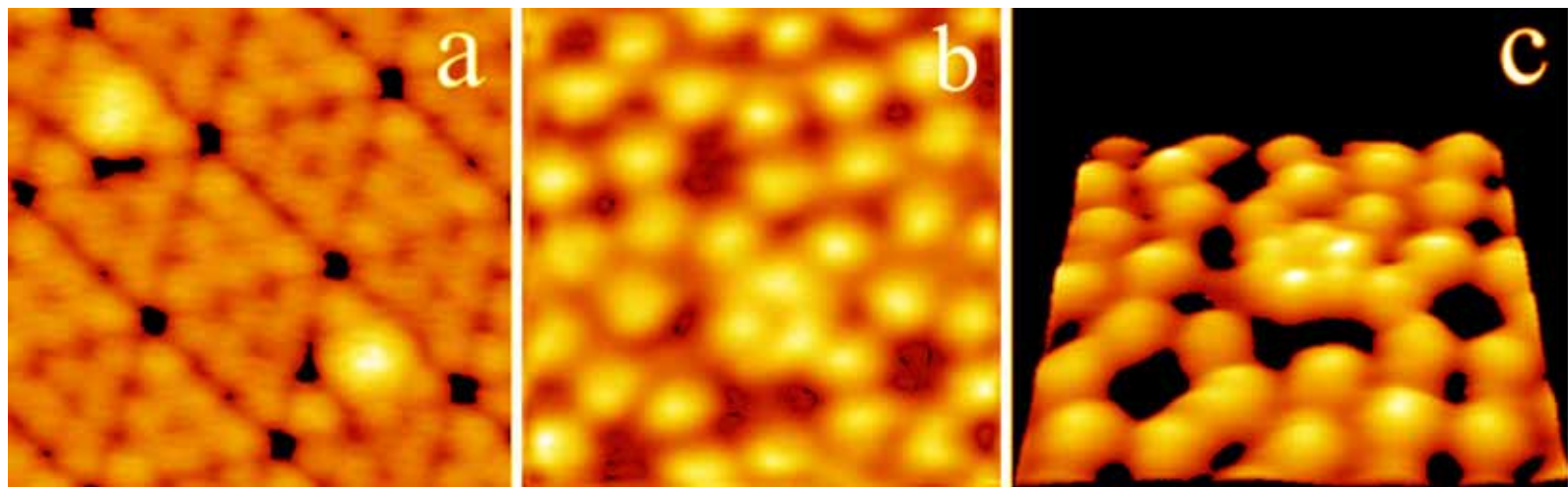
460



Si Magic Clusters on Si(111)-(7×7)



1. The spacing between the protrusions is $\sim 3.8\text{\AA}$, which is much larger than the Si-Si bond length (2.3\AA).
2. The magic number is estimated to be 9 to 15.



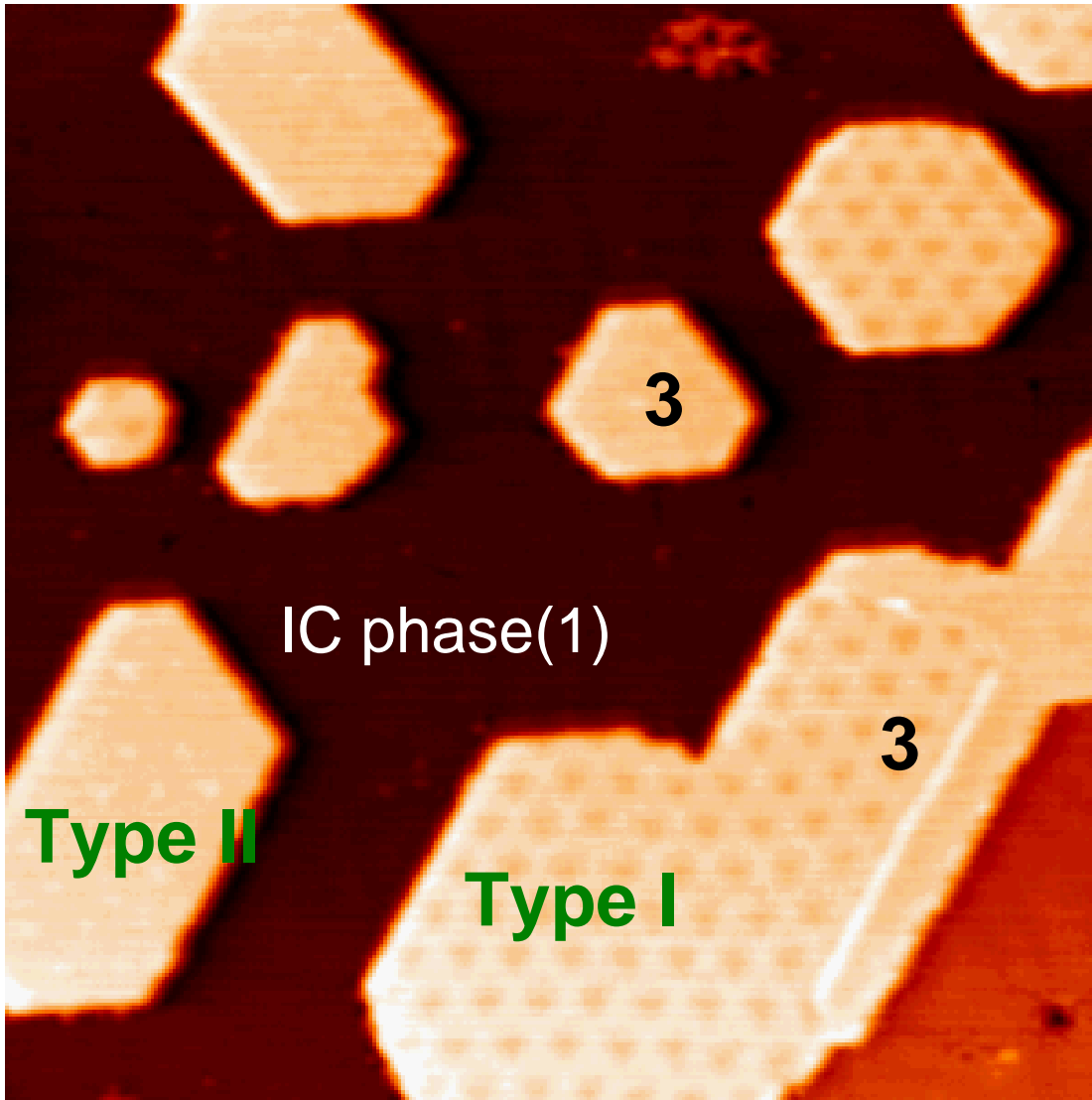
sample bias

-1.5 V

+1.8 V

+1.2 V

Pb islands on Pb/Si(111)

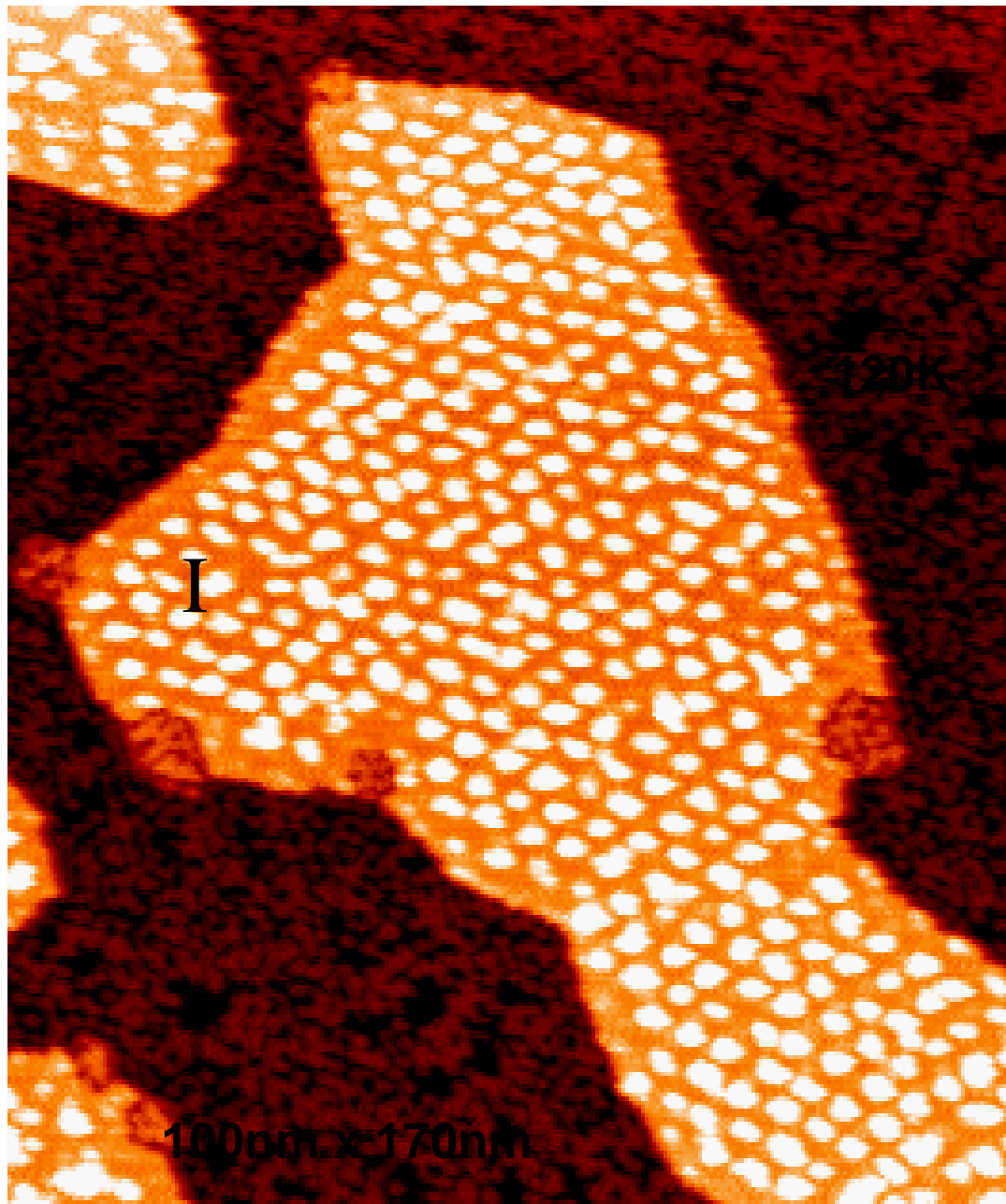


Deposit Pb on
Pb/Si(111) at
 $T \sim 200K$

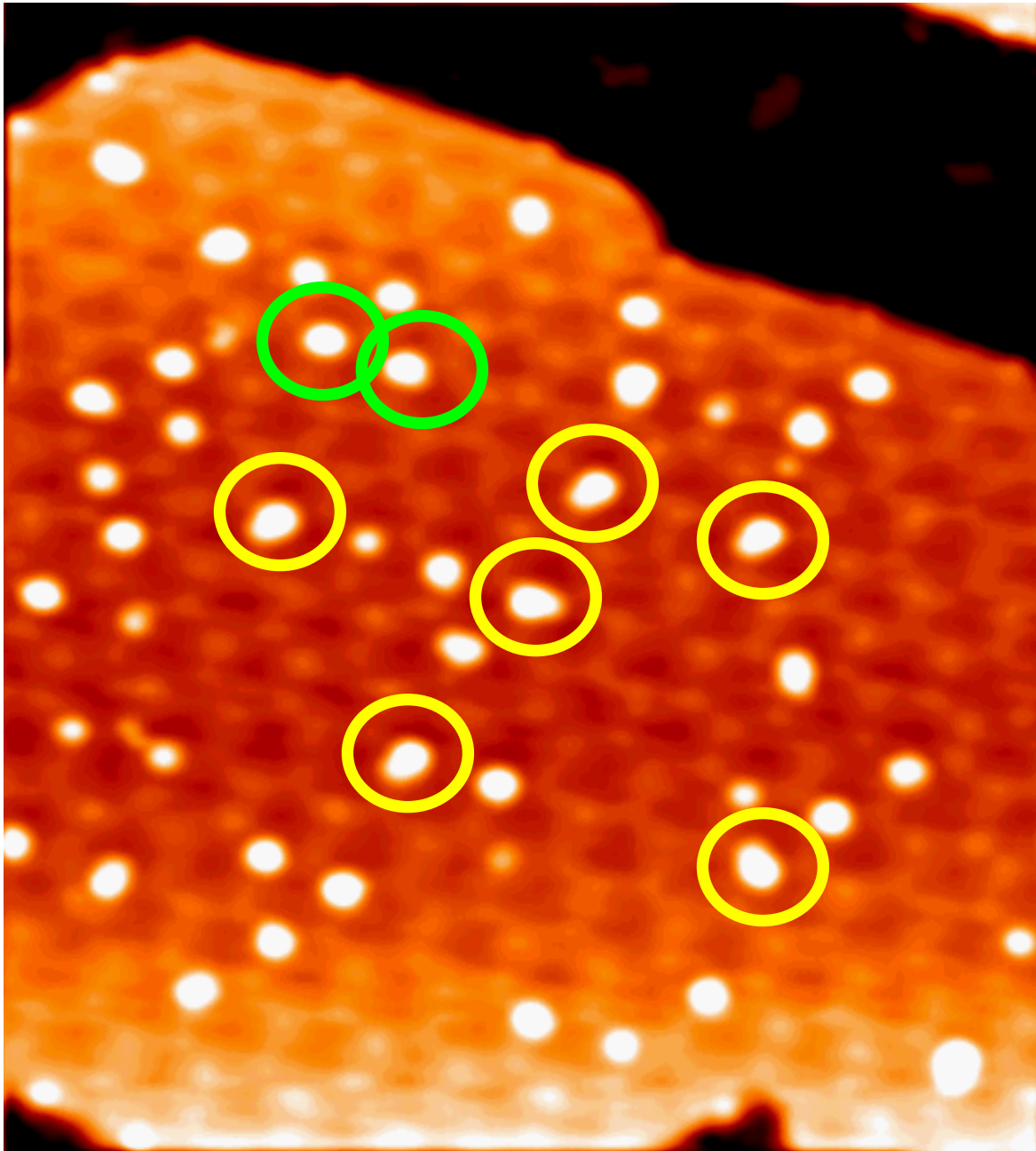
---Single
thickness

Sample bias :
+2V

Ref : PRL 90 (2003) 196603

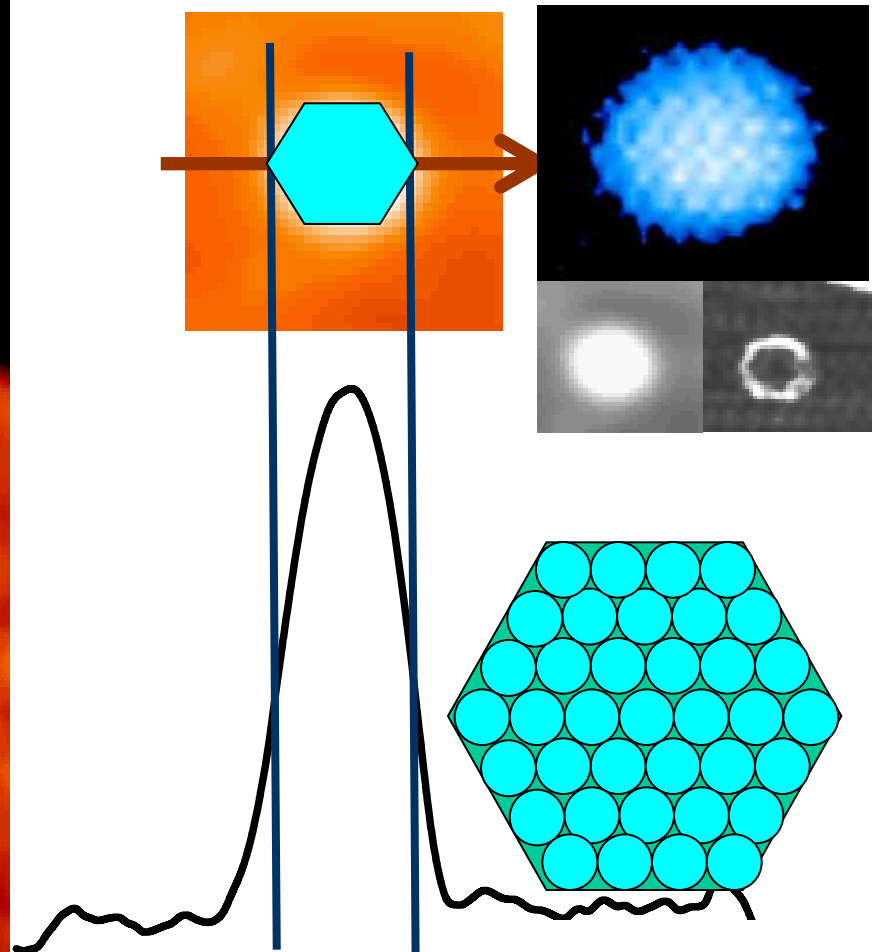
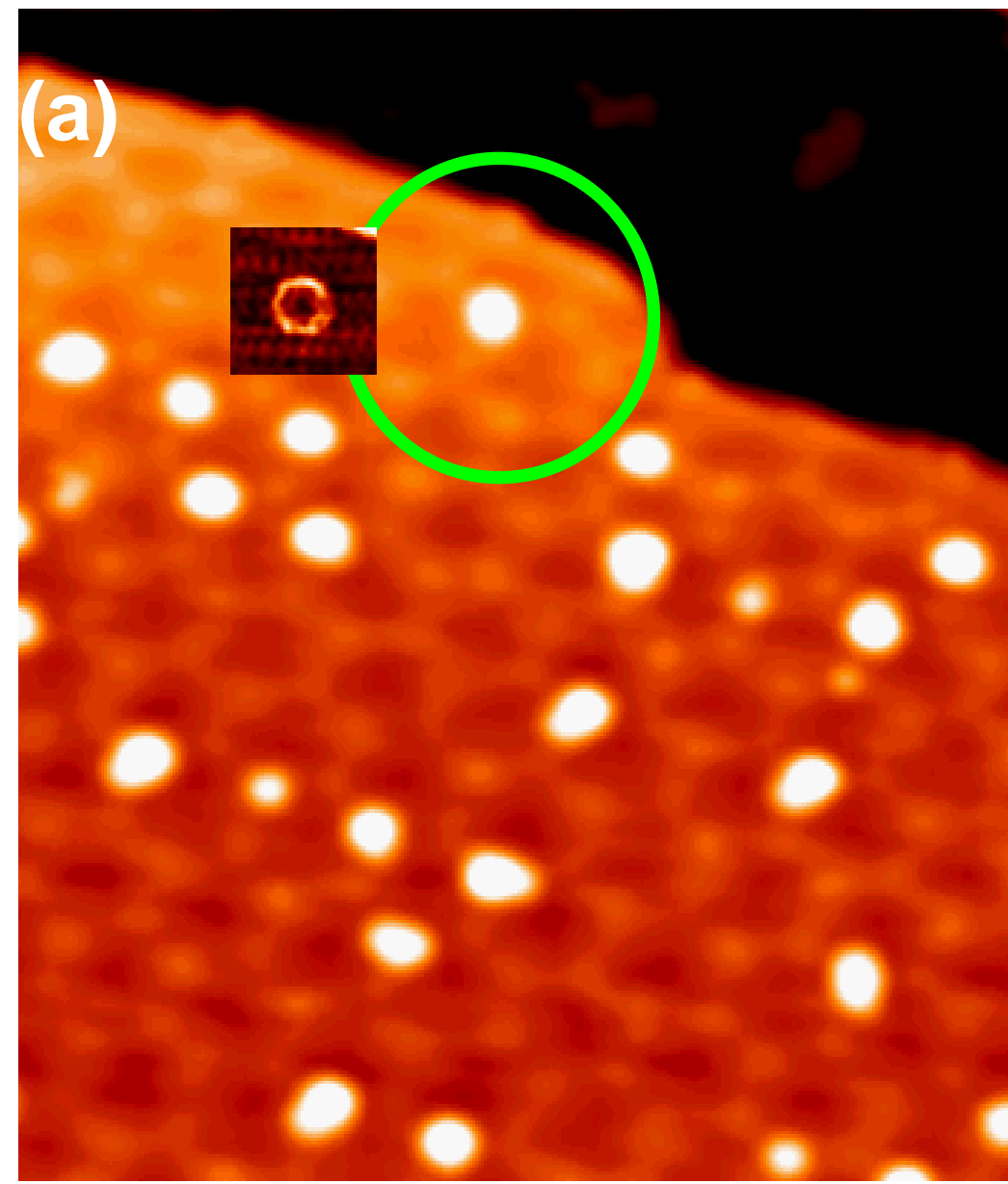


*Two-dimensional
Ag cluster arrays
on quantum Pb
islands*



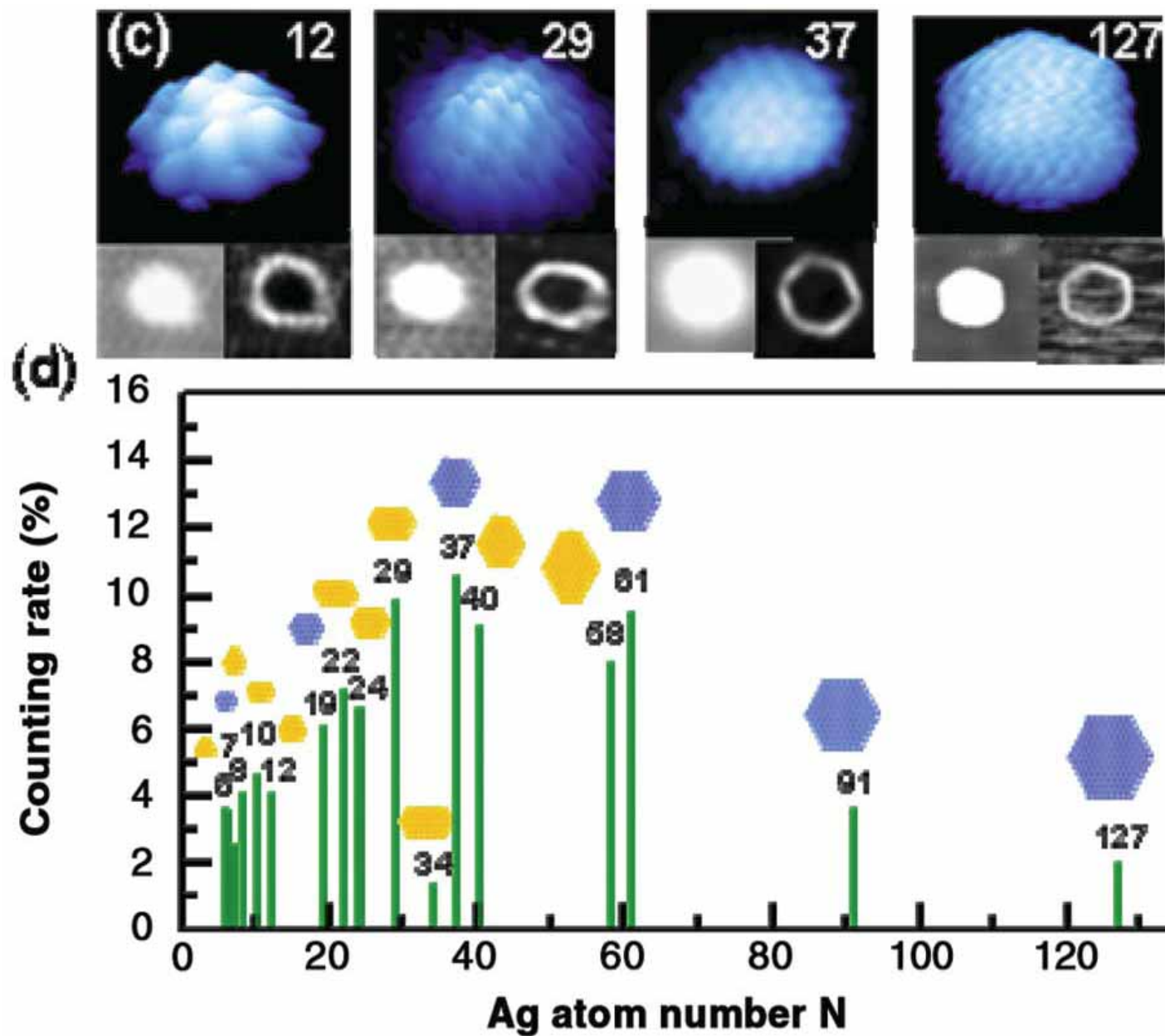
Deposit Ag
on Pb islands
at $T \sim 175K$

The size of the nanopucks

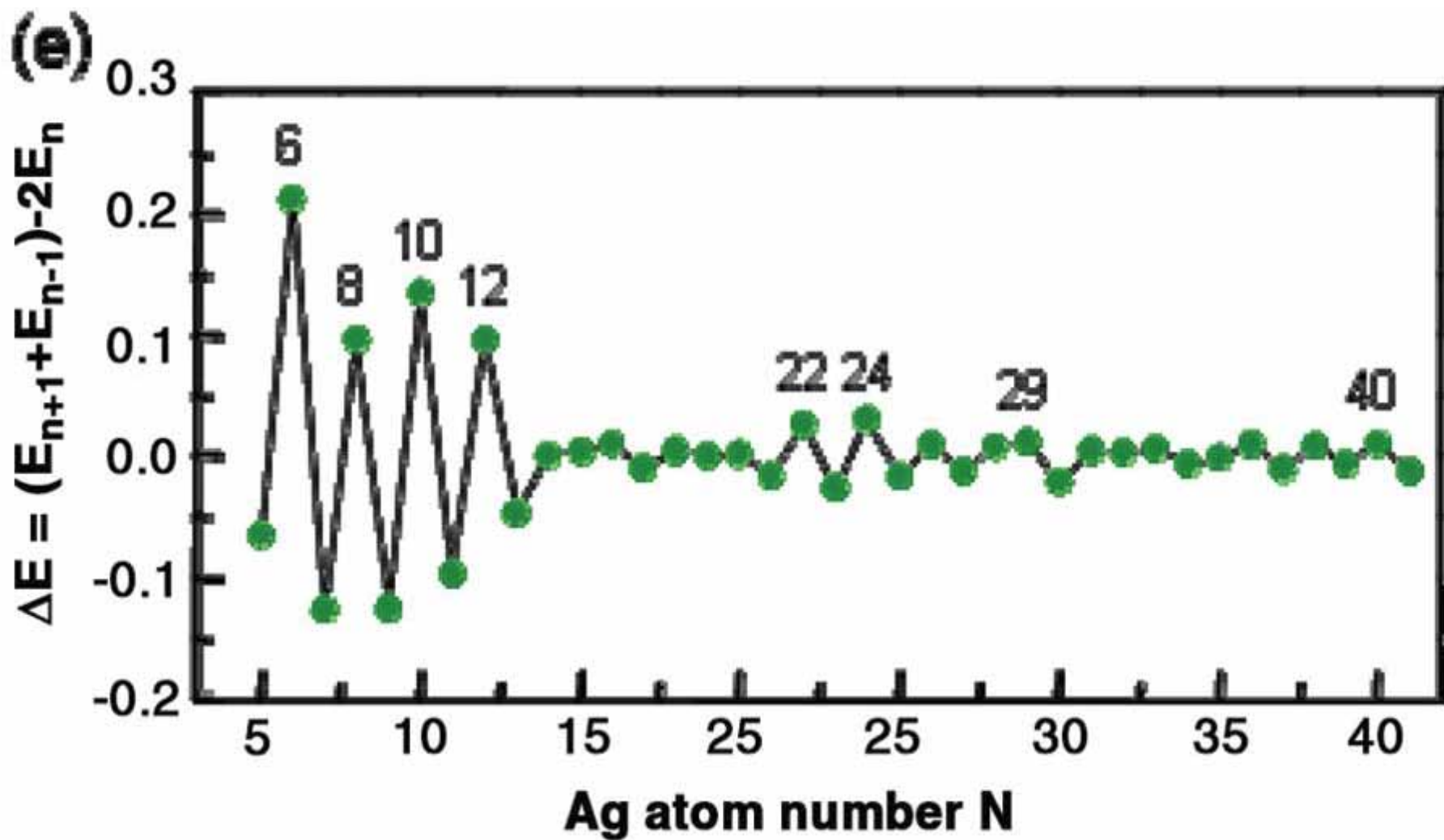


Hex. 37

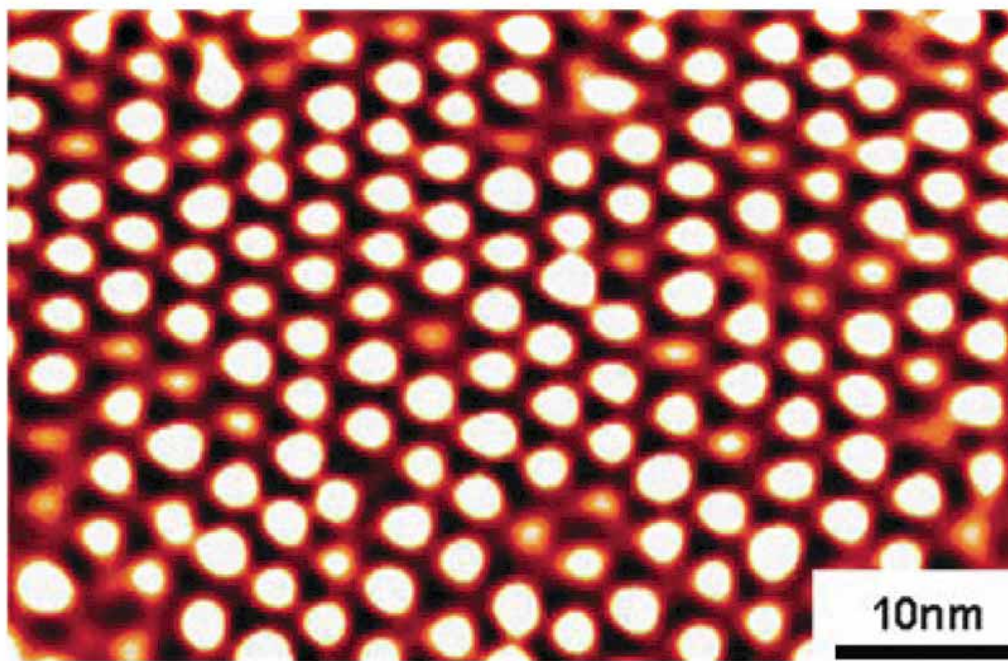
Size distribution of Ag nanopucks



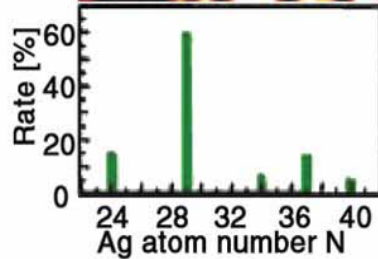
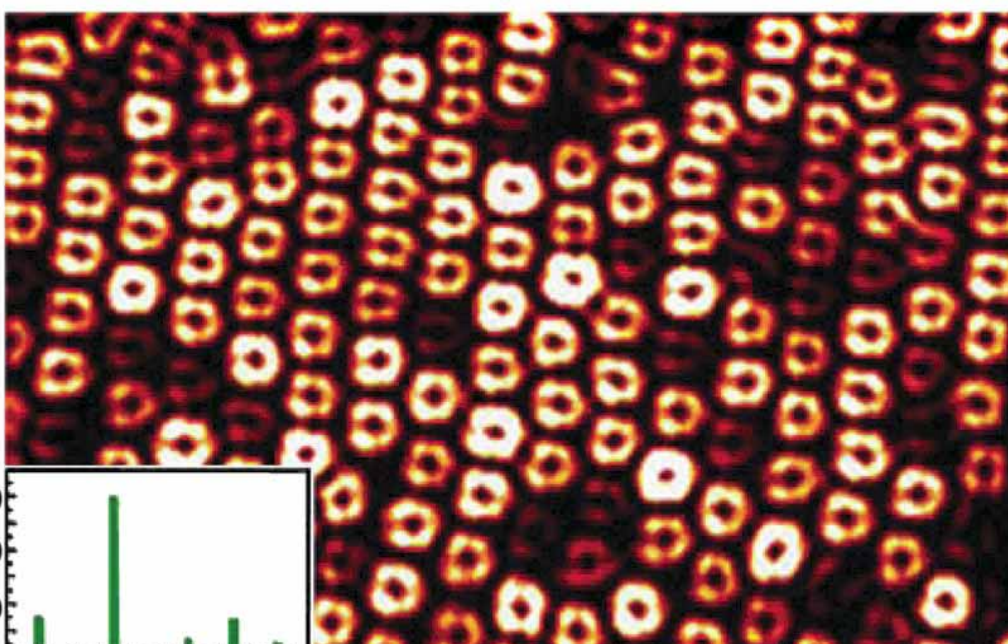
Stability of Ag nanopucks



(a)

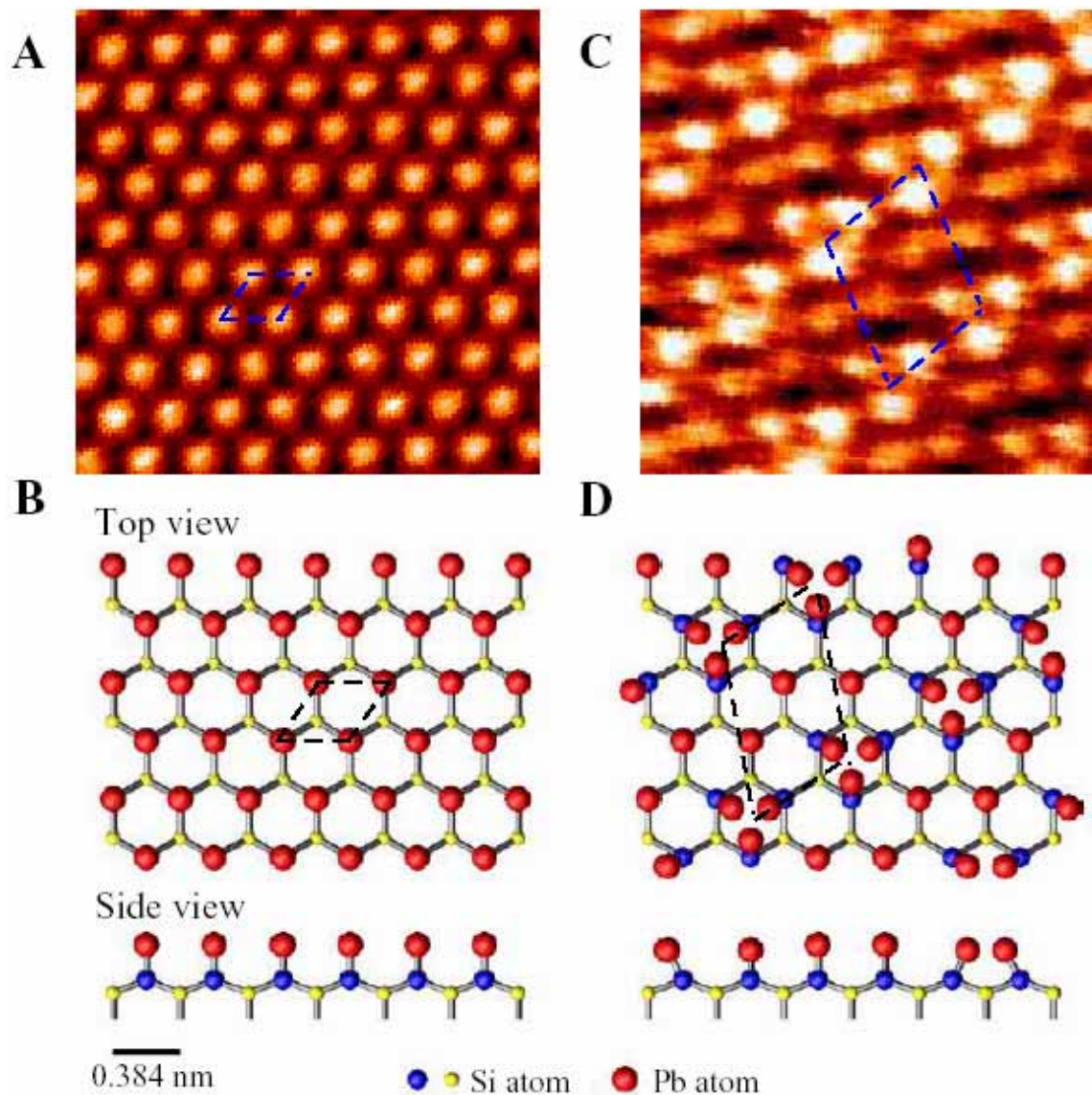


(b)

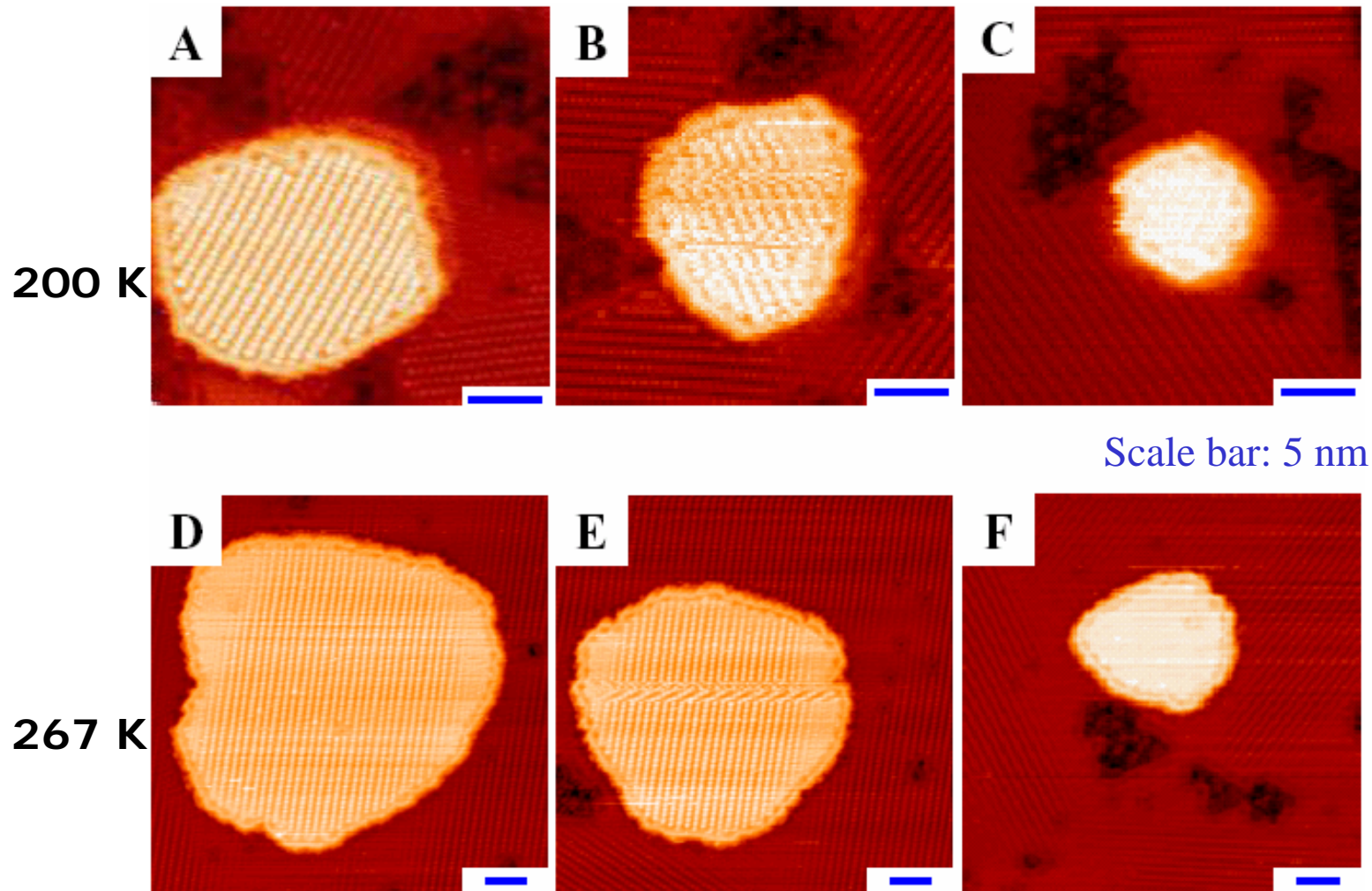


Reversible Surface Phase Transition

Pb/Si(111) $1\times 1 \leftrightarrow \sqrt{7} \times \sqrt{3}$

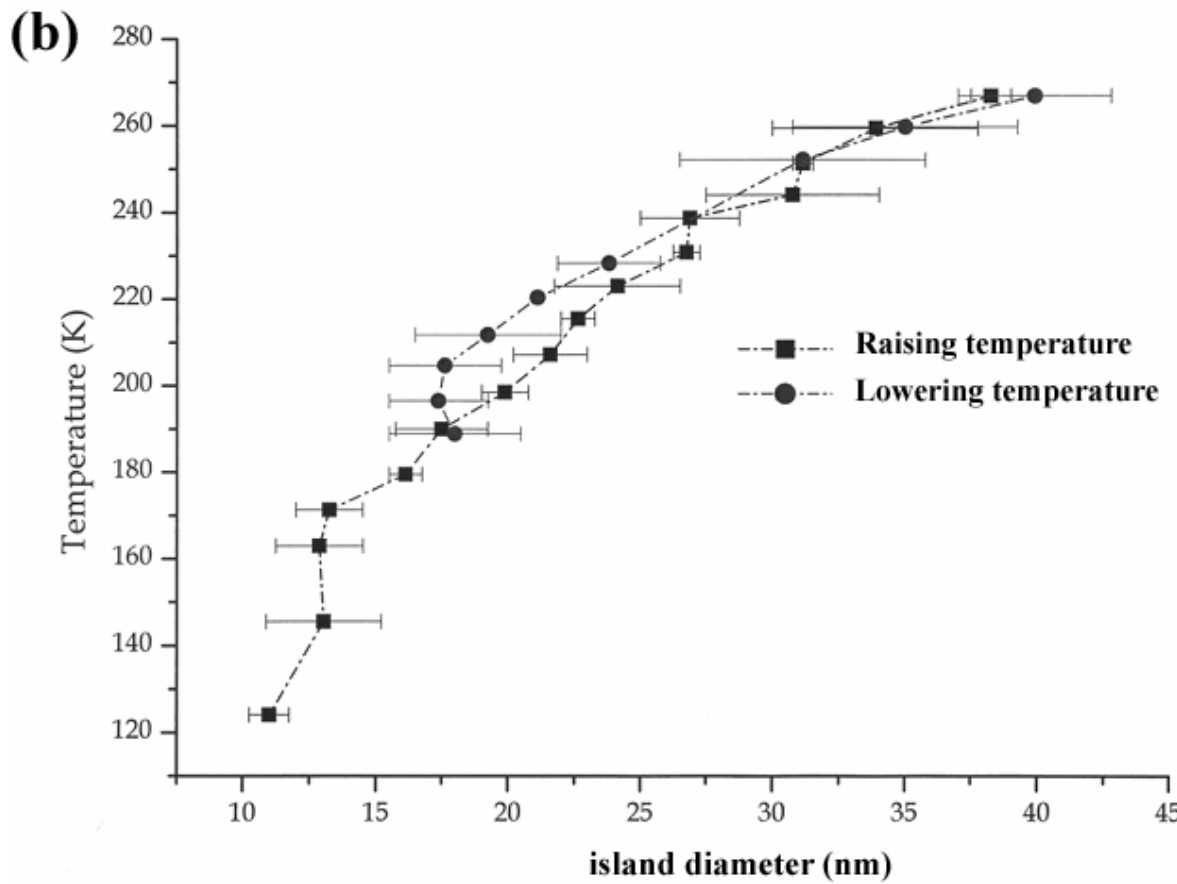
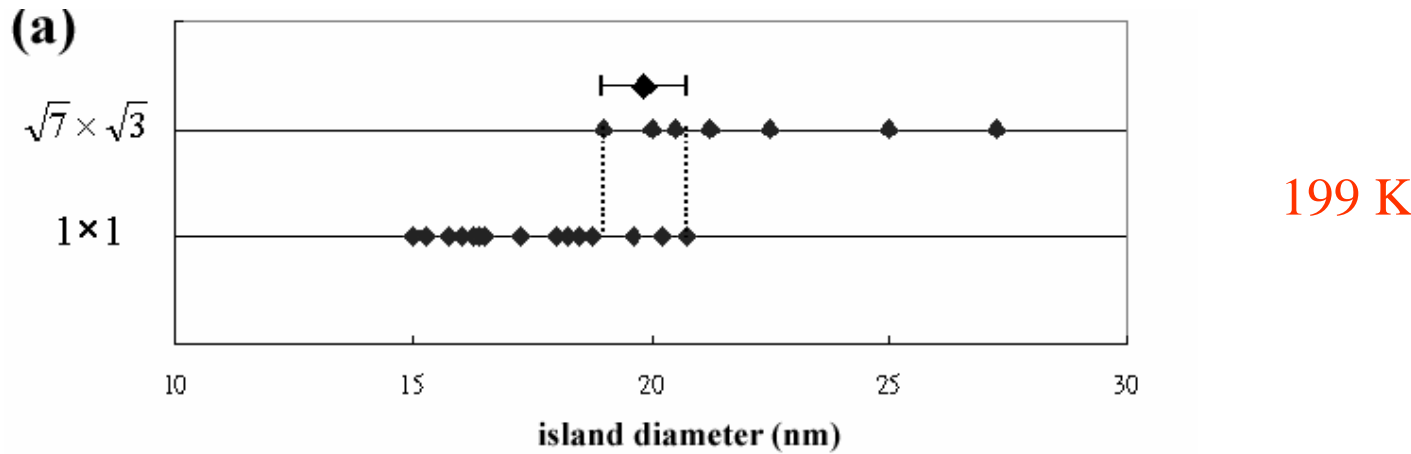


Size Effects on the Pb-Covered Si Islands



I.S. Hwang, et al., Phys. Rev. Lett. **93**, 106101 (2004)

Transition Temperature vs. Size



Temporal Fluctuations Near the Transition Temperature

Slow scan direction

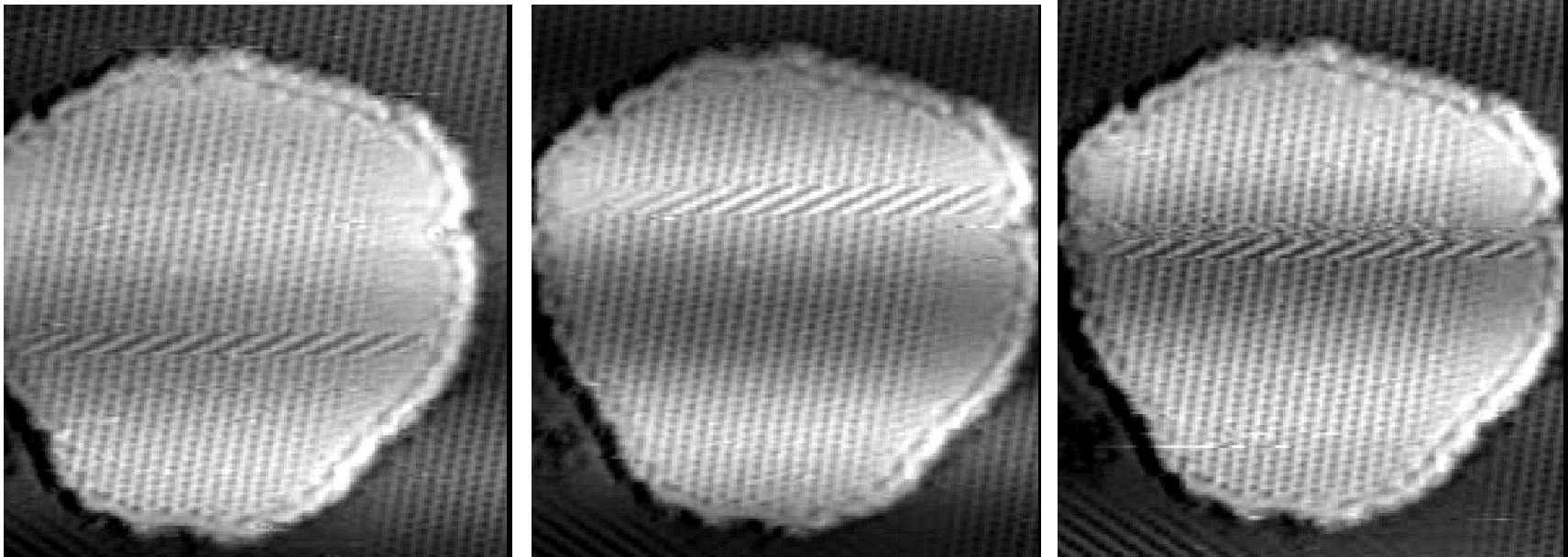
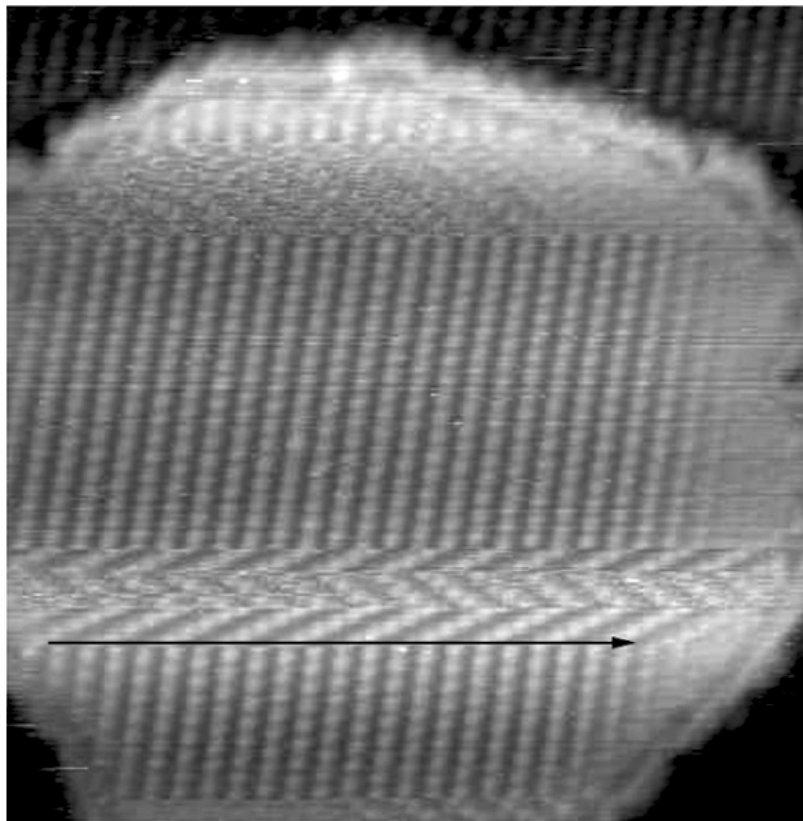


Image size: 34 nm × 38 nm

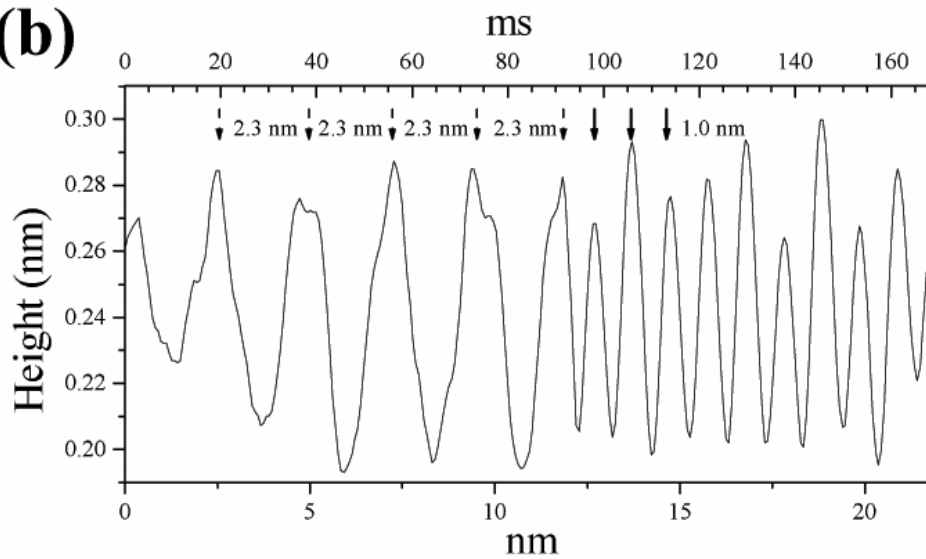
266 K

(a)

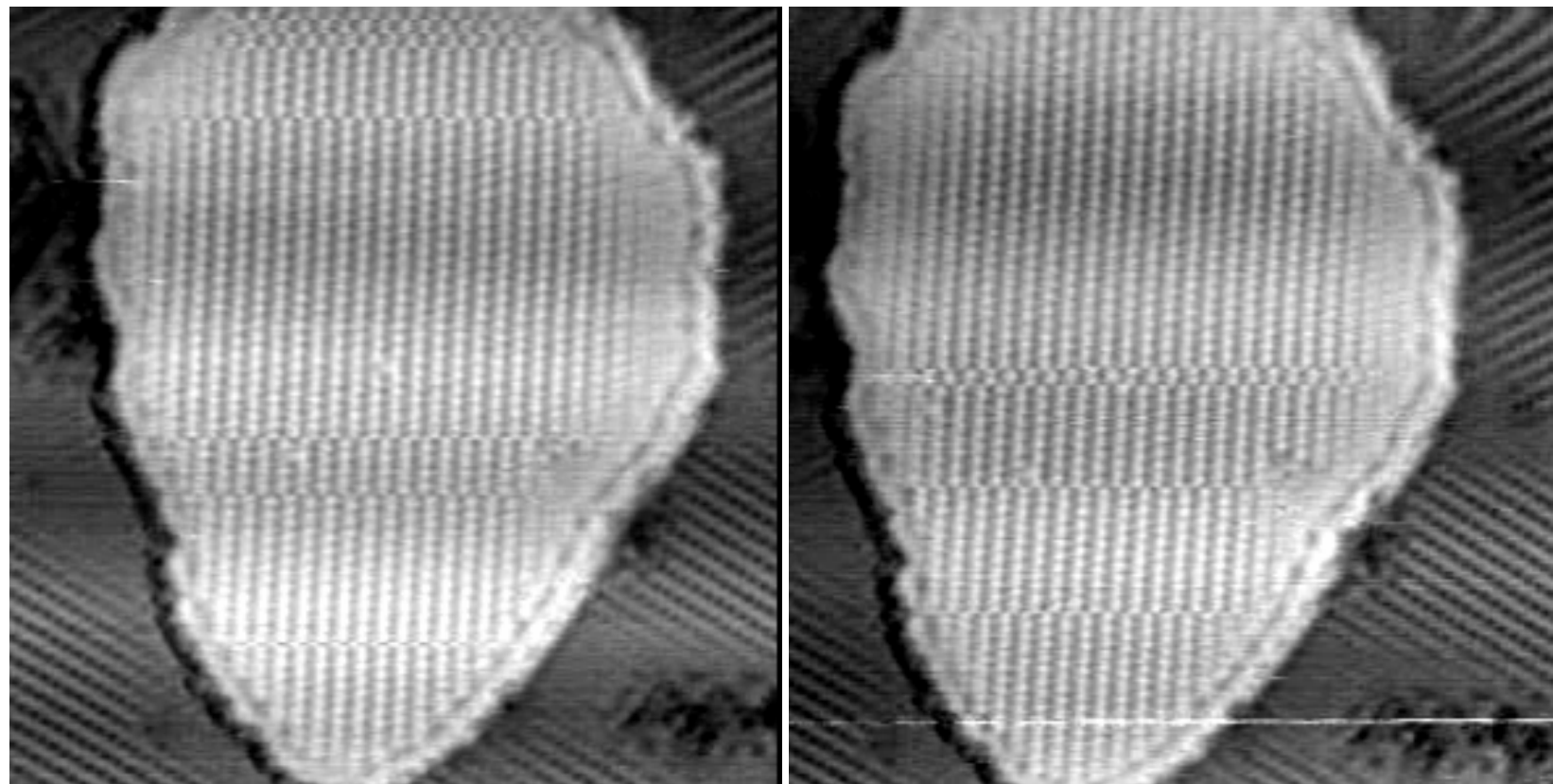


Slow scan direction

(b)



Temporal Fluctuations Near the Transition Temperature



260 K

Image size: 40 nm × 40 nm

Electrochemical Scanning Tunneling Microscopy

Angew. Chem. Int.
Ed. 40, 1162
(2001).

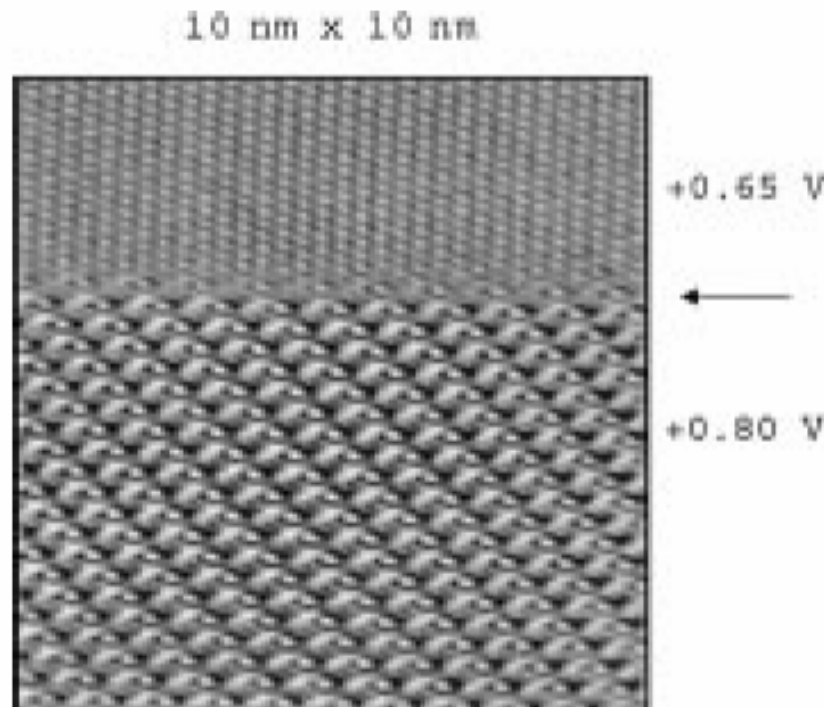


Figure 12. High-resolution STM image of Au(111) in 0.1M H₂SO₄. The upper part shows the Au(111) surface, atomically resolved, at +0.65 V versus SCE; the lower part shows the ordered adlayer of sulfate, formed by a potential step to +0.80 V versus SCE.

